IMPACT OF NUCLEOTIDE MODIFICATIONS ON IMMUNE STIMULATORY EFFECTS OF RNA

Dissertation

submitted to the

Combined Faculty of Natural Sciences and Mathematics

of the Ruperto Carola University Heidelberg, Germany

for the degree of

Doctor of Natural Sciences

presented by

Apothekerin Isabel Freund

Dissertation

submitted to the

Combined Faculty of Natural Sciences and Mathematics

of the Ruperto Carola University Heidelberg, Germany

for the degree of

Doctor of Natural Sciences

presented by

Apothekerin Isabel Freund

born in: Heidelberg

Oral-examination: 26.11.2018

IMPACT OF NUCLEOTIDE MODIFICATIONS ON IMMUNE STIMULATORY EFFECTS OF RNA

Referees:

Prof. Dr. Ralf Bartenschlager

Prof. Dr. Alexander H. Dalpke

ES IST WIE ES IST

TABLE OF CONTENT

LIST OF ABBREVIATIONS

A	adenosine
ADAR	adenosine deaminases acting on RNA
Am	2’-O-methylated adenosine
AP-1	activator protein 1
AAV	adeno-associated virus
bp	base pair
bRNA	bacterial RNA
C	cytosine
CARD	caspase activation and recruitment domain
Cas9	CRISPR-associated protein 9
cGAMP	cyclic guanosine monophosphate–adenosine monophosphate
cGAS	cyclic guanosine monophosphate-adenosine monophosphate synthase
CLR	C-type lectin receptors
Cm	2’-O-methylated cytosine
CRISPR	clustered regularly interspaced short palindromic repeats
crRNA	CRISPR RNA
D	dihydrouridine
DBD	DNA-binding domains
DNA	deoxyribonucleic acid
ds	double stranded
DSB	double strand break
ELISA	enzyme-linked immunosorbent assay
ER	endoplasmic reticulum
FC	fold change
G	guanosine
GDA	Gardiquimod-di-ethylene- glycol-azide
Gm	2’-O-methylated guanosine
GQI	Gardiquimod
gRNA	guide RNA
HDR	homology directed repair

I	inosine
IC_{50}	half maximal inhibitory concentration
iE-DAP	g-D-glutamyl-mesodiaminopimelic acid
IFN	interferon
IKK	IκB kinase
IL-6	interleukin 6
IRF	interferon regulatory factor
ISRE	interferon stimulated response elements
LBP	LPS-binding protein
LGP2	Laboratory of Genetics and Physiology 2
LPS	lipopolysaccharide
LRR	leucine rich repeat
MAPK	mitogen-activated protein kinase
MAVS	mitochondrial antiviral-signalling protein
MDA-5	melanoma differentiation associated gene 5
MDP	muramyl dipeptide
MFI	mean fluorescence intensity
MMA	mono-mannose
MOI	multiplicity of infection
mRNA	messenger RNA
MyD88	myeloid differentiation primary response 88
NA	nucleic acid
NFκB	nuclear factor kappa-light-chain-enhancer of activated B cells
NHEJ	non-homologous end joining
NLR	NOD-like receptors
NOD	nucleotide-binding oligomerization domain-like receptors
NOP 1	nuclear protein 1
nt	nucleotide
ORN	oligoribonucleotide
PAGE	polyacrylamide gel electrophoreses
PAM	protospacer adjacent motif
PAMP	pathogen-associated molecular pattern
PBMC	peripheral blood mononuclear cell

pDC	plasmacytoid dendritic cells
poly(I:C)	polyinosinic-polycytidylic acid
PRR	pattern recognition receptor
PYD	pyrin domain
R848	Resiquimod
RIG-I	retinoic acid inducible gene I
RISC	RNA-induced silencing complex
RNA	ribonucleic acid
RNAi	RNA interference
RPA	Resiquimod-polyethylene-glycol-azide
rRNA	ribosomal RNA
shRNA	short hairpin RNA
siRNA	short interfering RNA
ss	single stranded
STING	stimulator of interferon genes
T	thymidine
TALEN	transcription activator-like effector nuclease
TARBP1	Tar binding protein 1
TIR	Toll/interleukin-1 receptor
TLR	Toll-like receptor
Tm	2'-O-methylated thymidine
TMA	tri-mannose
TNF-α	tumor necrosis factor alpha
tracrRNA	*trans*-activating CRISPR RNA
TRAF	tumor necrosis factor receptor-associated factor
TREX	three-prime repair exonuclease 1
TRIF	TIR-domain-containing adapter-inducing interferon-β
tRNA	transfer RNA
U	uridine
Um	2'-O-methylated uridine
UNC93B1	uncoordinated 93 homolog B1
ZFN	zinc-finger nucleases
ψ	pseudouridine

1 SUMMARY

1.1 Abstract

Posttranscriptional RNA modifications are an important feature of self/non-self discrimination of nucleic acids by the innate immune system. Ribose 2'-O-methylation within RNA has been shown to limit recognition by Toll-like receptors (TLR) 7 and TLR8. In the natural RNA context, 2'-O-methylation of guanosine at position 18 (Gm18) within transfer RNAs (tRNAs) was identified to abolish RNA induced immune activation. However, the exact requirement of Gm18 within tRNA for affecting TLR responses remained unknown. Moreover, whether Gm18 plays a role as immune modulatory RNA modification in physiological settings or has different roles in pro- vs. eukaryotes was unexplored. Finally, preliminary data suggested the existence of further RNA modifications that affect immune recognition. This thesis therefore aimed to explore the function of Gm18 for immune regulation in more detail and to study further RNA modifications for immune regulatory properties.

In a combined chemical-immunological approach on human $tRNA^{Lys}_3$ which showed no TLR7 activation but lacked Gm18, this work identified a new immune-silencing modification: Tm, a double-methylation of uridine, at position 54 of human tRNAs was sufficient to decrease immune stimulation of TLR7. However, in contrast to Gm18, the effects were not dominant negative in co-stimulation experiments. Thus, for the first time an immune silencing modification in a natural RNA context has been deciphered.

To further define the inhibition of TLR7 and TLR8 activation by Gm18 modified RNA, a systematic variation of nucleotides within a conserved tRNA sequence was performed. The studies allowed identification of an optimized sequence motif antagonizing TLR7/8 responses. The minimal, naturally occurring GmGC tri-nucleotide motif within a 9-mer oligoribonucleotide was identified as most efficient to antagonize recognition of otherwise immune stimulatory RNA. The findings could be beneficial to design immune inhibitory oligoribonucleotides as therapeutic approach in autoimmune diseases associated with exaggerated TLR7/8 activation.

In further series of experiments mutants lacking Gm18 modification in either bacterial or eukaryotic tRNA were used to study the functional impact on overall immune stimulation. tRNA from an *Escherichia coli* (*E.coli*) mutant lacking the enzyme trmH that incorporates Gm18 showed increased immune stimulation. However, stimulation of human peripheral

blood mononuclear cells (PBMCs) and TLR8 deficient genetically engineered monocyte/macrophage–like BlaER1 cells, with whole *E.coli* wild-type and trmH deficient bacteria revealed RNA dependent recognition of *E. coli* but negligible effects of Gm18. Interestingly, results indicate that trmH mediated Gm18 modification might be subject to regulation under stress conditions. Similarly, CRISPR/Cas9 generated knockouts of TARBP1, the Gm18 methyltransferase in human cells, showed slightly increased immunostimulation for tRNA fractions but no change for whole RNA stimulation.

In summary, RNA 2'-O-methyl modification within tRNA is capable to limit immune recognition by TLR7/8, yet for manipulation of the overall immune recognition of bacterial or eukaryotic RNA the identified modifications alone seem to be insufficient.

1.2 Zusammenfassung

Posttranskriptionale Modifikationen von RNA sind ein wichtiger Aspekt der selbst/fremd-Unterscheidung von Nukleinsäuren durch das angeborene Immunsystem. Eine übergeordnete Rolle in der Erkennung von RNA spielt die 2'-O-Methylierung von einzelsträngiger RNA (ssRNA), da diese Art der Modifikation die Aktivierung der Toll-ähnlicher Rezeptoren (TLR) 7 und TLR8 inhibieren kann. Erforscht wurde dieser Effekt im natürlichen Kontext bakterieller tRNAs, welche eine 2'-O-Methylierung am Guanosin an Position 18 (Gm18) aufwiesen. Jedoch war der Einfluss von Gm18 in prokaryotischer oder eukaryotischer tRNA im physiologischen Kontext auf die Immunerkennung nicht bekannt. Zudem gaben unveröffentlichte Daten Hinweise auf weitere RNA Modifikationen, die die Immunostimulation beeinflussen können. Das Ziel dieser Arbeit war es, die Bedeutung von Gm18 für die Aktivierung des Immunsystems besser zu charakterisieren und weitere, neue immunmodulatorische RNA Modifikationen zu identifizieren.

In einem chemisch-immunologischen Ansatz wurde die native $tRNA^{Lys}_3$ untersucht, welche zwar keine Immunstimulation von TLR7 zeigte, jedoch nicht antagonisierend auf den Rezeptor wirkte. Tm, eine natürlich vorkommende Doppelmethylierung von Uridin an Position 54 in humanen tRNAs wurde als immunmodulatorische Modifikation identifiziert. Dabei bewirkte eine 2'-O-Methylierung von RNA zum ersten Mal eine Stummschaltung der RNA Erkennung über TLR7 ohne dessen zusätzliche Antagonisierung.

Um die Inhibition von TLR7 und TLR8 durch Gm18 besser charakterisieren zu können, wurden einzelne Nukleobasen einer konservierten tRNA Sequenz systematisch verändert. Dabei konnte ein optimiertes Sequenzmotiv identifiziert werden, welches eine TLR7- und

TLR8-Stimulation inhibiert. Das natürlich vorkommende, drei Nukleotid lange GmGC Motiv als Teil eines 9-mer Oligoribonukleotids, war am effizientesten um die Immunaktivierung durch stimulative RNA zu antagonisieren. Die Identifikation eines neuen Sequenzmotives zur Unterdrückung der RNA-Erkennung ist ein wichtiger Aspekt zur Gestaltung von inhibitorischen Oligoribonukleotiden für therapeutische Anwendungen die mit einer erhöhten TLR7/8 Aktivierung einhergehen.

In einer weiteren Versuchsreihe zur Untersuchung der physiologischen Relevanz von Gm18 wurden bakterielle und eukaryotische Mutanten verwendet, die kein funktionelles Enzym zur 2'-O-Methylierung von tRNAs an Position 18 aufwiesen. tRNAs isoliert aus *E. coli* die defizient für eben das Enzym trmH waren, zeigten einen Anstieg in der Immunstimulation. Die Infektion von humanen peripheren mononuklearen Blutzellen und TLR8 defizienten BlaER1 Zellen, einer Monozyten/Makrophagen-ähnlichen Zelllinie, mit lebenden *E. coli* Bakterien ergab eine RNA abhängige Erkennung dieser Bakterien, welche jedoch nicht durch die 2'-O-Methylierung von G18 beeinflusst wurde. Interessanterweise deuteten diese Infektionsversuche auf eine stressinduzierte Regulation der 2'-O-Methylierung hin. Isolierte tRNAs aus humane Zellen, die durch CRISPR/Cas9 Technologie defizient für die tRNA 2'-O-Methyltransferase TARBP1 waren, zeigten ebenfalls einen leichten Anstieg in der Immunstimulation.

Zusammenfassend zeigt diese Studie, dass die RNA-Erkennung durch TLR7 und TLR8 durch 2'-O-Methylierung von tRNA inhibiert werden kann. Jedoch, basierend auf den neusten Daten, ist die 2'-O-Methylierung von tRNAs nicht ausreichend um die Erkennung von lebenden Bakterien durch das angeborene Immunsystem zu beeinflussen.

2 INTRODUCTION

A variety of pathogens including viruses, bacteria and fungi can cause host-specific infections and it is a daily challenge of the immune system to recognize and neutralize those pathogens. The human immune system comprises the innate and the adaptive immune system. The innate immune system forms the first line of defence against invading pathogens and is able to recognize a broad range of so-called pathogen associated molecular patterns (PAMPs). PAMPs are highly conserved structures present in various pathogens but not in the host, therefore allowing the innate immune system a reliable discrimination between self and non-self [1-3]. Importantly, the innate immune system can be activated within minutes, leading to an unspecific immune response [4]. In contrast, the adaptive immune response arises with a delay of 4–7 days against specific antigens. Thus, cells of the innate immune system play a crucial role in controlling infection at early stages after pathogen encounter and link innate and adaptive immunity by presenting antigens to lymphocytes to initiate a specific immune response.

2.1 Pathogen recognition within the innate immune system

2.1.1 Pattern-recognition receptors and pathogen-associated molecular patterns

The innate immune system is the first line of host defence against invading pathogens. To ensure a fast immune response against a broad range of microbes and viruses cells of the innate immune system are equipped with a limited set of pattern recognition receptors (PRRs). PRRs are expressed among all kinds of immune cells but are also present in epithelial cells of skin, gut and lung or tissues of various organs [5-8]. Of note, each type of immune cell is equipped with a specific repertoire of receptors. For instance, human monocytes are expressing Toll-like receptor (TLR) 1, 2, 4, 5, 6, and TLR8, whereby TLR 1, 6, 7 and TLR9 are found in plasmacytoid dendritic cells (pDCs) [9]. Those receptors are not aimed to recognise unique pathogen specific antigens but so-called pathogen-associated molecular patterns (PAMPs) that are shared among different pathogens. Common PAMPs, exclusively present in microbes but not in host cells, are cell wall components like lipoteichoic acid (LTA) and lipopolysaccharide (LPS) of Gram-positive and Gram-negative bacteria, respectively [1, 10]. Those structures are mainly recognized by PRRs localized on the cell surface of different immune cells. The two major groups of surface transmembrane receptors are TLRs and C-type lectin receptors (CLRs). Upon ligand binding, intracellular downstream signalling is activated resulting in secretion of proinflammatory cytokines [2, 11]. Except for nucleotide-

binding oligomerization domain-like receptors, also known as NOD-like receptors (NLRs) which are involved in inflammasome formation, intracellular PRRs predominantly recognize nucleic acids (NA) like DNA and RNA. Beside cytosolic sensors such as cyclic GMP-AMP synthase (cGAS) and absent in melanoma 2 (AIM2) which are activated by double stranded DNA (dsDNA) or retinoic acid inducible gene I (RIG-I) and melanoma differentiation associated gene 5 (MDA-5) which are recognizing double stranded RNA (dsRNA), endosomal TLR3, 7, 8 and 9 are important in sensing various types of nucleic acids [12-14]. dsRNA activates TLR3, guanosine and uridine rich single stranded RNA (ssRNA) is recognized by TLR7 and 8 and unmethylated CpG dinucleotides (CpG DNA) found in bacterial DNA are able to activate TLR9. Since RNA and DNA are not exclusively present in pathogens but also in the host, nucleic acid sensing receptors need to discriminate between self and non-self. Beside the spatial restriction of nucleic acid sensing TLRs to the endolysosome, sequence dependent recognition and posttranscriptional modifications (see section 2.1.6 and 2.1.7) of RNA and DNA are key factors to avoid self-recognition and auto-immune response [6, 15, 16].

2.1.2 Excursus: Recognition of microbial cell wall components

To detect pathogens at an early stage of infection, microbial and fungal cell wall components are recognized by PRRs localized at the cell surface of immune cells. The two classes of receptors localized at the plasma membrane are transmembrane CLRs and TLRs. Most CLRs recognize carbohydrate motifs in a Ca^{2+} dependant manner resulting in the activation of IκB kinase (IKK) complex or mitogen-activated protein kinase (MAPK) leading to the secretion of proinflammatory cytokines [11]. Best described CLRs are Dectin-1 sensing β-glucan and Dectin-2 recognizing α-mannans. Dectin-1 has been shown to exhibit synergistic effects with cell surface receptors TLR2 and TLR4 up on specific ligand binding of each receptor [17, 18]. TLRs are type-1 transmembrane receptors possessing an extracellular domain containing variable numbers of leucine-rich-repeat (LRR) motifs and a cytosolic Toll/interleukin-1 receptor (TIR) domain necessary for downstream signalling. Beside TLR2 and TLR4, TLR1, TLR5 and TLR6 are found in the cell membrane of immune and epithelial cells. Unlike other TLRs, TLR2 is not known to form homodimers but functional heterodimers with TLR1 and TLR6 [19]. The heterodimers TLR2/TLR1 and TLR2/TLR6 are pre-formed at the cell surface and recognize triacyl and diacyl lipopeptides, respectively. A well described TLR2/TLR6 stimulus is LTA which is linked to the cell membrane of Gram-positive bacteria via diacylglycerol. Endogenous ligands like β-defensin-3, hyaluronic acid fragments and heat

shock proteins, known as “alarmins” and indicating tissue damage or necrosis are discussed to activate TLR2 [19, 20]. Furthermore, viral elements like glycoprotein B of cytomegalovirus or components of hepatitis B and C virus are described to activate TLR2/TLR6 heterodimer. Both heterodimers of TLR2 signal in a myeloid differentiation primary response 88 (MyD88)-dependent manner with downstream activation of MAPK and IKK complex and translocation of transcription factors activator protein 1 (AP-1) and nuclear factor kappa-light-chain-enhancer of activated B cells (NFκB), respectively [20]. In analogy to LTA, LPS is a major component of the outer membrane of Gram-negative bacteria. It is linked to the membrane of bacteria by Lipid A. This structure is conserved among Gram-negative bacteria and recognized by the TLR4/MD-2 complex. Of note, due to the chemical structure, LPS is forming micelles and LPS-binding protein (LBP) is needed to direct LPS monomers to the receptor. Activation of LPS-multi-receptor complex formed by TLR4 homodimer, MD-2, LBP and CD14 results in MyD88-dependent AP-1 and NFκB signalling and release of proinflammatory cytokines [21-24]. In addition, flagellated bacteria within the phylum γ-Proteobacteria and Firmicutes provide a further PAMP activating TLR5. The conserved D0 and D1 domain of flagellin forming the flagellum of those bacteria interacts with LRR9 loop of TLR5 [25]. Furthermore, intercellular delivered flagellin can activate the NLRC4 inflammasome. Upon ligand binding, nucleotide-binding oligomerization domain (NOD) like receptors (NLRs) containing N-terminal caspase activation domain (NLRC) assembles to a multiprotein complex recruiting pro-caspase-1 and resulting in caspase-mediated proteolytic cleavage of pro-IL-1β and pro-IL-18 into the active cytokines [26, 27]. As a response to intracellular pathogens, caspase-1 activation can induce pyroptosis to avoid bacterial or viral replication within the cell. In addition, NLRPs containing N-terminal pyrin domains (PYD) can form inflammasome complexes after stimulation with danger signals like ATP, microbial toxins and crystalline substances such as uric acid. The peptidoglycan components g-D-glutamyl-mesodiaminopimelic acid (iE-DAP) and muramyl dipeptide (MDP) are sensed by NOD1 and NOD2, respectively and induce secretion of proinflammatory cytokines [28, 29]. In summary, the recognition of cell wall components and flagellin by PRR induces inflammatory response of the innate immune system to eliminate invading pathogens.

2.1.3 Cytosolic nucleic acid sensing pathways

The occurrence of long dsRNAs in the cytosol is a hallmark of viral infection and replication. This kind of RNA is recognized by retinoic acid inducible gene I (RIG-I) like receptors (RLRs) such as RIG-I, melanoma differentiation antigen 5 (MDA-5) and Laboratory of

Genetics and Physiology 2 (LGP2) [12, 30]. RIG-I recognizes blunt end uncapped, 5′ di- and triphosphorylated dsRNAs and signals via two N-terminal caspase activation and recruitment (CARD) domains to activate mitochondrial antiviral-signalling protein (MAVS) [31]. Oligomerization of MAVS at the outer membrane of mitochondria allows recruitment of various downstream effectors, such as tumor necrosis factor receptor-associated factor (TRAF) 2, 5 and 6 and interferon regulatory factor (IRF)-3 and 7, leading to the rapid production of proinflammatory cytokines and type I interferons (IFNs), respectively. MDA5 downstream signalling is similar to RIG-I but activation is independent of terminal RNA structures. MDA5 molecules arrange around long dsRNA, forming long filaments which can activate MAVS [32]. Of note, LGP2 possesses no CARD domain indicating other functions than direct PAMP signalling. It is assumed that LGP2 assists MDA5 with double-stranded RNA binding and filament formation and therefore supports MDA5 but inhibits RIG-I [6, 29]. RLRs exclusively recognize RNA while recognition of cytosolic dsDNA is performed by absent in melanoma 2 (AIM2), resulting in inflammasome activation, and by the activation of cyclic GMP-AMP synthase (cGAS). Of note, cGAS acts not like other PRR with direct PAMP recognition and downstream signalling. Instead, upon binding of long dsDNA or y-formed DNA, the second messenger cyclic GMP-AMP (cGAMP) is produced [33]. cGAMP activates the endoplasmic-reticulum-resident protein stimulator of interferon genes (STING) resulting in the secretion of IFN-β and proinflammatory cytokines via IRF3 and NFκB, respectively [13]. In general, recognition of nucleic acids by the innate immune system was described as a main factor of antiviral response, but later studies could also show importance of bacterial NA recognition by the innate immune system [34-36]. In this regard, Leif Sander defined the concept of so-called vita-PAMPs: It was suggested that recognition of viable instead of dead bacteria adds a further quality (e.g. IL-12 induction) to the innate immune response. RNA was proposed as a feature that signifies viability. Due to a rapid degradation of RNA after microbial cell death the recognition of bacterial RNA by the innate immune system would indicate ongoing and present infectious danger to the host. Indeed experimental data showed that a robust innate immune response followed by adaptive antibody response was based on the recognition of bacterial mRNA thus serving as vita-PAMP [37]. Of note, isolated RNA of all kind of bacteria is sufficient to activate innate immune response [38, 39]. However, the impact of RNA recognition in the context of bacterial infections is less analysed. In contrast to a virus, different bacteria possess a variety of cell wall associated PAMPs (see section 2.1.2) which can be easily recognized by PRRs localized on the cell surface of immune cells. Nevertheless, non-redundant NA-dependant recognition of different bacteria by the immune system is

demonstrated. RNA-dependent recognition of bacteria is especially demonstrated for the Gram-positive streptococci *Streptococcus pyogenes* and *Streptococcus agalactiae* [40-42]. Furthermore, Eigenbrod *et al.* verified the TLR8-dependant recognition of *S. pyogenes* by the innate immune system [43]. However, a very recent publication of Leif Sanders working group also demonstrates a RNA-dependent recognition of Gram-negative *E. coli* when immune cells were stimulated with living or heat-killed bacteria [44]. Thus, in the following chapters described TLR8 is identified as receptor for the recognition of vita-PAMPs in humans.

2.1.4 Endosomal nucleic acid sensing pathways: Toll-like receptors

Nucleic acid recognizing TLRs are synthesized in the endoplasmic reticulum (ER), trafficked to the Golgi and shuttled to the endosome by the uncoordinated 93 homolog B1 (UNC93B1) [45]. Trafficking differs between different endosomal TLR; for instance TLR7 is shuttled directly to the endosome, whereby TLR9 traffics via the cell surface to the endosome [45]. Of note, those translocated TLRs are non-functional until they are proteolytically cleaved at their N-terminus within the acidic endolysosome [46, 47]. TLR9 is the only endosomal TLR sensing DNA motifs. It is activated by CpG dinucleotides with an unmethylated C5 of cytosine and signals in a MyD88-dependant manner to activate IRF7. Synthetic ligands are different classes of CpG desoxyoligoribonucleotide: CpG-A ODNs like ODN 2216 induce high levels of IFN-α and the maturation of plasmacytoid dendritic cells (pDCs), CpG-B ODNs (ODN 2006) activate B-cells but induce only weak secretion of IFN-α in pDCs and CpG C ODNs combine the features of previous described CpG class A and B [48-50]. ssRNA is recognized by the closely related TLR7 and TLR8. Beside viral and bacterial ssRNA, small synthetic molecules such as imidazoquinolines and nucleoside analogues activate TLR7 and 8 in a MyD88-dependent manner [43, 51]. Interestingly, TLR8 is described as non-functional in mice [52]. However, murine monocytes recognize ssRNA via the endosomal TLR13, which is not expressed in humans [36]. A unique feature of TLR13 is the recognition of a conserved sequence within the 23S ribosomal RNA of bacteria which is not present in eukaryotes [53-55]. Therefore, TLR13 is the only known TLR recognizing nucleic acids in a sequence-dependent manner. TLR3 is activated by the ribose-phosphate backbone of dsRNA longer than 40 base pairs (bp) and therefore has no specific sequence requirements. It is the only TLR signalling independent of MyD88. Upon binding of dsRNA or the synthetic analogue polyinosinic-polycytidylic acid (poly(I:C)) the adaptor molecule TIR-domain-containing adapter-inducing interferon-β (TRIF) is recruited and IRF3 mediated IFN-β secretion is facilitated [56-58]. Recently, TLR10 was described as an endosomal TLR also recognizing dsRNA. On the one

hand TLR10 seemed to sense dsRNA but on the other hand competed with TLR3 for ligand binding whereby a regulatory role of TLR10 in dsRNA-mediated IFN signalling was discussed [59].

2.1.5 Toll like receptors 7 and 8

ssRNA sensing PRRs are known to be involved in the antiviral response, but several studies demonstrated the importance of bacterial RNA recognition of the innate immune system [36]. As RNA is rapidly degraded upon microbial cell death, bacterial RNA has been suggested to function as a so-called vita-PAMP that helps the immune system to discriminate living from less harmful dead bacteria [37, 44, 60]. TLR7 and TLR8 are similar in sequence and function and are differentially expressed among various cell types. Both, TLR7 and 8 signal in a MyD88-dependent manner but TLR7 activation in plasmacytoid dendritic cells (pDCs) results in the secretion of high amounts of type I interferons whereby monocytes and macrophages predominantly produce proinflammatory cytokines like interleukin-6 (IL-6), IL-12p70 and tumor necrosis factor α (TNF-α) upon TLR8 stimulation [16, 61, 62]. Although both receptors are generally accepted to sense ssRNA, TLR7 is also discussed to recognize dsRNA [63]. Furthermore, both TLRs can be activated by small chemical imidazoquinoline components like Resiquimod (R848).

Recently, crystal structures of TLR7 and TLR8 dimers bound to their specific ligands have been published [64, 65]. Two different binding sites were identified, whereby the first binding site recognizing small chemical components seemed to be conserved among the receptors. It was localized in the dimerization interface and upon ligand binding TLR dimerization was induced. Of note, the second binding site responsible for RNA sensing differed regarding localisation and sequence specificity. In case of TLR7, the second binding site was localized in the dimerization interface and by electron density measurements a polyU 3-mer was identified to be bound. The second binding site of TLR8 was identified outside the dimerization interface and a UG or UUG oligoribonucleotide was bound. Furthermore, the first binding site of TLR7 and TLR8 was involved in RNA sensing by binding guanosine or uridine, respectively.

These results suggested that RNA needed to be partly degraded to produce single uridine nucleotides and 3-mer oligoribonucleotide residues for immune stimulatory effects. Within acidic lysosomes RNA is likely to be degraded due to hydrolytic enzymes including nucleases and phosphatases. Thus, a very recent assumption implies an endosomal ribonuclease upstream of TLR7 and TLR8 signalling processing the RNA for recognition. Nucleotide

binding to both binding sites was required to induce the m-shape formation of activated TLR7 and TLR8 dimers. Tight dimerization of the receptors upon ligand binding allows the recruitment of the adapter molecule MyD88 which contains a death domain required for the activation of downstream effectors. Downstream of TLR7 activation the transcription factor interferon regulatory factor (IRF) induces interferon stimulated response elements (ISRE) leading to the secretion of type-I interferons whereby TLR8 stimulation results in activation of NFκB and release of pro-inflammatory cytokines [6].

2.1.6 Host discrimination of self and non-self nucleic acids

In contrast to LPS or LTA, nucleic acids are not specific PAMPs of bacteria or viruses but are also present in the host. Consequently, recognition of self-RNA and self-DNA by the innate immune system, which could cause autoinflammatory disorders, must be prevented. Three main principles are described, which are supposed to minimize the risk of self-activation. One strategy is to limit the availability of host nucleic acids by the rate of degradation. Furthermore, NA sensing TLRs are localized in the endolysosome, where self-RNA and DNA has only limited access [16, 66]. However, spatial restriction of PRR and self-RNA like messenger RNA (mRNA) or transfer RNA (tRNA) within the cytosol is impossible. Therefore discrimination by sequence motifs, conformations and chemical modifications of RNA and DNA are important features for discrimination by the innate immune system. In case of DNA, degradation is crucial to avoid self-recognition. The cytosolic DNase three-prime repair exonuclease 1 (TREX1 or DNase III) impedes the accumulation of DNA derived from endogenous retroelements in the cytosol and thereby negatively regulates STING signalling [67]. In the endosome, DNase II plays a dual role in DNA recognition. On the one hand, DNAse II deficiency leads to a DNA-overload of the endolysosome resulting in self-DNA leakage to the cytosol, thus facilitating activation of cGAS and AIM2. On the other hand, processing of endosomal NA by DNase II is required for TLR9 activation by unmethylated CpG DNA [68, 69]. The principle of spatial restriction concerns all human endosomal TLRs.

Furthermore, the recognition of ssRNA by TLR7 and TLR8 is dependent on RNA sequence and modification [70, 71]. Favoured GU rich motifs are more abundant in bacterial and viral than in human RNA. An even more potent distinction of self and foreign RNA is based on chemical modifications. Incorporation of pseudouridine or base methylations has been described to decrease immune stimulation of host RNA [39]. Various studies have highlighted the importance of 2'-O-methylation of the ribose within eukaryotic tRNA and mRNA as the

most potent posttranscriptional modification impeding immune stimulation. Of note, 2'-O-methylation not only impairs TLR7 and TLR8 response but acts as an antagonist [72-74]. Cytosolic self RNA is protected from self-recognition by A to I conversion due to the enzyme adenosine deaminases acting on RNA (ADAR) [75, 76]. Furthermore, RNA formed outside the nucleus by viral replication shows a 5' triphosphate which is recognized by RIG-I [77]. Human mRNA transcribed in the nucleus is equipped with a five-prime cap (5′ cap) which abolishes the interaction with RIG-I and MDA5 [78]. 5' cap is characterized by an inverted 7-methylguanosine linked to the first transcribed nucleotide by a 5'–5' triphosphate bond and 2'-O-ribose methylation of the first (cap 1) and often the second (cap 2) nucleotide [79]. Consistent with TLR7 and TLR8 inhibition, the 2'-O-methylation within the cap structure seems to be crucial for self/non-self discrimination. Of note, this modification is not exclusively found in eukaryotes. Viruses like flaviviruses, coronaviruses and poxviruses have developed through evolutionary processes alternative 5'-elements including 2'-O-methylation avoiding recognition by the innate immune system [80]. Furthermore, several bacterial tRNA isoacceptors show 2'-O-methylation of guanosine at position 18 (Gm18). Those modified tRNAs were described to dominantly inhibit immune activation, even if otherwise stimulatory RNA is present [73]. The strategy of viruses as well as bacteria to modify their RNA in a manner avoiding immune recognition is heavily discussed as immune evasion mechanism [72, 81].

2.1.7 RNA modifications

Host and microbial RNA differ in kind and extent of posttranscriptional modifications. These differences in the modification profile allow the immune system to discriminate between self and nonself [39]. Karikó *et al.* demonstrated differences in immune stimulatory potential of different RNA species dependent on their evolutionary origin. Of note, bacterial total RNA potently activated innate immune cells, but not human total RNA. Furthermore, they observed a negative correlation of extent of modifications and immune stimulatory potential of RNA [39]. Of note, more than 150 different naturally occurring RNA modifications have been identified. Eukaryotic RNA in general is modified in higher frequency than prokaryotic RNA and types of modifications can be more complex. In human ribosomal RNAs (rRNAs) more than 210 modification sites including ribose 2'-O-methylation, pseudouridines, and base methylations are known. In relation to the size, tRNAs are the most frequent modified RNA species with an average of 13 modifications per molecule. The most frequent NA modifications consist of simple ribose or base methylations like Gm and Cm or m^5C and m^6A and base thiolation such

as s^2C, s^2U and s^4U. Further modifications are base isomerization, base reduction or deamination in case of pseudouridine (Ψ), dihydrouridine (D) or inosine (I), respectively [82, 83]. For more complex modifications, multiple base and/or ribose modifications can be introduced by different enzymes. Hypermodified nucleobases are usually found at position 34 and 37 of tRNAs. In general, the tRNA modification profile depends on nucleotide sequence and origin, whereby tRNAs from simple organisms such as bacteria and mitochondria are less modified compared to eukaryotic tRNA. Of note, some modifications such as 2'-O-methylation, Ψ, m^1G, t^6A and m^1A can occur in all kinds of tRNAs independent of their origin. tRNA modifications are posttranscriptionally introduced and each modification depends on a specific enzyme. Most enzymes are site and/or sequence specific and therefore chemically identical modifications at different positions within tRNAs require different enzymes (Fig. 2–1) [84, 85]. One example for diversity of enzymes is the bacterial methyltransferase trmH. It is responsible for the methylation of a conserved guanosine at position 18 (Gm18) in the D-loop of tRNAs. Based on their substrate specificity, trmH enzymes can be divided into two classes. Type I trmH expressed by *Thermus thermophiles* modifies all tRNA species at G18, whereas type II trmH found for example in *Escherichia coli* (*E. coli*)can modify only a subset of tRNA species. Homologues of trmH are described in lower as well as higher eukaryotes. In *Saccharomyces cerevisiae* (*S. cerevisiae*) the methyltransferase is called trm3 and in humans it is named TARBP1 [84, 86-89].

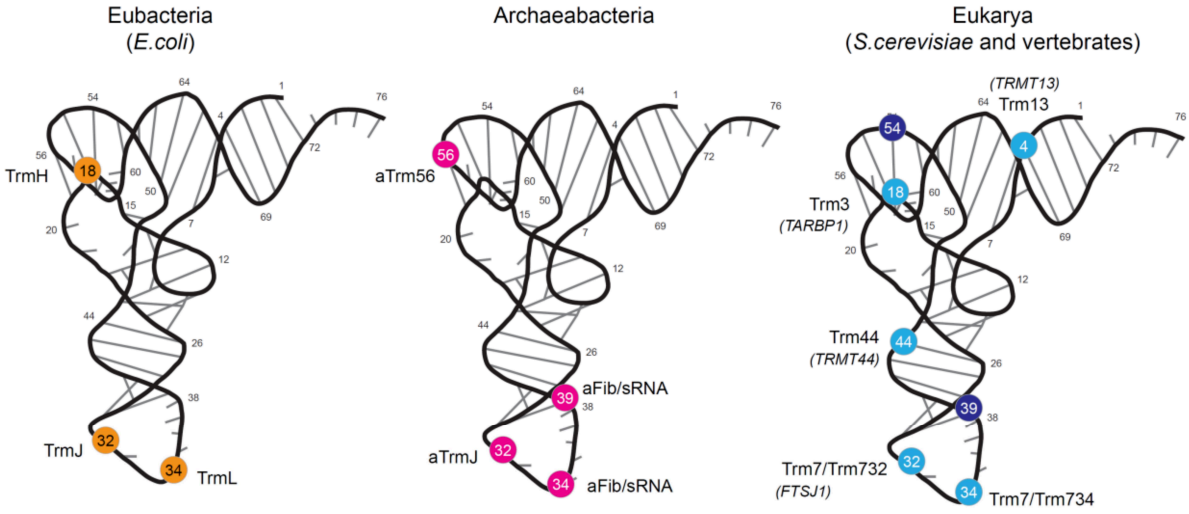

Fig. 2–1 Characterized positions of tRNA 2'-O-methylations and corresponding enzymes. tRNAs of Eubacteria (*E. coli/Bacillus subtilis*), Archaea (data almost exclusively from *H. volcanii*) and Eukarya (*S. cerevisiae* and various vertebrates) displayed in folded 3D structures. Highlighted 2'-O-methylated nucleotides: orange for Eubacteria, pink for Archaea, light blue colour corresponds to yeast modifications; additional known vertebrate positions are shown in dark blue. Homologous human protein names are written in italics. Figure adapted from Marchand *et al.* 2016.

Methylation of G18 is described to stabilize the L-shaped three-dimensional structure of tRNA. For instance, thermophilic bacteria tend to exhibit more excessively modified tRNA compared to bacteria growing at lower temperatures [90]. Furthermore, 2'-O-methylation within different types of RNAs is known to inhibit TLR7 and TLR8 response in human pDCs and monocytes, respectively. A single 2'-O-methylation at position 18 within certain tRNAs of *E. coli* is described to act as an antagonist for TLR7 and 8 [66, 70, 71, 91]. Hamm *et al.* demonstrated that 2'-O-methylated RNA binds with higher affinity to TLR7 compared to unmodified control. The competitive binding of modified and unmodified RNA and the much stronger interaction of 2'-O-methylated RNA and TLR7 might explain the dominant inhibitory potential of ribose methylated RNA [92]. A subsequent study identified a [DmR] motif (D= all but C; R= purine) as fundamental requirement to avoid TLR7 stimulation by 2'-O-methylation [93]. Besides pseudouridine, ribose methylation is one of the most abundant modifications within eukaryotic ribosomal RNA. Around fifty or rather one hundred 2′-O-methylation sites within yeast or human rRNA are described [94, 95]. These ribose methylations in rRNA are introduced by fibrillarin or nuclear protein 1 (NOP1) in humans or yeast, respectively. NOP1 is described to be crucial for cell viability and among other diverse functions, fibrillarin is involved in early processing and modification of pre-rRNA, ribosome assembly and cell growth [96, 97]. 2'-O-methylation of rRNA is promoting ribosomal structures and seems to be essential for stability and function [98]. In particular, diversity of functions renders RNA modifications to an essential feature of immune modulation, RNA stabilization and cell viability.

2.2 Genome editing

The complete sequencing of the human genome [99] facilitates new opportunities to study the function of various genes and encoded proteins. For long times, genes were knocked out randomly by using chemicals, radiation or virus integration within different organisms [100]. Due to the identifications of human gene sequences in combination with shortly after published RNA interference (RNAi), a tool for targeted specific gene knockdown became available [101]. The use of short interfering RNA (siRNA) or short hairpin RNA (shRNA) induces sequence specific degradation of mRNA by activation of the RNA-induced silencing complex (RISC). Of note, knock-down efficiencies of 100% are hardly possible and a complete loss-of-function situation cannot be mirrored [102]. To examine a target specific knock-out situation in a cell or organism, so called genome editing tools are necessary. The

first site-specific disruption of a gene succeeded by the usage of zinc-finger nucleases (ZFNs) [103]. Engineered DNA-binding domains (DBD) recognizing specific target sequences of sense and antisense strand of DNA were fused with the restriction enzyme FokI. Upon DNA-binding of both DBD, FokI domains form a dimer and initiate nuclease activity resulting in double strand breaks (DSB) near the binding sites [104, 105]. Transcription activator-like effector nucleases (TALENs) act in a similar manner. Programmed DBDs contain highly homologous repeats of 33-35 amino acids which are recognizing DNA regions of 15-20 bp. Similar to ZFNs, pairs of DBDs are fused to nucleases and direct the restriction enzymes to genomic target sites to induce DSB [106]. Subsequently, two different DNA repair mechanisms could be activated: the highly accurate homology-directed repair (HDR) and the more error-prone non-homologous end joining (NHEJ). The more frequently induced NHEJ results in insertions or deletions (indels) in the DNA target-site resulting in frame shift mutations [107]. However, as TALENs and ZFNs are based on protein-DNA interaction, knock-out of new target genes requires time-consuming engineering and cloning of new pairs of proteins [100, 108]. Recently, the new and more powerful genome editing tool clustered regularly interspaced short palindromic repeats (CRISPR)-associated protein 9 (Cas9) was identified [109, 110]. The CRISPR/Cas9 system exhibits fundamental differences compared to TALENs and ZFNs: i) Cas9 endonuclease is RNA guided and sequence specificity results from Watson-Crick base pairing ii) Cas9 provides intrinsic nuclease activity iii) the same Cas9 can be combined with various guide RNAs (gRNAs) to easily target a broad range of genes and no protein engineering is necessary. Due to the ability to cut DNA in a sequence specific manner, the CRISPR/Cas9 system is also termed “molecular scissors” and meanwhile it is the most widely used genome editing tool [108, 111].

2.2.1 CRISPR/Cas9-System

Surprisingly, many bacteria and archaea possess a pathogen specific adaptive immune system. It is based on the acquisition of foreign phage or plasmid associated DNA fragments to the genome to rapidly recognize and degrade foreign NA in case of reinfection [112]. Those fragments are incorporated into the host CRISPR locus as so called protospacers and upon a second infection CRISPR RNAs (crRNAs) are transcribed to guide Cas9 dependant DNA cleavage. Processed crRNAs are combined with noncoding *trans*-activating CRISPR RNA (tracrRNA) to create a mature guide RNA (gRNA). Of note, for genome editing tools crRNA and tracrRNA can be fused to a single chimeric sgRNA which interacts with Cas9 [108, 110]. The most widely used CRISPR/Cas9 system to create gene knock-in or knock-out originates from

Streptococcus pyogenes. To activate Cas9-gRNA complex in the target cell a protospacer adjacent motif (PAM) immediately 3' of the target sequence is required [113]. *Streptococcus pyogenes* derived Cas9 requires the PAM sequence NGG. Cas9 endonuclease activity results from the two nuclease domains HNH nuclease domain and RuvC-like nuclease domain. Upon double strand brakes (DSBs), the most commonly induced DNA repair mechanism is the non-homologous end joining (NHEJ) pathway which can induce insertions or deletions by re-ligation of open DNA ends using DNA ligase IV. The more accurate homology directed repair (HDR) mechanism, however, requires a DNA molecule as repair template. In case of the CRISPR/CAS9 genome editing tool an artificial DNA template, mimicking the sister chromatid, is co-transfected to target cells. Within HDR mediated gene conversion the template's homology regions are integrated into the target sequence, enabling the introduction of precise mutations such as insertion of reporter genes or a codon replacement [114, 115]. In the meantime, different expression systems are available to achieve best possible efficiency. The simplest variant for easy-to-transfect cell types like HEK293 cells are plasmids encoding for Cas9 and a gRNA scaffold and the usage of standard transfection reagents. Lentiviral and adeno-associated virus (AAV) transduction can be used for *in vivo* applications and are common methods to express CRISPR/Cas9 machinery in primary cells. Plasmid based expression systems often comprise a reporter gene like GFP to preselect transfected cells. Microinjection or electroporation of *in vitro* transcribed Cas9 mRNA and gRNA is one method to generate genetically modified embryos, or Cas9-gRNA complex consisting of Cas9 protein and *in vitro* transcribed gRNA can be delivered into cells using cationic lipids. Transient RNA or protein based CRISPR/Cas9 systems may decrease off-target effects due to limited Cas9 activity [115-117]. The choice of an appropriate CRISPR/Cas9 system depends on the cell type or organism and the underlying question which demands for a gene knock-in or knock-out.

2.3 Objectives of this study

Eukaryotic as well as prokaryotic posttranscriptional RNA modifications can alter the immune stimulatory potential of various RNA species. Yet, important aspects remain poorly understood. Of note, more than 150 different posttranscriptional RNA modifications have been identified, but so far, only 2'-O-methylation was described as a natural immune inhibitory modification. It is thus conceivable that post-transcriptional modifications other than 2'-O-methylation can alter innate immune responses towards RNA. Furthermore, the sequence-context of 2'-O-methylation within tRNAs (Gm18) seems to play a major role in antagonizing immune response but a specific sequence motif remains to be further characterized. Moreover, the dominant inhibitory effect of Gm18 within bacterial tRNAs was only shown for isolated isoacceptors or total tRNA preparations but the impact on the stimulatory potential of total RNA preparations or whole microbial organisms remains unclear. The physiological relevance of RNA modifications within their natural context for self/non-self discrimination or as a potential immune escape mechanism has not yet been investigated. To answer those upcoming questions three work-packages were defined:

(i) To uncover immune inhibitory modifications other than Gm18, human $tRNA^{Lys}_3$ which is lacking 2'-O-methylation but has previously been demonstrated not to induce immune activation should be studied in detail.

(ii) To characterize the optimal sequence-context of 2'-O-methylation that is necessary and sufficient to inhibit TLR7 and TLR8 activation, permutations studies using artificial oligoribonucleotides should be performed.

(iii) To elucidate a redundant or non-redundant role of tRNA 2'-O-methylation for immune activation, the stimulatory potential of total RNA preparations derived from prokaryotic or eukaryotic sources and whole microbial organisms employing Gm18-methyltransferase deficient mutants should be examined.

3 MATERIALS AND METHODS

3.1 Materials

3.1.1 Devices and Instruments

Table 3-1: List of instruments used in the study

Device	Type & Manufacturer
AutoMACS™	Miltenyi Biotec, Bergisch-Gladbach
Balance	EW600-2M, Kern & Sohn GmbH, Balingen
Bioanalyzer	Agilent Technologies GmbH, Berlin
Blotting chamber	Biometra, Jena
Centrifuges	Multi 3 SR, Heraeus Instruments, Hanau
	Multi 3 SR+
	Sigma 2K15, B. Braun, Melsungen
Confocal microscope	Leica TCS SP5, Leica Microsystems, Mannheim
Counting chamber	Neubauer 0.00025mm2/0.1 mm/ Brand GmbH, Schwerin
Electrophoresis chamber	Perfect Blue Mini S, Peqlab, VWR, Radnor, Pennsylvania, USA
	Perfect Blue Mini M, Peqlab, VWR, Radnor, Pennsylvania, USA
ELISA reader	Sunrise/ Tecan, Crailsheim
Fine scale	MC1 Research RC 210 P, Wiegetechnik Knoll, Ketsch
Flow cytometer	BD FACSCanto™, BD Biosciences, San Diego, USA
	BD FACSMelody™, BD Biosciences, San Diego, USA
Gel Documentation-System	CN-3000.WL, Peqlab, VWR, Radnor, Pennsylvania, USA
Heat block	AccuBlock, digital dry bath, Eppendorf, Hamburg
Incubators	BBD6220i/ Heraeus Instruments, Hanau
Microscope	Leica DMLS, Leica Microsystems GmbH, Wetzlar
MidiMACS™ Separator	Miltenyi Biotec, Bergisch-Gladbach
McFarland bioMérieux DensiCHECK Plus	bioMérieux, Marcy-l'Étoile, France

Orbital Shaker	Mini Rocker MR-1, Peqlab, Radnor, Pennsylvania, USA Heidolph 1010/ Hilab, Karlsruhe
pH-Meter	Seven Easy, Mettler Toledo, Gießen
Power supply	Power Pac HC, BioRad, München Consort E835/ Sigma-Aldrich, Steinheim
qPCR cycler	StepOne Plus, Applied Biosystems, Darmstadt
SDS-PAGE system	perfectBlue™ Twi S, Peqlab, VWR, Radnor, Pennsylvania,
Spectrophotometer	NanoDrop®ND-1000, Peqlab, VWR, Radnor, Pennsylvania,
Sterile bench	Hera Safe KS 12, Heraeus Instruments, Hanau
Thermocycler	Primus 25 advanced®, Peqlab, VWR, Radnor, Pennsylvania, USA Primus 96 advanced® gradient, Peqlab, VWR, Radnor, Pennsylvania, USA
Typhoon scanner	GE Healthcare, Solingen, Germany
UV platform	ECX-26M, Peqlab, Radnor, Pennsylvania, USA
Vortexer	Heidolph Reax 2000/ Hilab, Karlsruhe
Water bath	Temp, Julabo Labortechnik GmbH, Seelbach

3.1.2 Software

Table 3-2: List of software used in this study

Sofware	Description & Version
Bio-Capt	Gel visualisation, Vilber Lourmat GmbH
FACSDiva	BD Bioscience, San Diego
GraphPad Prism	Version 6.05, GraphPad Software, Inc. San Diego, USA
ImageJ	1.46r developed at the National Institutes of Health, USA
Inkscape	0.92.0 r15299, licensed GPLv2
LAS AF	2.6.0.7266, Leica Microsystems, Solms
Magellan V	Tecan, Grödig, Austria
NanoDrop	3.0.1, Nanodrop Technologies, Rockland, USA
R software	Version 3.3.0, Package drc (Team 2013; Ritz *et al.*2015)

3.1.3 Consumables

Table 3-3: List of consumables used in this study

Consumable	Manufacturer
Blotting membrane	Immobilon-P Transfer, Millipore, Billerica, USA
Blotting paper	Whatman GB003, Whatman GmbH, Dassel
Cannula	22G, 27G or 29G, BD Biosciences, Heidelberg
Cell culture flasks	Cellstar, 25cm^2 /75 cm^2 /175 cm^2 Greiner Bio-One GmbH, Frickenhausen
Cell culture plates	6- /12- /24- /96-well plates, Cellstar, Greiner Bio-One
Culture plates for microscopy	glass bottom dish (35 mm), Ibidi GmbH, Martinsried
Cell scraper	Greiner Bio-One GmbH, Frickenhausen
ELISA plates	96-well, half area, Greiner Bio-One GmbH, Frickenhausen
Eppendorf tubes	0.5 ml, 1.5 ml, 2 ml, Eppendorf AG, Hamburg
FACS tubes	BD Falcon^{TM} 5 ml, BD Biosciences, Heidelberg
Falcon tubes	15 ml, 50 ml, Greiner Bio-One, Frickenhausen
Nanosep MF, Bio-Inert Membrane, purple, 0,45 µm	Pall Laboratory, Dreieich
LD columns	Miltenyi Biotec, Bergisch-Gladbach
Pipette tips	Hinged Rack Pipette tips, Corning, New York, USA
qPCR plates	MicroAmp, Fast 96-well reaction plate (0.1 ml), AppliedBiosystems, UK
Scalpel	Feather disposable scalpel, Feather Safety Razor, Osaka, Japan
Syringe	BD Discardit II, 2 ml, 5 ml 10 ml; BD Bioscience, Heidelberg

3.1.4 Chemicals and reagents

Table 3-4: List of chemicals and reagents used in the study

Chemical/ Reagent	Manufacturer
Acrylamide stock solution	Carl Roth GmbH, Karlsruhe
Agarose	Eurobio, Courtaboeuf, France
Ammonium acetate	J.B. Baker, Deventer, Netherlands
Ammonium persulphate (APS)	Sigma-Aldrich, Taufkirchen
Ampicillin	Sigma-Aldrich, Taufkirchen
Antibiotic-Antimycotic 100x	Invitrogen, Karlsruhe, Germany
Aqua ad injectabilia	B. Braun, Melsungen
BbsI #R3539	New England Biolabs (NEB), Ipswich, USA
β- Estradiol	Sigma-Aldrich, Steinheim
β-Mercaptoethanol	Sigma-Aldrich, Steinheim
Boric acid	Bernd Kraft, Duisburg
Bovine serum albumin (BSA)	Sigma-Aldrich, Taufkirchen
Bromphenol blue	Sigma-Aldrich, Steinheim
Chloroform: Isoamylalkohol	AppliChem, Darmstadt
Dulbecco's Modifed Eagle Medium (DMEM)	Biochrom AG, Berlin
EDTA	AppliChem GmbH, Darmstadt
Ethanol, undenatured	Riedel-de Haën AG, Seelze
Diethyl pyrocarbonate (DEPC)	Sigma-Aldrich, Steinheim
DOTAP	Carl Roth GmbH, Karlsruhe
Eukitt mounting medium	Sigma-Aldrich, Taufkirchen
FACSClean™	BD Bioscience, Heidelberg
FACSFlow™	BD Bioscience, Heidelberg

FastRuler™ Ultra Low Range DNA Ladder	Ambion, life technologies, Darmstadt
Fetal calf serum (FCS)	Gibco™, Invitrogen, Karlsruhe
Formamid	AppliChem GmbH, Darmstadt
Q5 High-Fidelity DNA Polymerase #M0491S	New England Biolabs (NEB), Ipswich, USA
Geneticin (G418)	Carl Roth GmbH, Karlsruhe
Glucose	Sigma-Aldrich, Steinheim
Glycin	VWR, Radnor, Pennsylvania, USA
Heparin	Ratiopharm, Ulm
Hoechst 34580 (Trihydrochloride salt)	Sigma Aldrich, Taufkirchen
IL-3	PeproTech, Rocky Hill, USA
Isopropanol	Riedel-de Haën AG, Seelze
Kanamycin	AppliChem GmbH, Darmstadt
5x Ligase Reaction Buffer	Life Technologies, Darmstadt
Lipofectamine	Life Technologies, Darmstadt
Luria-Bertani (LB) Broth	AppliChem GmbH, Darmstadt
Lysozyme	Sigma-Aldrich, Taufkirchen
Lyticase	Sigma-Aldrich, Taufkirchen
M-CSF	PeproTech, Rocky Hill, USA
Methanol	Riedel-de Haën AG, Seelze
10x NEB buffer	New England Biolabs (NEB), Ipswich, USA
NEB2 buffer	New England Biolabs (NEB), Ipswich, USA
N',N',N',N'- tetra-methylethylenediamine (TEMED)	Sigma-Aldrich, Taufkirchen
Opti-MEM Reduced Serum Media	Life Technologies, Darmstadt
Pancoll human	PAN™ Biotech, Aidenbach
Paraformaldehyde (PFA)	Merck, Darmstadt

Penicillin/Streptomyin (100x)	Sigma-Aldrich, Taufkirchen
Penicillin/Streptomycin solution (P/S)	PAA Laboratories, Pasching, Austria
Peptone	Sigma-Aldrich, Steinheim
peqGREEN	Peqlab, VWR, Radnor, Pennsylvania, USA
Poly-D-lysine hydrobromide	Sigma-Aldrich, Steinheim
Q5® High-Fidelity DNA Polymerase	New England Biolabs (NEB), Ipswich, USA
RiboRuler high range RNA ladder, 2x RNA loading dye	Life Technologies, Darmstadt
Roti®-Mount FluorCare DAPI	Carl Roth GmbH, Karlsruhe
Rotiphorese sequence gel system and sequence concentrate	Carl Roth GmbH, Karlsruhe
RPMI 1640 Medium (1x)	Biochrome AG, Berlin
SDS	AppliChem GmbH, Darmstadt
SOC medium	New England Biolabs (NEB), Ipswich, USA
Sodium carbonate	Sigma-Aldrich, Steinheim
Sodium chloride	Sigma-Aldrich, Steinheim
Sorbitol	Sigma-Aldrich, Steinheim
SYBR Green PCR Master Mix Fast	Applied Biosystems, Foster City, USA
SYBR Gold Nucleic Acid Gel Stain	Life Technologies, Darmstadt
T4 DNA Ligase #EL0014	Life Technologies, Darmstadt
Tetramethylethylenediamine (TEMED)	AppliChem GmbH, Darmstadt
Triton X-100	Merck, Darmstadt

TRIS	AppliChem GmbH, Darmstadt
TRIS/HCl	AppliChem GmbH, Darmstadt
TRIzol® Reagent	Life Technologies, Darmstadt
Trypan blue	Sigma-Aldrich, Taufkirchen
Tween 20	Sigma-Aldrich, Taufkirchen
Yeast extract	AppliChem, Darmstadt

3.1.5 Buffers and Solutions

Table 3-5: List of Buffers and solutions used for western blot

Buffer	Ingredients
Acrylamide stock solution	30% (v/v) acrylamide and bisacrylamid solved 29:1
Blocking Buffer	1 x TBS; 0.1% (v/v) Tween 20; 5% (w/v) BSA
Enhanced chemilumi-nescence (ECL) substrate	PerkinElmer, Rodgau
SDS blot buffer	25 mM TRIS-OH (pH 8.3); 192 mM glycin; 10% (v/v) methanol
SDS-PAGE Running buffer	25 mM TRIS-OH (pH 8.3); 192 mM glycin; 0.1% (w/v) SDS
SDS sample buffer (4x)	200 mM TRIS-HCl (pH 6.8); 20% (v/v) β-mercaptoethanol; 8% (w/v) SDS; 40% (v/v) glycerol; 0.04% (w/v) bromphenol blue
Separating gel buffer (3x)	1.5 M TRIS-HCl (pH 8.8); 0.4% (w/v) SDS
Stacking gel buffer (2x)	1 M TRIS-HCl (pH 6.8); 0.8% (w/v) SDS
10 x TBS	100 mM TRIS-HCl (pH 8.0); 1.5 M NaCl
Wash Buffer (TBST)	1 x TBS; 0.1% (v/v) Tween 20

Table 3-6: Buffers and solutions used for ELISA

Buffer	Ingredients
ELISA blocking buffer (IFNα)	1 x PBS; 0.5% (w/v) BSA; 0.05% (v/v) Tween 20
ELISA blocking buffer (IL-6, TNF-α)	1 x PBS; 10% (v/v) FCS

ELISA coating buffer	0.1 M sodiumcarbonate: 8.4 g $NaHCO_3$, 3.6 g Na_2CO_3; adjust to pH 9.5; ad 1000 ml H_2O
ELISA washing buffer	1x PBS; 0.05% (v/v) Tween 20
10x PBS	80 mM di-sodiumhydrogenphosphate; 20 mM sodium di-hydrogenphosphate; 1.4 M NaCl; pH 7.4

Table 3-7: Buffers and solutions used for nucleic acid preparation

Buffer	Ingredients
TRIS Buffer	121 g TRIS (1 M); ad 1000 ml DEPC-H_2O; pH 7,5
DEPC water	1 ml DEPC ad 1000 ml H_2O; autoclaved before use
10x TBE	108 g TRIS; 55 g Boric acid; 40 ml 0,5 M Na_2EDTA; ad 1 l DEPC-H_2O
50x TAE	60,5 g TRIS; 14,25 ml acetic acid, 25 ml 0,5 M EDTA (pH 8); 250 ml DEPC-H_2O
PAGE RNA loading dye	90% formamid + 10% 10x TBE
Y1 Buffer	100 mM EDTA; 1 M sorbitol; 0,1% ß-mercaptoethanol; pH 7,4

Table 3-8: Media and solutions used for cell culture

Media	Supplements
DMEM Culture Medium	10% (v/v) heat-inactivated FCS; 1% (v/v) P/S
DMEM Transfection Medium	10% (v/v) heat-inactivated FCS
RPMI Culture Medium	10% (v/v) heat-inactivated FCS; 1% (v/v) P/S
RPMI Tranfection Medium	10% (v/v) heat-inactivated FCS or 2% (v/v) heat-inactivated human serum
Trypan blue solution	2 mg/ml trypan blue in 1x PBS
Trypsin solution	0.05% trypsin; 0.02% EDTA in 1x PBS

Table 3-9: Media and solutions used for microbiology, autoclaved before use

Media	Ingredients
LB medium	20 g LB broth ad 100 ml dH_2O
Y1 Buffer	1,46 g EDTA, 9,1 g Sorbitol ad 50 ml dH_2O
YPD medium	20 g peptone; 10 g yeast extract; ad 975 ml dH_2O; pH 6,5

3.1.6 Kits

Table 3-10: List of commercial kits used for the study

Kit	Manufacturer
BD OptEIA™ human IL-6 ELISA set	BD Biosciences, Heidelberg
BD OptEIA™ human TNF-α ELISA set	BD Biosciences, Heidelberg
CD19 MicroBeads, human	Miltenyi Biotec, Bergisch-Gladbach
DNeasy Blood & Tissue Kit	Qiagen, Hilden
ExtractMe total RNA Kit	BLIRT S.A., Gdansk, Poland
Fast SYBR green master mix	Applied Biosystems, Darmstadt
QIAquick Gel Extraction Kit	Qiagen, Hilden
High capacity cDNA reverse transcription Kit	AppliedBiosystems, Darmstadt
Monarch® PCR & DNA Cleanup Kit	New England Biolabs (NEB), Ipswich, USA
Human pDC Isolation Kit II	Miltenyi Biotec, Bergisch-Gladbach
PureLink™ HiPure Plasmid Filter Maxiprep	Life Technologies, Darmstadt
IFN-α ELISA Kit human	eBioscience, Frankfurt

CellTiter 96 Aqueous One solution proliferation Kit (MTS)	Promega, Madison, USA
NucleoBond® RNA/DNA 80/400	Macherey-Nagel, Düren
RNeasy Total RNA Kit	Qiagen, Hilden

3.1.7 Primers and guide RNAs

Table 3-11: List of primers used for this study

Target	Forward (5' – 3')	Reverse (5' – 3')
hIFN-α	AACTCTACCAGCAGCTGAATGAC	CATGATTTCTGCTCTGACAACC
hIFN-β	ATGACCAACAAGTGTCTCCTCC	GGAATCCAAGCAAGTTGTAGCTC
hIL-6	GGATTCAATGAGGAGACTTGC	GTTGGCTCAGGGGTGGTTAT
hGAPDH	ACGGATTTGGTCGTATTGGGC	TTGACGGTGCCATGGAATTTG
hTARBP1	ACTCCTGGCCTTACGTCTAAATC	ACGGCTGCTAGCACTTCCAC
hTNF- α	GCCCAGGCAGTCAGATCATCTTC	TGAGGTACAGGCCCTCTGATGG

Table 3-12: List of guide RNAs used for this study

gRNA	Forward (5' – 3')	Reverse (5' – 3')
gRNA#1	CACCGGACCCCCGGGCCCTGCTTG	AAACCAAGCAGGGCCCGGGGGTCC
gRNA#2	CACCGCTTGGGGCGCTGTGCCAAG	AAACCTTGGCACAGCGCCCCAAGC
gRNA#3	CACCGGGCGCAGGCGCGCTCCCGG	AAACCCGGGAGCGCGCCTGCGCCC
gRNA#4	CACCGCGGCGCGCGAGGTGGCTGC	AAACGCAGCCACCTCGCGCGCCGC
gRNA#5	CACCGCTCGTGCGTCCGCCTGGCC	AAACGGCCAGGCGGACGCACGAGC
gRNA#6	CACCGCTTCCTTCTGCAGCGGCTCG	AAACCGAGCCGCTGCAGAAGGAAGC
gRNA#7	CACCGGGCGCTCGGCAAATGGAGT	AAACACTCCATTTGCCGAGCGCCC
gRNA#8	CACCGCAAATGGAGTGGGTGCTCG	AAACCGAGCACCCACTCCATTTGC
gRNA#9	CACCGGAGGCATCCGCGGAGCGCG	AAACCGCGCTCCGCGGATGCCTCC
gRNA#10	CACCGGTACCTCGTGCCACTGCTG	AAACCAGCAGTGGCACGAGGTACC
gRNA#11	CACCGCGAGCAGATCGCGCAGCGC	AAACGCGCTGCGCGATCTGCTCGC
gRNA#12	CACCGCGGCGCCAGGCGCGCGCCAC	AAACGTGGCGCGCGCCTGGCGCCGC
gRNA#13	CACCGAGCACGCGCCGGCGGTGGCG	AAACCGCCACCGCCGGCGCGTGCTC

gRNA#14	CACCGCAGCCAGCGCGGCCGCCAGC	AAACGCTGGCGGCCGCGCTGGCTGC
gRNA#15	CACCGCTGCCGCGCGCCTCCTCGTC	AAACGACGAGGAGGCGCGCGGCAGC

3.1.8 Oligoribonucleotides

Table 3-13: List of oligoribonucleotides used for the study

Oligoribonucleotide	Sequence 5' – 3' *
Unmodified 26-mer	GU GGG GUU CCC GAG CGG CCA AAG GGA
2'-O-Me 26-mer Pos.17	GU GGG GUU CCC GAG XGmG CCA AAG GGA
2'-O-Me 26-mer Pos.18	GU GGG GUU CCC GAG CXmG CCA AAG GGA
2'-O-Me 26-mer Pos.19	GU GGG GUU CCC GAG CGmX CCA AAG GGA
2'-O-Me 26-mer Pos.20	GU GGG GUU CCC GAG CGmG XCA AAG GGA
2'-O-Me 15-mer	CCC GAG CGmG CCA AAG
2'-O-Me 9-mer	GAG CGmG CCA
2'-O-Me 7-mer	AGC GmGC C
2'-O-Me 5-mer	G CGmG C
2'-O-Me 9-mer Pos.1	GmG CCA AAGG
2'-O-Me 9-mer Pos.2	CGmG CCA AAG
2'-O-Me 9-mer Pos.3	G CGmG CCA AA
2'-O-Me 9-mer Pos.4	AG CGmG CCA A
2'-O-Me 9-mer Pos.5	GAG CGmG CCA
2'-O-Me 9-mer Pos.6	C GAG CGmG CC
2'-O-Me 9-mer Pos.7	CC GAG CGmG C
2'-O-Me 9-mer Pos.8	CCC GAG CGmG
2'-O-Me 9-mer Pos.9	U CCC GAG CGm
5' Atto 549 ssRNA 40	GCC CGU CUG UUG UGU GAC UC
5' Atto 488 Gm18	GU GGG GUU CCC GAG CGmG CCA AAG GGA
MH662	GCA AGC UGA CCC UGA AGU UC**X** U [#]
MH662-Gm8	GCA AGC UGmA CCC UGA AGU UCC U
ssRNA 40	GCC CGU CUG UUG UGU GAC UC

* highlighted in grey: permutated nucleobase; [#] **X** = C8-alkyne-dtCE phosphoramidite (Glen-Research)

3.1.9 Antibodies

Table 3-14: list of anti- human (except otherwise specified) antibodies used for the study.

Antigen	Species/ Labeling	Application	Manufacturer
β-actin	Rabbit	Western blot	GeneTex, Hsinchu City, Taiwan
CD 19	APC	Flow cytometry	BD Bioscience, Franklin Lakes, USA
CD 86	PE	Flow cytometry	Cell Signaling Tech., Danvers, USA
MHC II (HLA-DR)	APC	Flow cytometry	BioLegend Inc, San Diego, USA
Anti-Rabbit IgG	HRP-conjugated	Western blot	Cell Signaling Tech., Danvers, USA
TARBP1	Rabbit	Western blot	Abcam, Cambridge, United Kingdom

3.1.10 Vectors

Table 3-15: List of vectors used for the study

Vector	Description
#1451 Cas9 plasmid	pSSV 9; short CMV; Shalem; Cas; #49535 Addgene kindly provided by AG Grimm, Heidelberg
#1529 gRNA Scaffold	pBSU6 BbsI (x2) F+E scaffold RSV-GFP kindly provided by AG Grimm, Heidelberg

3.1.11 Stimuli

Table 3-16: List of stimuli used for the study

Stimulus	Final concentration	Manufacturer
Cl264	1 µg/ml	InvivoGen, San Diego, USA
CpG-ODN 2006	1 µM	InvivoGen, San Diego, USA
CpG-ODN 2216	1 µM	InvivoGen, San Diego, USA

Gardiquimod (GQI)	as indicated	Provided by Helm Group, Johannes Gutenberg-University of Mainz
Gardiquimod-di-ethylene- glycol-azide (GDA)	as indicated	Provided by Helm Group, Johannes Gutenberg-University of Mainz
Resiquimod (R848)	Unless otherwise stated: 1 µg/ml	InvivoGen, San Diego, USA
Resiquimod- poly-ethylene- glycol- azide (RPA)	as indicated	Provided by Helm Group, Johannes Gutenberg-University of Mainz
Lipopolysaccharide (LPS) *Salmonella minnesota* (smooth form)	0.1 µg/ml	Provided by U. Seydel (Bortsel)
TL8-506	0.1 µg/ml	InvivoGen, San Diego, USA

3.1.12 Organisms

Cell lines

Table 3-17 List of cell lines used for the study

Cell line	Description
A549	Human alveolar cell line (AG Dalpke)
BlaER1 wt and TLR8 KO	B cell line derived from Burkitt lymphoma cell line Seraphina expressing transcription factor C/EBPa upon 17-β-estradiol addition.* All BlaER1 cells were kindly provided by Prof. Dr. Holger Heine, Research Center Borstel
Beas-2B	Human bronchial epithelial cell line (AG Dalpke)
HEK293	Human embryonic kidney cell line (AG Dalpke)
THP-1	Tohoku Hospital Pediatrics 1, acute monocytic leukaemia cell line (AG Dalpke)

* B-cell like BlaER1 cells can be transdifferentiated to monocyte/macrophage-like cells (see section 3.2.1.2)

Table 3-18: Culture conditions of cell lines used for the study

Cell line	Growth	Culture Media
A549	adherent	DMEM,10% (v/v) heat-inactivated FCS; 1% (v/v) P/S
BlaER1	suspension	RPMI,10% (v/v) heat-inactivated FCS; 1% (v/v) P/S
Beas-2B	adherent	RPMI,10% (v/v) heat-inactivated FCS; 1% (v/v) P/S
HEK293	adherent	DMEM,10% (v/v) heat-inactivated FCS; 1% (v/v) P/S
THP-1	suspension	RPMI,10% (v/v) heat-inactivated FCS; 1% (v/v) P/S

Bacteria and yeas strains

Unless otherwise stated, *E. coli* and *S. cerevisiae* where purchased from *E. coli* Genetic Stock Center CGSC, Yale University and Euroscarf, Johann Wolfgang Goethe-University Frankfurt, respectively.

Table 3-19: Microorganism used for the study

Strain	Genotype	Culture Media
Staphylococcus aureus	ATCC 25923	LB-medium
E. coli parental strain BW25113	Δ(araD-araB)567, ΔlacZ4787 (::rrnB-3); λ-, rph-l, Δ(rhaD-rhaB)568, hsdR514	LB-medium
E. coli ΔtrmH JW3626-1	Δ(araD-araB)567, ΔlacZ4787 (::rrnB-3); λ-, rph-l, ΔtrmH 755::kan, Δ(rhaD-rhaB)568, hsdR514	LB-medium supplemented with Kanamycin (50 µg/ml)
competent *E. coli*	NEB 5-alpha New England Biolabs (NEB), Ipswich, USA	LB-medium
S. cerevisiae parental strain Y00000	MATa; his3Δ1; leu2Δ0; met15Δ0; ura3Δ0	YPD-Medium
S. cerevisiae Δtrm3 Y03809	BY4741; MATa; his3Δ1; leu2Δ0; met15Δ0; ura3Δ0; YDL112w::kanMX4	YPD-Medium supplemented with G418 (Geneticin) (200 µg/ml)

3.2 Methods

3.2.1 Cell culture

3.2.1.1 Cell lines

Cell lines (Table 3-17) were cultured in 15 ml growth media as indicated in Table 3-18 in T-flasks (75 cm^2) at 37°C, 5% CO_2 and 95% humidity in an incubator. Cells were split twice a week at an approximate confluence of 80-90%. Adherent cells were washed with PBS and passaged 1:10 or 1:20 using trypsin solution. Suspension cells were centrifuged for 5 min at 1,300 rpm and passaged 1:10 or 1:20 in fresh media.

3.2.1.2 BlaER1 trans-differentiation and purification.

B-cell like BlaER1 cells were trans-differentiated into monocyte/macrophage-like cells prior stimulation experiments. Therefore, BlaER1 cells were harvested and 1 million cells/well of a 6-well plate were centrifuged for 10 min at 1,300 rpm in a 50 ml Falcon tube. The supernatant was discarded and the cell pellet was resuspended in 3 ml/well RPMI medium supplemented with 10% FCS, 1% Pen/Strep, 10 ng/ml IL-3, 10 ng/ml M-CSF and 150 nM b-Estradiol. Plates were incubated at 37 °C and 5% CO_2. At day 2 and 5 the cells were harvested by pipetting up and down and cells of one genotype were collected in one Falcon tube and centrifuged at 1,300 rpm for 10 min. To the remaining cells in the 6-well plate, 2 ml of fresh medium was added and after centrifugation the cell pellet was resuspended in 1 ml media per collected well. 1 ml of the cell suspension was transferred into the 6-well plate and cells were incubated at 37 °C and 5% CO_2. After one week, residual B-cells like BlaEr1 cells were sorted using AutoMACS magnetic cell sorter system. The trans-differentiated BlaER1 cells were harvested and cells of one genotype were collected in a 50 ml Falcon tube. Double the amount of cells needed for stimulation experiments were centrifuged for 10 min at 1,300 rpm. CD19 negative, trans-differentiated monocyte/macrophage like BlaER1 cells were sorted by using CD19 MicroBeads, human kit according to manufacturer's instructions. CD19 negative fraction was collected and cells were centrifuged at 1,300 rpm for 10 min. Cells were resuspended in RPMI supplemented with 10% FCS and 2 x 10^5 cells in 250 µl medium were transferred into a 48-well plate. To avoid pre-activation of BlaER1 cells due to MACS sorting, cells were rested for 20 h at 37 °C, 5% CO_2. For microarray analysis technical duplicates were performed and after 5 h of stimulation duplicates were pooled for further RNA extraction using RNeasy mini kit including an on-column DNase treatment.

3.2.1.3 Isolation of human peripheral blood mononuclear cells (PBMCs)

PBMCs were isolated from heparinized fresh blood of voluntary healthy donors as approved by the local Ethic Committee Heidelberg (admission number: S-716/2017) by density gradient centrifugation. To 50 ml Falcon tubes 15 ml Pancoll (density 1.077 g/ml) was added and blood pre-mixed with equal volume of PBS was carefully layered on top of the Pancoll. Tubes were centrifuged at 1,800 rpm for 20 min at RT without deceleration. The white ring of PBMCs at the interphase of Pancoll and serum was collected and transferred into fresh 50 ml Falcon tubes. White rings of two different Falcon tubes were pooled in one fresh Falcon tube, filled up to 50 ml with PBS and centrifuged at 1,300 rpm for 10 min at RT. Supernatant was discarded and cells were resuspended in 50 ml PBS. PBMCs were pelleted again at 1,000 rpm for 15 min at RT. After discarding the supernatant cells were resuspended in 10 ml PBS and pooled into one tube. PBS was added to a total volume of 50 ml and the Falcon tube was centrifuged at 1,300 rpm for 10 min at RT. Supernatant was discarded and cells were resuspended in 10 ml RPMI supplemented with either heat inactivated FCS 10% or 2% human serum. Cell number was determined by counting in a Neubauer chamber after diluting the cells 1:10 in Trypan blue.

3.2.1.4 Stimulation of cells

Cells were seeded at density of 50,000- 300,000 cells/well in 50-200 µl medium in flat bottom plates as indicated in the figure legend. All stimulations were performed in duplicate wells and cells were incubated in a humidified incubator at 37 °C and 5% CO_2. Unless otherwise specified, stimuli were added to the well at a volume of 50 µl, whereby the amount of stimulus was calculated for duplicates + 10%. For transfection experiments, RNA was encapsulated with DOTAP at a ratio of 3 µl DOTAP per 1 µg of RNA in 20-50 µl Opti-MEM Reduced Serum media and incubated for 10 min at room temperature. After encapsulation, transfection medium supplemented with 10% FCS or 2% human serum was added to a total volume of 110 µl. For co-transfection experiments different types of RNA were mixed prior encapsulation with DOTAP at indicated ratios. As positive control, cells were stimulated with bacterial RNA, small molecules like R848 and GQI and CpG2216. Cell free supernatants were collected after 20 h and secreted cytokines were measured by ELISA. mRNA expression levels were determined by qRT-PCR at indicated time-points.

3.2.1.5 Infection of cells

Infection experiments were performed in the same setup like stimulation experiments with indicated MOI of living bacteria or yeast. Standardisation of CFU was approximated by

McFarland 0.5, 1 or 3. For bacteria a McF 0.5 equivalents approximately 1.5 x 10^8 CFU/ml and McF 3 ≅ 9 x 10^8 CFU/ml. Due to size differences, McF 1 of yeast equivalents approximately 1 x 10^7 CFU/ml. Stimuli were prepared in cell culture media to avoid growth media dependent cell toxicity. 1.5 h post infection bacteria or yeast were killed by addition of antibiotics (P/S) or Antibiotic-Antimycotic solution as indicated in the different experiments.

3.2.2 Immunoassays

3.2.2.1 Enzyme-linked immunosorbent assay (ELISA)

Secreted cytokines were quantified in cell free supernatants by sandwich-ELISA. Cytokine levels were determined in half area plates according to an adjusted manufacturer's protocol. Usage of half-area plates allowed the reduction of indicated antibodies by 75% and amount of sample and substrate by 50%. Depending on donor variation, supernatants were used pure or diluted in ELISA blocking buffer. Absorbance measurements were performed at 490 nm with reference wavelength at 650 nm with the Tecan Sunrise plate reader. Quantification of cytokines was determined using a four parameter regression curve plotted by the Magellan V software.

3.2.2.2 Flow cytometry

Cell sorting

To preselect transfected HEK cells of CRISPR/Cas9 induced TARBP1 knock-out experiments, GFP positive cells were sorted by BD FACSMelody™. Of note, only transfected cells expressing the plasmid encoding for the guide RNA scaffold were capable to express GFP. To this end, 48 h post transfection cells were harvested and diluted to a total volume of 600 µl in DMEM + 2% FCS. Cell suspension was filtrated through a 40 µm cell strainer (Sarstedt, Nümbrecht) into a sterile FACS tube and stored at 4 °C until sorting. GFP signal was detected in the FITC channel and 50% of the highest GFP^+ cells were sorted at flow rate of 1 into a sterile FACS tube.

Detection of surface markers

To check for the upregulation of CD86 and MHC class II molecules at the cell surface of BlaER1 cells, 2 x 10^5 stimulated (o/n) cells were transferred into FACS-tubes and mixed with 500 µl of PBS supplemented with 2% FCS (FACS buffer). Tubes were centrifuged at 300 g for 5 min at 4 °C and supernatants were discarded. Cells were washed in 100 µl FACS buffer

and after centrifugation (300 g, 5 min) resuspended in 100 µl FACS buffer. Antibodies were added according to the dilution suggested by the manufacturer and shortly vortexed. As negative controls cells without addition of the antibody were included. After 15 min at 4 °C in the dark, cells were shortly vortexed and centrifuged (300 g, 5 min). Supernatant was discarded and cells were washed twice with 300 µl FACS buffer. Finally, cells were resuspended in 500 µl FACS buffer and analysis was performed with a BD FACSCanto™.

3.2.2.3 Confocal microscopy

5 x 10^5 cells were seeded to poly-D-lysine treated Ibidi glass bottom dishes (35 mm). 700 µl of poly-D-lysine solution was added to each dish and incubated for 10 min at RT. After 6 to 20 h cells were adherent and were transfected with labeled RNA (5 µg/ml). At indicated time points medium was removed and cells were fixed with 4% PFA in PBS for 20 min at RT. All incubation steps were performed in the dark to avoid bleaching of the fluorescent dyes. Cells were washed three times with 500 µl PBS and permeabilized with 0.1% Triton-X-100 in PBS for 15 min at RT. After three washing steps, samples were blocked with 5% BSA in PBS for 30 min at RT and subsequently incubated with MHC class II antibody (1:100 in 5% BSA) for 1 h. Samples were washed three times and stained with Hoechst (1 µg/ml) for 20 min. Slides were washed three times with PBS and mounted with DAPI containing mounting medium.
Confocal microscopy was performed with Leica TCS SP5 confocal microscope (488- and 561-nm laser) and HCX PL APO 63x/1.4 oil objective.

3.2.3 Molecular Biology

3.2.3.1 RNA preparation from stimulated cells

Total cellular RNA was extracted by adding 250 µl lysis buffer (ExtractMe total RNA kit) to each well of the 96-well plate. Duplicate wells were pooled to a 1.5 ml Eppendorf reaction tube and stored at -80 °C for further use. RNA isolation was performed according to the ExtractMe total RNA Kit protocol including on-column DNase digestion and RNA was eluted with 25 µl nuclease-free water. RNA quality and quantity was determined by NanoDrop spectrophotometer with respect to 260/230 nm and 260/280 nm ratios.

3.2.3.2 cDNA synthesis

Total RNA was reverse transcribed using 10 µl isolated RNA in a total reaction volume of 20 µl with High Capacity cDNA RT Kit according to the manufacturer's instructions. As a control 4 randomly picked samples (2.5 µl each) were pooled and reaction mixture without reverse transcriptase (noRT) was added to exclude genomic DNA contamination. Cycler conditions were set up as followed: 25 °C for 10 min, 37 °C for 120 min, 85 °C for 5 min, storage at 4 °C. cDNA preparations were diluted in nuclease- free water at 1:4 ratio.

3.2.3.3 Quantitative real time PCR (qRT-PCR)

For qRT-PCR analysis, SYBR®Green PCR Master Mix Fast was used. The reaction mixture was prepared as followed:

Component	Volume [µl]
H_2O	7.9
fw- primer (50 pM)	0.05
rv- primer (50 pM)	0.05
SYBR®Green PCR Master Mix	10
Template	2

The analysis was performed in duplicates on a StepOne Plus RT PCR cycler in 96-well format. noRT and non-template controls as well as melt curve analysis served as specify control. Cycling conditions were programmed as followed: 95 °C 20 sec; 40 x [95 °C 3 sec; 60°C 30 sec]; melt curve: 95 °C 15 sec, 60 °C 60 sec, 95 °C 15 sec.
Relative expression of target gene mRNA was calculated by ΔCT compared to GAPDH:
($rE = 2^{(-\Delta CT)}$)

3.2.4 RNA preparation

3.2.4.1 Standard TRIzol protocol for total RNA preparation

All solutions and buffer used for RNA preparations were prepared with DEPC or MilliQ water to avoid RNase contamination. Workplace and devices were cleaned with RNase-ExitusPlus before starting RNA purification.

E. coli wt and ΔtrmH strains were grown o/n in 10 ml LB medium at 37 °C, 250 rpm and trmH deficient mutant was selected by Kanamycin (50 ng/ml) in 50 ml Falcon tubes. The next

day, the overnight culture was diluted 1:20 to a final volume of 100 ml and bacteria were grown 3-5 hours until mid-log phase in 250 ml Erlenmeyer flask. Bacteria were pelleted at 3,000 g, 10 min and treated with lysozyme (c=40 mg/ml, 20 min at 37°C): Cell suspension was frozen at -80 °C for minimum 30 min before TRIzol reagent treatment. 5 ml Trizol were added and cell pellet was resuspended. After 5 min at RT, 1 ml chloroform was added and samples were vortexed for 15 sec. After 5 min at RT samples were centrifuged for 60 min at 4,000 g and 1 ml of aqueous phase was pipetted in 2 ml reaction tubes. 830 µl isopropanol were added to each reaction tube and samples were incubated for 10 min at RT. Subsequently centrifugation was performed at > 12,000 g, 4 °C for 10 min. Pellets were washed with 1 ml 75% ethanol and centrifuged 5 min, 7,500 g, 4 °C. Purity and quantity of extracted RNA was validated by NanoDrop measurement.

S. cerevisiae wt and Δtrm3 deficient mutant (mutant grown with Geneticin 200 µg/ml) were cultured in 10 ml YPD-Media at 30 °C and 300 rpm in a 50 ml Falcon tube. After 15-20 h, the yeast culture was re-inoculated if growth rate was low. Well grown yeast cultures (OD > 0.7) were diluted 1:10 to a final volume of 100 ml in a 250 ml Erlenmeyer flask and cells were cultured for further 5-10 h. Cells were harvested (3,000 g, 10 min) and treated for 30 min at 30 °C with 100 U Lyticase in Y1 Buffer supplemented with 0.1% β-Mercaptoethanol, pH 7,4. Cell suspension was frozen o/n before TRIzol treatment as described before.

HEK cells were harvested using Trypsin-solution and pelleted at 1,300 rpm, 15 min. Supernatant was discarded and cells were lysed by using TRIzol reagent and a following freezing step at -80 °C for minimum 1 h. To improve RNA release, the TRIzol suspension was aspirated into a sterile 10 ml syringe using a 20 G cannula and cells were lysed by shear forces in the cannula. Of note, HEK cells were not frozen before TRIzol extraction. RNA was extracted according to previous described TRIzol extraction protocol

3.2.4.2 Starvation of cells

E. coli or *S. cerevisiae* were cultured o/n from glycerol stock as described in 3.2.4.1. Pre-cultures were seeded at 0.05 OD_{600nm} and were grown in 200 ml culture media at indicated temperature until 1.5 OD_{600nm}. Of note, stationary phase had to be avoided. Cultures were splitted, whereby 100 ml cell suspension was used for TRIzol RNA isolation of non-starved cells as a control. The remaining 100 ml were used for starvation by 5 min, 4,500 g, 4 °C centrifugation followed by resuspension of the pellet in 100 ml PBS 1x. OD_{600nm} was measured and cells were incubated at 190 rpm at indicated temperature for 24 h. Final OD_{600nm} was taken and RNA was isolated by TRIzol protocol.

To starve HEK cells, one T175 flask was splitted 1:5 and 1:20 into two new T175 flasks. The 1:5 splitted HEK cells reached 100% confluence within 2-3 days and the culture media turned into light orange to yellow, whereby 1:20 splitted HEK cells reached only 70-80% confluence and culture media was still pink. For RNA isolation, cells were treated as indicated in 3.2.4.1.

3.2.4.3 TRIzol protocol to extend the yield of tRNA

50-100 ml bacterial or yeast culture in exponential phase (around 0.7-1.5 OD_{600nm}) were centrifuged 5 min at 4,500 g and 4 °C. The pellets were resuspended in 5 ml 1 x PBS and centrifuged 5 min, 4,500 g, 4 °C. For subsequent cell lysis, pellet was resuspend in 3 ml of TRIzol Reagent (samples can be stored at -20 °C). Samples are aliquoted to three 2 ml Eppendorf tubes and centrifuge for 5 min, > 12,000 g at RT. The supernatant was transferred in a new tube and incubated for 5 min at RT to get complete ribonucleoprotein dissociation. Per 1 ml Trizol, 200 µl chloroform were added and incubated 2-3 min at RT followed by 15 min centrifugation at 12,000 g at RT. The aqueous phase containing RNA was transferred in a new tube without touching the organic phase. 500 µl isopropanol were added, mixed well and incubated for 10 min at RT. Subsequently centrifugation was performed at > 12,000 g, 4 °C for 10 min. Pellets were washed twice in 1 ml 75% EtOH (Samples can be stored at – 20 °C) and centrifuged 5 min, 7,500 g, 4 °C. Of note, if pellets were washed only once with EtOH, 260/230 nm and 260/280 nm ratio measured by NanoDrop was below 1.8 and RNA was not suitable for stimulation experiments. Pellets were dried and resuspended in the appropriate volume of RNase free water.

3.2.4.4 Preparation of specific RNA species

Column based RNA purification

RNA purification was performed by Macherey-Nagel NucleoBond® RNA/DNA columns following the manufacturer's instructions including on column rDNase treatment. The kit allowed the isolation of different RNA species due to distinct KCl concentrations for nucleic acid elution. After a washing step with buffer R1, RNAs were eluted according to the following table adapted from manufacturer's protocol:

	tRNA	rRNA	whole RNA
Elution buffer	R0/R4 at a ratio 1:2	1. R0/R4 to elute tRNA 2. R4	R4
KCl concentration	575 mM	575 mM 1150 mM	1150 mM

After elution, 2.5 ml (AXR 80) or 5 ml (AXR 400) of isopropanol were added and samples were incubated for 15 min on ice, centrifuged for 25 min at 10,000 g, 4 °C and washed with 1 ml ethanol 85%. After a second centrifugation step the supernatant was discarded, pellets were dried and dissolved in RNase-free water. Concentrations were measured by NanoDrop and the samples were stored at -80 °C.

Agarose gel based RNA purification

tRNA and rRNA were prepared out of a 2% agarose gel prepared with 80 ml 1x TAE buffer and 6 µl pegGREEN to visualize the RNA. Up to 30 µg of sample were loaded with 2x RNA loading dye at a final volume of minimum 10 µl. Electrophoresis was performed at 100 V for about 40 min. Corresponding RNA bands were cut out of the gel as followed: To avoid the influence of UV light on the RNA preparation, an additional reference RNA sample and a RNA ladder were loaded into the left two pockets of the gel. Before visualisation, the gel was cut in two pieces, one reference part and one part for RNA preparation. Only the ladder and the reference sample were examined on an UV platform. Reference RNA was cut out and served as a marker to cut the corresponding RNA bands out of the RNA preparation gel. Gel slices were put into a 2 ml reaction tube, mashed with a scalpel and 500 µl ammonium acetate 0.5 M was added. Reaction tubes were stored for minimum 1 h at -80 °C and shaken o/n at 500 rpm and room temperature. The next day, RNA containing ammonia acetate solution was transferred to a Nanosept filter and incubated for 10-20 min. Filters were centrifuged at 10,000 g, 4 °C. The flow through was collected, transferred to a 2 ml reaction tube and 1,250 µl ethanol were added to precipitate RNA. Samples were stored for 1-2 h at -80 °C and centrifuged for 60 min at 10,000 g, 4 °C. The supernatant was discarded and pellets were washed with ethanol 70%. After a second centrifugation step (60 min, 10,000g, 4 °C) supernatant was taken out carefully to remove most of the ethanol and pellets were dried at RT. RNA was dissolved in nuclease-free water and RNA amount was measured by NanoDrop. For further quality control, RNA was examined on a control gel to exclude RNA degradation during the purification process.

Polyacrylamide gel electrophoresis (PAGE) based tRNA isolation

This protocol was mainly adapted from Patrick Keller, Helm Group, Johannes Gutenberg-University of Mainz.

To purify tRNA, a denaturing 10% PAGE supplemented 0.8 M urea (Rotiphorese-Sequencing-Gel System) was prepared as followed in a western blot chamber:

Component	Volume
Sequencing gel diluent	12.5 ml
Sequencing gel concentrate	10 ml
Sequencing gel buffer	2.5 ml
APS	150 µl
TEMED	15 µl

After polymerisation, 1x TBE buffer was added and pockets were rinsed with buffer to remove precipitated urea. The empty gel was run for 20-30 min at 150 V. Samples were mixed with denaturating loading dye (90% formamide + 10% 10x TBE) in a ratio of 1:2 to a total volume of minimum 20 µl. Immediately before loading the samples, pockets were rinsed again with 1x TBE buffer. To empty pockets, 10 µl of 6x loading dye were added and Fast Ruler ultra-low range DNA ladder was used as size marker. The PAGE was run first at 100 V and after 30 min voltage was increased to 150 V for 1- 1.5 h until the yellow dye run out of the gel. The gel was stained with 10 µl SYBR Gold in 100 ml 1x TBE buffer for 15 min at 100 rpm and washed with 100 ml 1x TBE for 5 min in the dark. RNA was detected with Typhoon scanner (Blue laser 488/520; 300V) and a picture of the gel was printed in real size to cut tRNA bands. Gel slices were put into a 2 ml reaction tube, mashed and 500 µl ammonia acetate 0.5 M were added. All subsequent steps were performed according to the RNA preparation out of agarose gels.

3.2.4.5 Bacterial RNA preparation of *Staphylococcus aureus* ATCC 25923

Bacteria were grown in LB medium at 37 °C, 250 rpm until mid-log phase. Bacteria were pelleted at 3,000 g, 10 min and treated with lysozyme (c=40 mg/ml, 20 min at 37°C). Cell suspension was frozen at -80 °C for minimum 30 min before RNA isolation using TRIzol reagent as described in section 3.2.4.1. Extracted RNA was further purified using RNeasy mini kit including an on-column DNase treatment. Purity and quantity of bacterial RNA (bRNA) preparations was validated by NanoDrop measurement.

3.2.5 Biochemistry

3.2.5.1 Western blot

To analyse protein expression of different cells, a 12% SDS-PAGE was prepared and 100,000 cells were washed with ice cold PBS, lysed with 10 µl 1x SDS sample buffer, and incubated at 95 °C for 10 min. The total amount of sample was loaded to the SDS-PAGE and PAGE was run for 1.5 h at 100 V. Proteins were transferred to a nitrocellulose membrane by semidry blotting procedure (2.5 mA/cm^2 membrane for 90 min). Unspecific binding was blocked by incubating the membranes in 1x TBST supplemented with 3% BSA for at least 1 h. According to the protein size, membrane was cut and incubated with specific primary antibodies (TARBP1 1:1,000 and β-actin 1:5,000 diluted in 3% BSA) overnight at 4°C and agitation. Membranes were washed three times for 5 min with 1x TBST at room temperature. Blots were incubated with HRP-conjugated secondary antibody (anti-rabbit-HRP 1:4,000) diluted in 1x TBST supplemented with 3% BSA for 1 h at room temperature and washed three times for 5 min with 1x TBST. Proteins were detected using an enhanced chemiluminescence (ECL) substrate by digitally imaging the emission. Contrast adjustments were applied to all parts of a figure.

3.2.5.2 Cell viability assay

To examine the survival of stimulated PBMCs, bioreducable MTS was used. The number of metabolically active cells was directly proportional to the quantity of the coloured formazan product. CellTiter 96 Aqueous One solution proliferation kit (MTS) was used according to the manufacturer's instructions to determine cell viability of stimulated PBMCs in a 96-well plate format. To each well (400,000 cells/well in 100 µl media) 20 µl of the CellTiter solution were added and PBMCs were incubated for 3 h at 37 °C in a humidified, 5% CO_2 atmosphere. Cell viability was assessed by measuring the absorbance of produced formazan at 492 nm in a Tecan sunrise photometer.

3.2.6 Genome editing

To investigate the relevance of TARBP1 for the recognition of human tRNA by PBMCs, methyltransferase deficient HEK cell mutants were created via CRISPR/Cas9. The guide RNAs (gRNAs) using a NGG PAM sequence were designed by using Blue Heron webpage (www.blueheronbio.com). Guide RNAs with a GC content between 60 and 80% were chosen and blasted to check for off target effects. Localization of all gRNA sequences (listed in Table

3-12) are shown below. The gRNAs scaffold expression was regulated by an U6 promotor which preferred a leading guanosine in the gRNA sequence. If gRNA sequence did not start with a G, an additional guanosine was added to the sequence (guide RNA #12- 15) The DNA oligos for cloning were ordered from Eurofins Genomics according to following scheme:

5' CACC N20 3'
3' N20 CAAA 5'

Depicted is antisense (-) strand of TARBP1; yellow highlighted: primer sequences; red highlighted: gRNA sequence localized on the sense (+) strand; green highlighted: gRNA sequence localized on the antisense (-) strand; white letters: start codon

ACT CCT GGC CTT ACG TCT AAA TCA TTC TTG TGT TTT CAT GAC TTA TTT TTA ATG
CAG ATG TCC AGA ACC AAT TTC AGA CCT ACT GTG TCA GTC TCT TTG TGG ATG GTG
CCC ATC ATG CAA CGT TTG GAA AAT AAT CTA AAG TGA TTC TGC TGT GTT CCA TCT
GTG AAC TGG TTT ATG CTC ACA GGC ACG CCT GAT TTA GGG TCC TGG GCA GAC CAA
CCT CCA ATC AGG AAT CGA TGA AGC TGG TGT AGA TAC TAC ATT AAC TTT TAA CGA
AGG CCT CGT TTC TCC TAA AAA TAA GAG ACC AGG TGG GTT CTA TCT AGG CAG GGT
TGG TGG CAG GAA CCC AAG GGA AGC TGA GCT GCA CCA AGC CGG GCT GGG ATC
CCC CTC TCT GC GGC CGC GCG CCC GGC TCCGT CGG CGC ACG CGC ACG TAG GGG
CCG GCC GGT CCT GTG CGC ACG CAT CGC ACA CGC CGG CGC CTT CCT TTG GGA GCC
CGG GCC GGT GGC GCG GGC GCT CGG CAA **ATG** GAG TGG GTG CTC GCG GAA GCG
CTG CTC TCG CAG AGC CGG GAC CCC CGG GCC CTG CTT GGG GCG CTG TGC CAA
GGG GAG GCA TCC GCG GAG CGC GTG GAG ACG CTG CGC TTC CTT CTG CAG CGG CT
C GAG GAC GAG GAG GCG CGC GGC AGC GGG GGC GCA GGC GCG CTC CCG GAG GCG
GCG CGC GAG GTG GCT GCA GGG TAC CTC GTG CCA CTG CTG CGG AGC CTG CGC GG
A CGC CCC GCG GGC GGC CCG GAC CCC AGT CTG CAG CCT CGC CAC CGC CGG CGC
GT G CTG AGG GCG GCG GGC GCG GCC CTG CGC TCG TGC GTC CGC CTG GCC GGG CG
T CCG CAG CTG GCG GCC GCG CTG GCT GAG GAG GCG CTG CGC GAT CTG CTC GCC
GGG TGG CGC GCG CCT GGC GCC GAG GCT GCC GTG GAA GTG CTA GCA GCC GT

3.2.6.1 Cloning of guide RNA

1 µg of the backbone (#1529) was digested with 10 units BbsI according to the manufacturer's protocol. The digested plasmid was loaded into a 1.5% agarose gel (100 V, 50 min). Consequently, the vector was purified using the QIAquick Gel Extraction Kit according to the manufacturer's instructions. In the meantime, 2.5 µl of forward and reverse gRNA oligonucleotides (100 µM) were annealed in 5 µl NEB2 buffer and 45 µl of nuclease free water by an initial heating step (95 °C, 5 min.) and the following cool down to room temperature. The annealed gRNA solution was diluted 1:200 in nuclease-free water and subsequently used for ligation. 50 ng digested backbone and 1 µl gRNA solution were ligated using 1 µl T4 DNA ligase according to the manufacturer's instructions.

3.2.6.2 Transformation and purifications of plasmids

10 ng plasmid DNA were added to 50 µl NEB 5-alpha competent *E. coli* and carefully mixed before incubating for 30 minutes on ice. For transformation, heat shock was performed at 42 °C for 30 seconds followed by 5 minutes incubation on ice. To allow the *E. coli* to recover, 100 µl SOC medium were added and bacteria were incubated at 37 °C for 1 hour at 300 rpm. Bacteria were spread on war Ampicillin selection plates and incubated at 37 °C overnight. The digested, non-ligated backbone used as a negative control. After 24 h, one colony per plate was picked and inoculated in 200 ml LB-medium supplemented with Ampicillin (100 µg/ml). Flasks were shaken at 37 °C and 200 rpm overnight. The plasmid DNA was isolated using PureLink™ HiPure Plasmid Filter Maxiprep Kit according to the manufacturer's instructions. DNA concentration was determined by NanoDrop.

3.2.6.3 Transfection of HEK cells and selection of potential knock-out clones

One day prior infection 1.5 x 10^4 HEK293 cells/well were seeded in 200 µl antibiotic free DMEM supplemented with 10% heat inactivated FCS in a 96-well plate. To transfect the cells, DNA-mixes were prepared as followed:

gRNA-Mix: 0.2 µg Cas9 plasmid (#1451) + 0.2 µg cloned gRNA plasmid (#1529) + 25 µl Opti-MEM

Lipofectamine-Mix: 0.5 µl Lipofectamine + 25 µl serum-free medium (incubation 10 min at RT)

25 µl gRNA-Mix + 25 µl Lipofectamine-Mix were gently mixed and incubated for 30 min at RT. Into each of two wells of the 96-well plate, 25 µl of the gRNA/Lipofectamine mixture were added and HEK cells were transferred to a 48-well plate after 24 h. The next day, cells were harvested using Trypsin-solution and resuspended in DMEM supplemented with 2%

heat inactivated FCS. HEK cells expressing the eGFP encoding gRNA scaffold plasmid were sorted by BD FACSMelody™. Positively selected cells underwent a limiting dilution which calculated for a single cell in every second well in a 96-well plate. After one week of growth, single cell colonies were transferred into a 6-well plate and were splitted after 3 days to obtain HEK cells for western blot analysis. All clones were screened for a TARBP1 knock-out on protein level to preselect clones for sequencing analysis. Six clones were picked and DNA was isolated using DNeasy Blood & Tissue Kit. For all six clones a PCR with indicated primers was performed (Table 3-11) and PCR products were purified using Monarch® PCR & DNA Cleanup Kit according to manufacturer's protocol. PCR conditions are indicated in Table 3-20

Table 3-20: PCR reaction mix and cycler conditions

Reaction mix		**Cycler conditions**		
Component	**Amount**	**Temperature**	**Time**	
Q5® DNA Polymerase	25 µl	98 °C	1 min	
Primer fw (50 pM)	0.5 µl	98 °C	30 sec	35x
Primer rv (50 pM)	0.5 µl	67.5 °C	30 sec	
Template	100 ng	72 °C	1 min	
Nuclease free water	ad 50 µl	72 °C	5 min	

Purified PCR products were sent to GATC Biotech GmbH for Sanger sequencing. Sequences were analysed using CRISP-ID (Dehairs, J. *et al.* CRISP-ID: decoding CRISPR mediated indels by Sanger sequencing Sci. Rep. 6, 28973; doi: 10.1038/srep28973 (2016))

3.2.7 Statistical analysis

Unless otherwise indicated, data was analysed using GraphPad prism version 6.05. Significant differences were assessed by two-way ANOVA including multiple comparison tests or linear regression model. P-values are indicated by ns (not significant, $P > 0.05$), * ($P \leq 0.05$), ** ($P \leq 0.01$), *** ($P \leq 0.001$).

Section 4.2.1: Dose-response model was calculated by R software 3.4.1 and the package drc with best fitting model for each RNA oligoribonucleotides. Unmodified GG ORN: log-logistic function (three parameters), native Lys3: Weibull function (two to four parameters), modified GmG ORN: log-logistic function (two parameters).

Section 4.3: IC50 values and curve fit for inhibitory RNA oligoribonucleotides were calculated using R software version 3.4.1 and the package drc (R Core Team 2013; Ritz *et al.* 2015) Responses fit well to a log-logistic function (with 2–4 parameters) with exception of IFN-α for the CGm18GU and unmodified motif (best model: fractional polynomial-logistic dose–response functions). The error bars represent the confidence interval of the model.

4 RESULTS

The main focus of this thesis was the analysis of posttranscriptional RNA modifications with regard to their impact on innate immune stimulation. The first part of the results section gives an overview of the method establishment and explains advantages and disadvantages of different RNA isolation methods. The following three chapters address different aspect of RNA modifications. In Chapter 4.2 a new immune modulating RNA modification is identified. The next chapter 4.3 describes an optimized inhibitory tri-nucleotide motif based on a naturally occurring tRNA modification. In the last chapter 4.4, the relevance of RNA modifications for whole organism recognition is studied.

4.1 Method establishment

4.1.1 Purity of RNA species depends on the way of purification

The quality of RNA for stimulation experiments is determined by several factors including DNA contamination, degradation of RNA by nucleases or physical and chemical stress or the 260/230 nm and 260/280 nm ratio indicating phenol and guanidine or protein contaminations, respectively. Of note, RNA with 260/230 nm and 260/280 nm ratios >1.8 are in general accepted as pure RNAs. Furthermore, to examine the immune stimulatory effect of specific RNA species, contaminations with other kinds of RNA must be avoided. Therefore, we established several isolation methods to either purify total RNA or defined RNA species as described in section 3.2.4 considering the above described criteria. In case of ribosomal RNA purification and stimulation experiments we mainly focused on the 23S and 16S, 25S and 18S and 28S and 18S rRNA subunits of *E. coli*, *S. cerevisiae* and human cells, respectively. A couple of different methods as partly published in literature were evaluated. The results indicate the purity of RNA is greatly influenced by the purification method, as shown below in detail.

4.1.1.1 Purification of distinct RNAs based on 'NucleoBond RNA/DNA columns' can lead to cross-contamination by DNA and RNA species

At first, a commercial purification kit assigned to be able to purify different RNA species, was tested. Side by side purification of tRNA and rRNA or total RNA from TRIzol total RNA preparations by NucleoBond RNA/DNA columns was reported to be possible due to RNA elution along a KCl gradient (see section 3.2.4.4). Purified RNA species were subsequently examined on a 1.5% agarose gel to check for DNA contamination, RNA degradation and

RNA cross-contamination. Although all RNA samples were treated with DNase I according to the manufacture's protocol, various samples showed DNA contaminations (Fig. 4–1, No. 2). Furthermore, some tRNA preparations showed rRNA residues which were co-eluted within tRNA fractions (Fig. 4–1, No. 1). The depicted agarose gel was representative for different tRNA preparations showing rRNA contaminations. Moreover, the physiological proportion of tRNA within a cell was estimated with approximately 10% of total RNA and 90% of the total RNA samples were expected to be rRNA. Yet, not all total RNA samples fulfilled these criteria and were therefore not suitable for immune stimulation experiments that should mimic physiological RNA conditions. Of note, we never noticed any RNA degradation due to column-based RNA purification.

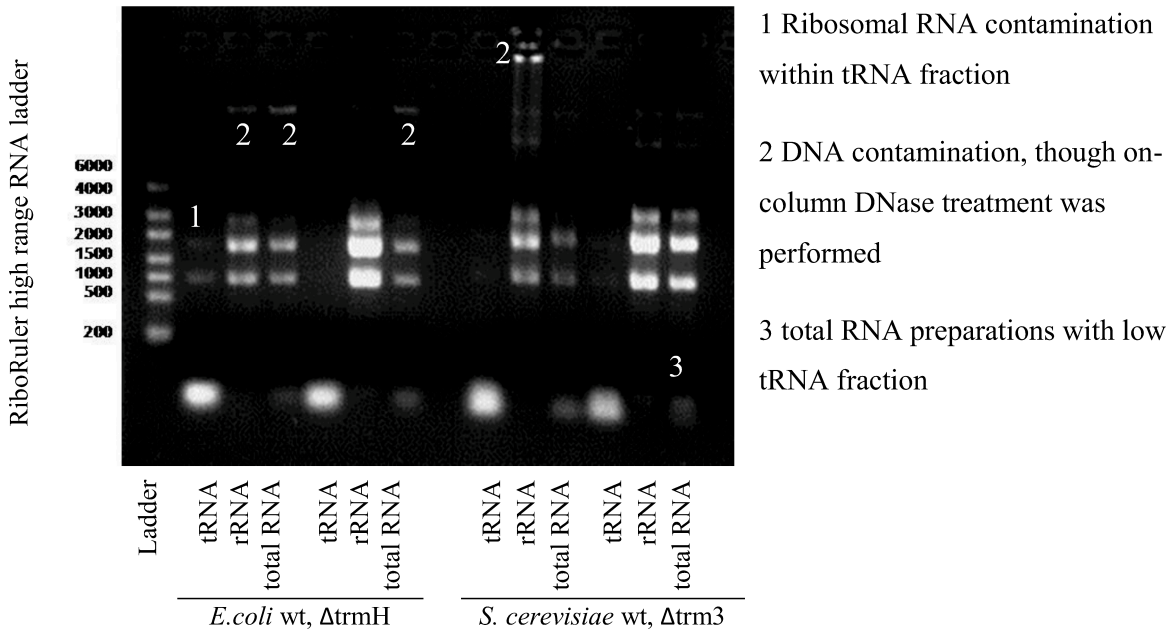

Fig. 4–1 Agarose gel of column-based isolated RNA species. 1.5% Agarose gel was stained with peqGREEN and 2 µg of each RNA was mixed with 2x loading dye and loaded into the pockets. The agarose gel run for 45 min at 100 V and was subsequently analysed under UV light.

Altogether, column-based RNA purification did not result in RNA preparations with reproducible high quality. DNA and RNA cross-contamination made those samples inappropriate for further stimulation experiments. Caution should be paid to publications claiming to use such a method for immune stimulation with defined RNA species unless quality controls are shown.

4.1.1.2 tRNA isolation from denaturating polyacrylamide gel induces higher levels of proinflammatory cytokines compared to tRNA isolated from agarose gel

Size of transfer RNAs can differ from roughly 70-100 nucleotides. With 120 nucleotides, the 5S rRNA subunit is only slightly larger compared to tRNAs and might co-elute in the tRNA fraction by column-based tRNA purification. Furthermore the resolution of 1-2% agarose gel is inadequate to discriminate tRNAs from 5S rRNAs. To this end, we decided to purify tRNAs from a denaturing 10% PAGE supplemented 0.8 M urea as described in section 3.2.4.4. The separation efficiency of PAA gels was much higher compared to agarose gels, where tRNAs could easily be discriminated from 5S rRNA (Fig. 4–2). To isolate the tRNAs only, the RNA fraction at the bottom of the gel (dashed square) was cut and tRNAs were extracted from the gel slices (section 3.2.4.4).

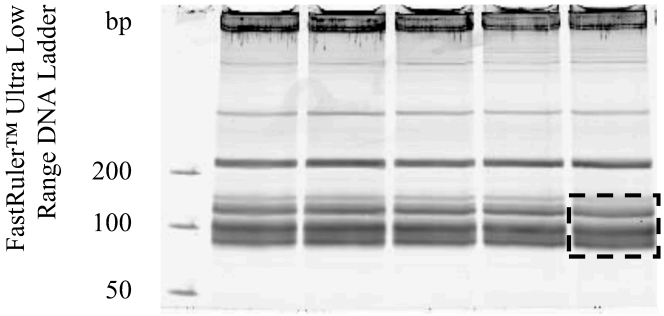

Fig. 4–2 TRIzol sample separated via PAGE. PAA gel was stained with SYBR Gold Nucleic Acid Gel Stain and visualized by Typhoon scanner. Dashed square indicated tRNA fraction of total RNA samples isolated by TRIzol reagent.

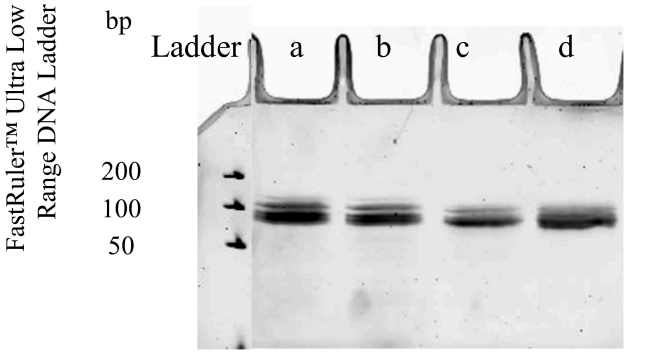

Fig. 4–3 Quality control of isolated tRNAs. PAGE purified tRNAs of *E. coli* wt (a), *E. coli* ΔtrmH (b), *S. cerevisiae* wt (c), *S. cerevisiae* Δtrm3 were examined on a second PAA gel to evaluate size of isolated RNAs and to exclude NA contaminations.

Subsequently, PBMCs were stimulated with isolated tRNAs of different human cell lines. Of note, TNF-α levels induced by human tRNAs seemed to be quite high and were against the expectation based on previous results suggesting that highly modified human tRNA should not show activation of TLR8 within monocytes. Thus, we decided to extract tRNA side by side from PAA gels and agarose gels to investigate a potentially gel-dependent stimulatory effect of tRNA samples. Of note, when tRNAs were isolated from an agarose gel, the tRNA fractions were cut quite stringent at the upper part to avoid 5S rRNA contaminations. Stimulation of human PBMCs with differentially isolated tRNAs showed significant

differences with regard to their immunestimulatory potential dependent on the type of RNA isolation (Fig. 4–4). TNF-α release was significantly decreased for THP-1 and Beas2B tRNAs (0.5 µg/ml) purified from an agarose gel compared to PAA gel purification. In case of A549 and HEK tRNAs, the samples showed the same trend, however results were not significant. Of note, IFN-α release by human pDCs was not affected by the way of tRNA purification (data not shown). TLR7-based type I IFN read-out was more insensitive towards contaminations, as human pDCs possess a limited set of PRRs and PAA gel impurities were not capable to trigger IFN-α release. Compared to monocytes that are expressing TLR2 and TLR4 and are known to recognize a broad spectrum of ligands, pDCs mainly express endolysosomal NA-sensing TLRs [9].

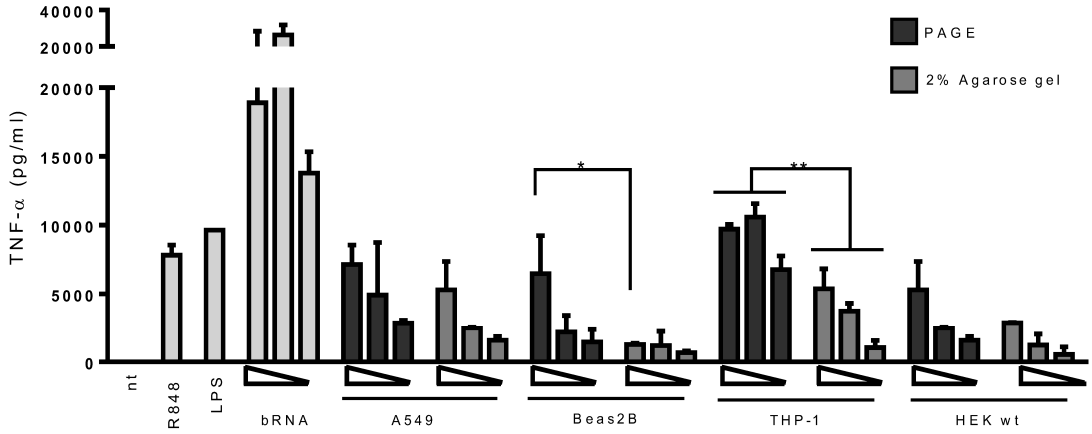

Fig. 4–4 Stimulation of human PBMCs with isolated tRNAs from human cell lines by either purification from PAGE or 2% agarose gel. 200,000 PBMCs/well in a final volume of 100 µl were stimulated with DOTAP-encapsulated tRNAs. Triangles indicate concentrations of tRNAs of 0.5, 0.25 and 0.125 µg/ml. TNF-α was measured in cell-free supernatants by ELISA. tRNA samples were prepared from either a 2% agarose gel or denaturating PAGE by cutting the corresponding tRNA bands and subsequent tRNA purification.

As a conclusion, all further RNA samples (tRNA, rRNA and total RNA) for stimulation experiment were purified from agarose gels by excision in order to prevent distortion of results caused by the way of RNA purification.

4.1.2 Serum dependent secretion of interferon-α and proinflammatory cytokines

According to the literature, peripheral blood mononuclear cells (PBMCs) are cultured in RPMI supplemented with either 10% FCS or 2% human serum. In our lab, we commonly used RPMI supplemented with 10% FCS to culture isolated human PBMCs for stimulation experiments. Of note, detected type I interferon levels upon PBMC stimulation were rather low in our assays compared to publications of other labs. Therefore, we decided to directly

compare the cytokine and IFN-α release of PBMCs either cultured with 10% FCS or 2% human serum. Human serum was prepared from healthy donors and heat inactivated at 56 °C for 30 minutes. Of note, only allogenic but no autologous serum was used for PBMC cultures. PBMCs were stimulated with 1 µg/ml R848 as a classical TLR7/TLR8 ligand inducing IFN-α release in pDCs upon TLR7 activation and proinflammatory cytokine secretion of monocytes by TLR8 stimulation. LPS served as a TLR4 ligand which could only activate monocytes as TLR4 is not expressed on the cell surface of pDCs. RPMI with the corresponding serum was added without any additional stimulus to the non-treated control to check for pre-activation of PBMCs or an activating effect of human serum. Of note, most experimental read-outs of this project were based on RNA-dependent induction of proinflammatory cytokines and IFN-α. Therefore, DOTAP-encapsulated bacterial RNA (bRNA) was transfected at three different concentrations to human PBMCs to examine the effect of FCS and human serum on cytokine release triggered by RNA. Indeed, human serum was capable to boost the release of both, IFN-α and TNF-α for donor 1 (Fig. 4–5 A, B) as well as for donor 2 (Fig. 4–5 C, D). In case of donor 1, IFN-α secretion induced by bRNA was significantly increased for all three concentrations by human serum, whereas R848 dependent IFN-α release reached similar results for FCS and human serum. PBMC stimulation of donor 2 demonstrated similar results, whereby the increase of IFN-α level by human serum was less pronounced compared to donor 1. Of note, overall TNF-α levels were significantly increased in the presence of human serum compared to FCS for both, donor 1 and donor 2.

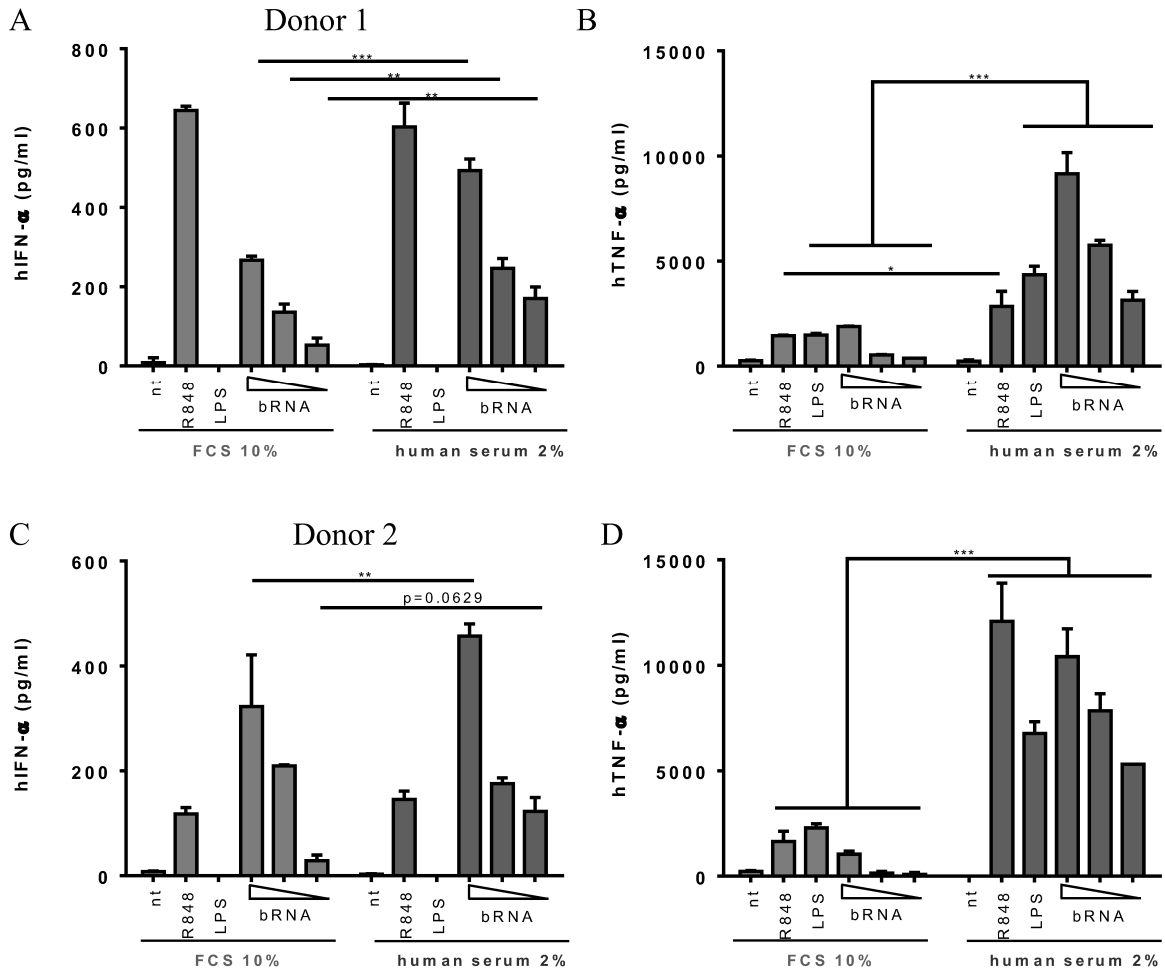

Fig. 4–5 Stimulation of human PBMCs in the presence of either 10% FCS or 2% human serum. Isolated PBMCs (200,000/well) of two healthy donors were stimulated side by side in RPMI supplemented with FCS or human serum. IFN-α and TNF-α secretion was detected in cell free supernatants by ELISA Triangles indicate concentrations of bRNA of 0.5, 0.25 and 0.125 µg/ml. Secreted IFN-α (A) and TNF-α (B) of donor 1 and donor 2 (C-D) secreted after 20 h of stimulation. Stimulation experiments were performed in duplicate wells. Shown are means + SD

In summary, a serum dependent IFN-α and TNF-α secretion was demonstrated by human PBMCs. Immune stimulation induced by RNA was significantly increased in PBMCs cultured in RPMI supplemented with 2% of human serum. This observation was important to develop a more sensitive experimental setup for RNA-dependent immune stimulation of PBMCs.

4.1.3 Interferon-α secretion depends exclusively on plasmacytoid dendritic cells

It is an accepted fact, that IFN-α secretion upon TLR7 stimulation within PBMCs is exclusively linked to pDCs [38, 73, 118]. However, frequently the question arose again, if IFN-α is indeed exclusively produced by pDCs. Former experiments of the working group demonstrated the absence of IFN-α within stimulated PBMCs if pDCs were depleted. However, depletion experiments did not mirror potential interactions of activated pDCs with other immune cells leading to altered IFN-α secretion pathways. To quantify the pDC-dependent IFN-α secretion within PBMCs compared to pDCs alone we negatively selected pDCs (human pDC Isolation Kit II) with MACS LD-columns on a MidiMACS™ Separator according to the manufacturer's protocol. Of note, AutoMACS™ separation resulted in 63% purity of pDCs only. Consequently, we stimulated isolated pDCs and PBMCs of the same donor to compare secreted IFN-α levels. As expected, stimulation of both cell populations resulted in a similar IFN-α release, thereby indicating pDCs as sole source for interferon secretion (Fig. 4–6). Of note, purity of isolated pDCs was rather low but enriched pDC population showed equal IFN-α levels compared to PBMCs.

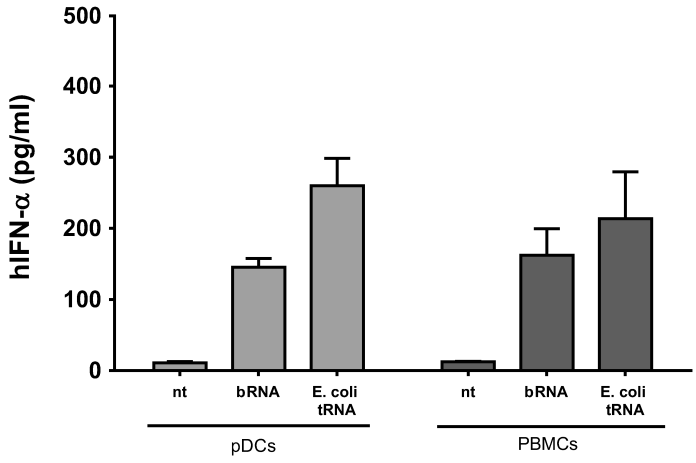

Fig. 4–6 Stimulation of isolated pDCs and PBMCs. 10,000 pDCs or 400,000 PBMCs per well were stimulated in a 96-well flat bottom plate. 1µg/ml DOTAP-encapsulated RNA was transfected to the cells and IFN-α release was measured in cell free supernatants by ELISA. Stimulation experiment was performed in duplicate wells. Shown was means + SD

4.2 Identification of a new modification in human $tRNA^{Lys}_3$ that decreases TLR7 stimulation

This study was performed in cooperation with the working group of Prof. Dr. Mark Helm, Institute of Pharmacy and Biochemistry, Johannes Gutenberg-University of Mainz. All tested tRNA modivariants were created by Patrick Keller, Helm Group. All modivariants were equal in tRNA sequence but differed in kind and amount of modifications.

Previous studies have demonstrated a great variability of native tRNA isoacceptors with regard to their immune stimulatory properties. Yet, the corresponding *in vitro* transcribed tRNAs were uniformly stimulatory [73], indicating that not the sequence but posttranscriptional modifications enabled the discrimination of "self" and "non-self". The 2'-O-methylation of certain nucleotides like Gm18 within tRNAs was identified as a dominant inhibitory modification on TLR7 and TLR8. Of note, human $tRNA^{Lys}_3$ which lacks Gm18 was likewise identified as a non-stimulatory naturally occurring tRNA (Fig. 4–7) [70, 73, 91, 93].

To examine the unknown immunosilencing modification pattern, a Colicin D-based molecular surgery approach was performed. Colicin D is a bacteriocine secreted by *E. coli* and acts as a tRNase which was described to cleave the four bacterial isoacceptors of $tRNA^{Arg}$ in the anticodon-loop between position 38 and 39 *in vivo* [119]. Of note, Colicin D was capable to also cleave mammalian $tRNA^{Lys}_3$ at a precise position within the anticodon loop *in vitro.*

This finding facilitated the creation of modivariants of $tRNA^{Lys}_3$ which were analysed for their immunosilencing potential. Furthermore, single modified tRNAs were synthetized to identify the modification that is crucial to inhibit TLR7 response within PBMCs.

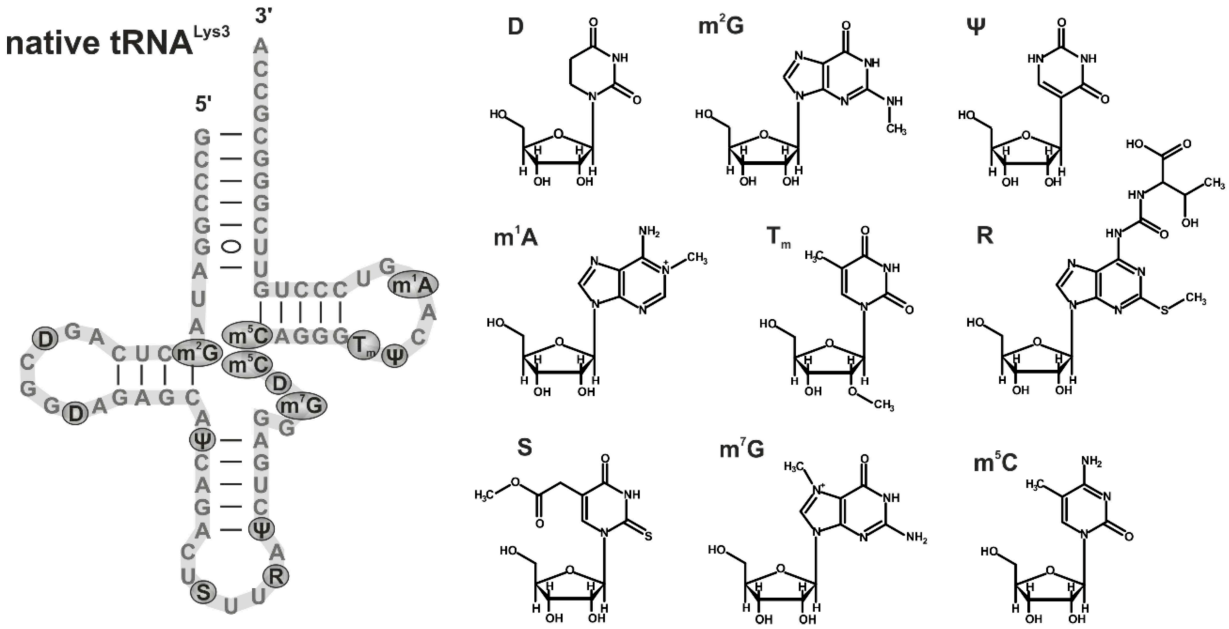

Fig. 4–7 RNA modifications in mammalian tRNA$^{Lys}_3$. The left part depictures native tRNA$^{Lys}_3$ and on the right part corresponding modifications (illustrated as grey circles) with structural formulas. D = Dihydrouridine, m2G = N2-methylguanosine, Ψ = Pseudouridine, m1A =1-methyladenosine, Tm = m5Um = 2'-O-methylthymidine/5,2'-O-dimethyluridine, R = t6A = 2- methylthio-N6-threonylcarbamoyladenosine, S = mcm5s2U = 5-methoxycarbonylmethyl-2-thiouridine, m7G = 7-methylguanosine, m5C = 5-methylcytidine (according to modomics RNA modification database[120]) Figure adapted from Keller *et al.* 2018

4.2.1 Native tRNA$^{Lys}_3$ is non-stimulatory but does not act as TLR7 antagonist

Synthesized unmodified tRNA$^{Lys}_3$ and native tRNA$^{Lys}_3$ were titrated on human PBMCs to check for differences in immune stimulation. Bacterial RNA (bRNA) and the small molecule R848 served as positive control for TLR7-dependent pDC activation within PBMCs. Absence of IFN-α secretion in the non-treated control excluded unspecific pre-activation of PBMCs. Bacterial RNA and the unmodified tRNA$^{Lys}_3$ control induced similar IFN-α levels in human PBMCs, whereas native tRNA$^{Lys}_3$ did not stimulate TLR7 (Fig. 4–8 A). Therefore, the lack of immune stimulation by native tRNA$^{Lys}_3$ was not linked to tRNA sequences but to its posttranscriptional modifications. To investigate dominant inhibitory effects of tRNA$^{Lys}_3$ on TLR7, co-transfection experiments with different concentrations of non-stimulatory native tRNA$^{Lys}_3$ together with constant amounts of otherwise stimulatory bacterial RNA were performed (Fig. 4–8 B). The previously described 2'-O-methylated 26-mer ORN (see section 4.3) served as a positive control for dominant inhibition of TLR7 and antagonisation of bRNA induced IFN-α release. An unmodified GG ORN (previously described unmodified control) which did not decrease secretion of type I IFN served as specificity control for inhibition of TLR7. Of note, the co-transfection of bRNA and tRNA$^{Lys}_3$ did not attenuate bRNA induced

IFN-α production, indicating that $tRNA^{Lys}_3$ was non-stimulatory but, unlike Gm, did not act as TLR7 antagonist.

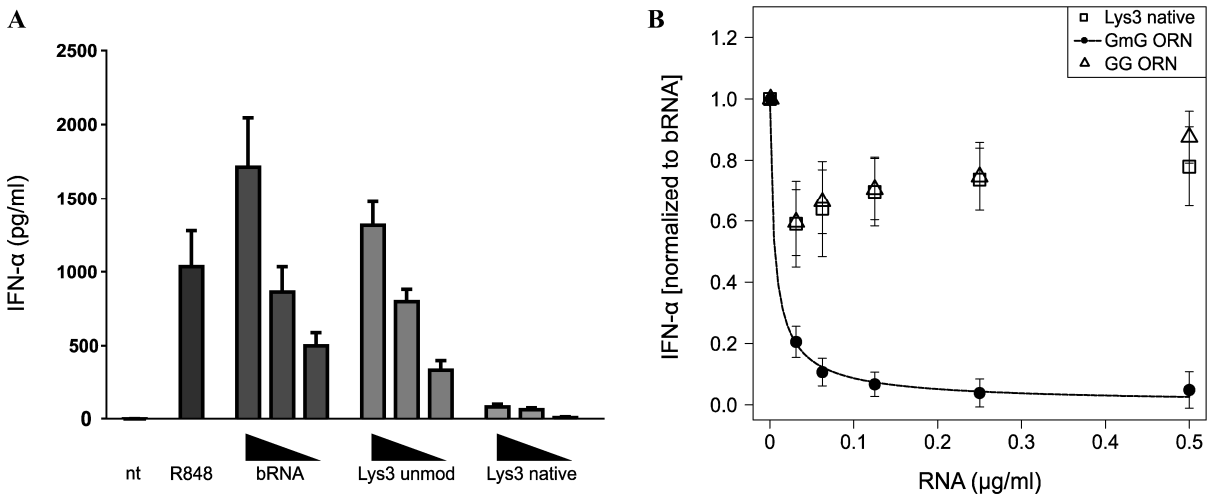

Fig. 4–8 Induction of IFN-α release by native and unmodified $tRNA^{Lys}_3$ and effect of $tRNA^{Lys}_3$ on bRNA-dependant TLR7 activation. Human PBMCs (200,000/well) were treated with indicated stimuli. Cytokine levels were determined in cell-free supernatants by ELISA. (A) Cells were stimulated for 20 h with R848 (1µg/ml) and DOTAP encapsulated bacterial RNA, unmodified and native $tRNA^{Lys}_3$. Triangles indicate concentrations of RNA of 0.5, 0.25 and 0.125 µg/ml. Shown bars represent the stimulation of 3-6 individual donors in duplicate wells +SEM. (B) Human PBMCs of three individual donors were co-stimulated in duplicate wells with a constant amount of bacterial RNA (0.5 µg/ml) and five different concentrations of indicated RNAs (0.5, 0.25, 0.125, 0.0625, 0.03125 µg/ml). To account for donor variation data were normalized to secretion of IFN-α induced by bacterial RNA alone. Dose-response model was calculated by R software. Figure adapted from Keller *et al.* 2018

4.2.2 IFN-α release induced by splint ligated full length 5' and 3' $tRNA^{Lys}_3$ modivariants indicates an immunosilencing modification within the 3' part.

As the human $tRNA^{Lys}_3$ was heavily modified, a cleavage reaction previously established by the group of Mark Helm mediated by so-called DNAzymes was not possible [73, 121]. Consequently, modivariants with identical sequence but different post-transcriptional modifications were created by Patrick Keller, Helm group, by the usage of Colicin D. Native $tRNA^{Lys}_3$ was cut at the anticodon site and 5' and 3' parts of tRNA were purified. tRNA fragments were combined with synthetic, unmodified RNA followed by different enzymatic treatments to end up with full length RNAs consisting of 50% of modified native RNA and 50% of an unmodified ORN (Fig. 4–9 A). Compared to native Lys3, only the splint ligated 5' tRNA (mv#1) fragment showed significantly increased IFN-α level. Mv#2 consisting of the native 3' fragment and an unmodified 5' fragment displayed clearly reduced IFN-α secretion

similar to native $tRNA^{Lys}_3$. These results indicated an immunosilencing modification within the 3' fragment of the tRNA (Fig. 4–9 B)

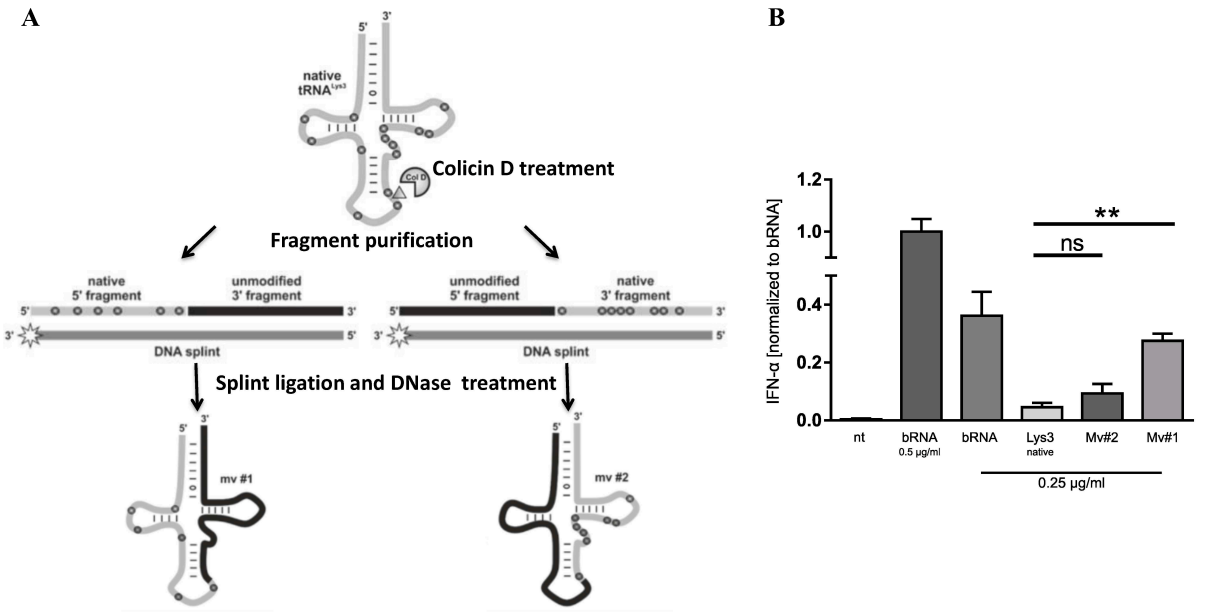

Fig. 4–9 Preparation of Lys3-modivariants and their immunestimulatory activity compared to native $tRNA^{Lys}_3$. (A) Native $tRNA^{Lys}_3$ was treated with Colicin D and the two 38 nt long fragments were purified by PAGE. Subsequently, DNA hybridization to the 3' fragment was performed to enable separation of the double-stranded RNA/DNA hybrid and simultaneous isolation of both tRNA fragments. RNAs were then treated with DNase I and a thermosensitive alkaline phosphatase (FastAP, Thermo Fisher Scientific). Prephosphorylated tRNA fragments were annealed together with unmodified RNAs on splint DNA and subsequently ligation and DNase treatment resulted in full length tRNAs mv#1 and mv#2 (Patrick Keller). (B) Human PBMCs of three individual donors were stimulated in duplicate wells with DOTAP encapsulated RNA species at indicated concentrations. 20 h post transfection IFN-α levels were measured in cell-free supernatants. Results were normalized to IFN-α levels induced by 0.5 µg/ml bRNA to account for donor variation. Each bar illustrates mean +SEM. (A) Figure adapted from Keller *et al.* 2018

4.2.3 A single 2'-O-methylated thymidine within tRNA decreases immune stimulation

Based on the previous observation, indicating an immonosilencing modification within the 3' fragment, the modification pattern of $tRNA^{Lys}_3$ was analysed. Of note, none of the modifications present within the 3' fragment of native $tRNA^{Lys}_3$ had previously been described as immunosilencing. As former studies identified 2'-O-methylation as an immunomodulatory modification, 5, 2'-O-dimethyluridine (Tm) at position 54 was identified as a candidate for immune suppression and further examined. A $tRNA^{Lys}_3$ modivariant containing a single Tm within an otherwise unmodified tRNA context was created by splint ligation. Therefore, commercial ORNs and a single 5, 2'-O-dimethyated uridine (Tm) were ligated using a DNA splint to receive a full length, single modified tRNA. Subsequently,

PBMCs were stimulated with Tm54 tRNA as well as native and unmodified $tRNA^{Lys}_3$ as controls. Introduction of Tm modification reduced immune stimulation of the tRNA by almost 50% compared to unmodified full-length tRNA (Fig. 4–10 B). Of note, native $tRNA^{Lys}_3$ showed even less stimulation indicating further modifications contributing to the immunosilencing phenotype. Previous results suggested that the dominant inhibitory effect of 2'-O-methylation is dependent on the corresponding nucleobase. To further investigate the immunosilencing effect of Tm on TLR7 and immunosilencing capacity of other 2'-O-methylated nucleotides at position 54, nucleobases at that position were permutated. Of note, only the two purines adenosine and guanosine but not the pyrimidines cytosine and uridine were able to abrogate immune stimulation when being 2'-O-methylated (Fig. 4–10 B). Interestingly, cytokine release induced by Tm modified tRNA was in between 2'-O-methylated pyrimidines and purines. Of note, the base methylation of uridine (rT) alone did not decrease cytokine release compared to an unmodified control.

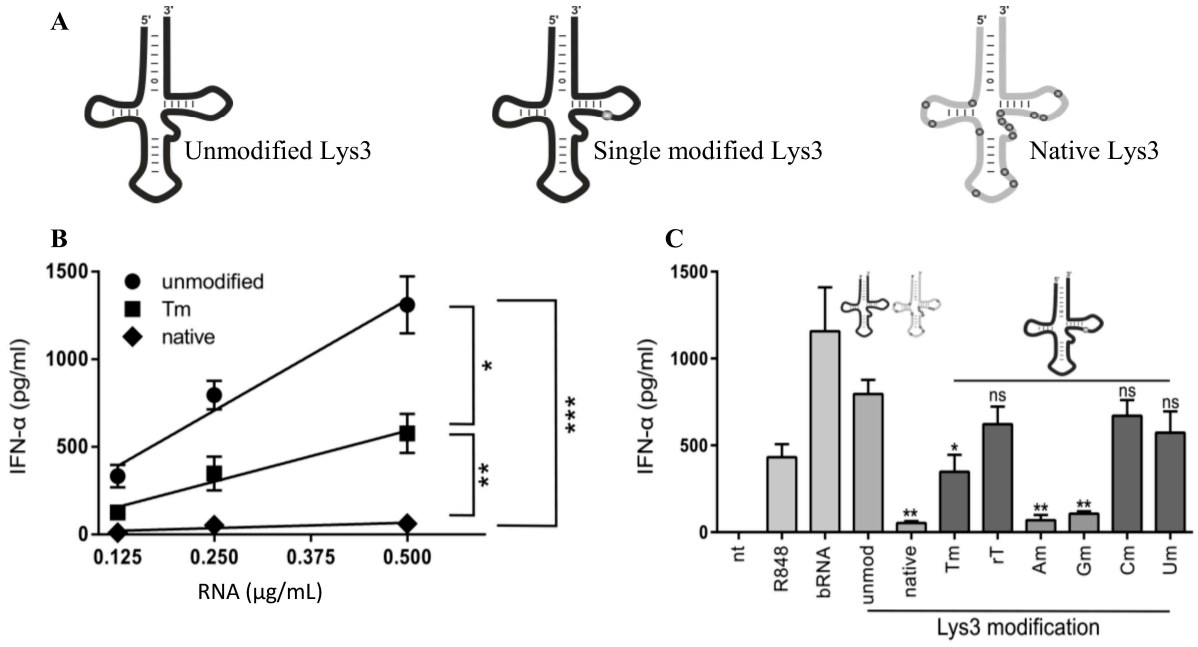

Fig. 4–10 Immune stimulation of single Xm54 modified tRNAs. (A) Modification pattern of unmodified, single modified and native, fully modified $tRNA^{Lys}_3$. (B) Isolated human PBMCs were stimulated at indicated concentrations of tRNAs encapsulated with DOTAP (0.5, 0.25 and 0.125 µg/ml). IFN-α release was detected in cell free supernatants by ELISA 20 h after stimulation. Linear regression was calculated by GraphPad Prism. (C) Transfection of single modified tRNAs at position 54 at a final concentration of 0.25 µg/ml. R848 and bRNA were used as a positive control for TLR7 stimulation. IFN-α secretion was compared to unmodified tRNA control. All stimulations were performed in duplicate wells on three individual donors. Shown are mean + SEM. Figure adapted from Keller *et al.* 2018

In summary, this study could confirm the non-immune stimulatory character of human native $tRNA^{Lys}_3$. In relation to the immunosilencing potential of the 3' fragment of native Lys3 tRNA, 2'-O-methylthymidine (Tm) was identified as a sufficient modification to decrease but not completely impede immune stimulation. In contrast to previous identified 2'-O-methylated guanosine (Gm18), Tm54 within native $tRNA^{Lys}_3$ did not antagonize TLR7 activation.

4.2.3.1 Bioconjugation of immune stimulatory small molecules to RNA to enhance immune response – a side project-

This study was performed in cooperation with the working group of Prof. Dr. Mark Helm, Institute of Pharmacy and Biochemistry, Johannes Gutenberg-University of Mainz. All tested RNAs were created by Isabell Hellmuth, Helm group.

So far, all investigated posttranscriptional RNA modifications were from natural origin. However, those naturally occurring RNA modifications were inhibitory on immune stimulation or did not affect the RNA recognition by TLRs. Immune stimulatory RNA modifications were not identified, yet. Though, an increase of immune stimulation by RNA modifications might be a useful tool for mRNA based vaccinations [122-124]. In a recent study from van Hoeven *et al.* the application of a TLR7/TLR8 ligand based on the chemical structure of imidazoquinolines as a potent adjuvant for pandemic influenza vaccines was described [125]. Of note, due to small molecular size of imidazoquinolines like R848, usage as vaccine adjuvants has not passed clinical testing, yet. Their rapid diffusion from the injection site might cause systemic immune activation leading to adverse side effects of vaccination [126]. To avoid this problem, conjugation of R848 to influenza virus A antigens to immobilize small molecules gave promising results regarding antibody and cell mediated immune responses [127]. Furthermore, RNAs were described as potent adjuvants for vaccination by activating different RNA sensors like TLR7 and TLR8 [128, 129]. Moreover, mRNA based vaccines cannot only possess adjuvant activity but at the same time encode for the desired immunogenic antigen, therefore combining signal one and signal two required for robust T-cell activation. Based on these studies, we set out to investigate the effect of bioconjugation of imidazoquinolines to an eGFP model mRNA to boost TLR stimulating activity of mRNA while retaining translational competence.

4.2.3.2 Co-stimulation of PBMCs with eGFP mRNA and small molecules shows minor effects on overall IFN-α release

Click-chemistry was performed by Isabell Hellmuth. Covalently binding of the immune stimulatory TLR7 ligands Resiquimod (R848) and Gardiquimod (GQI) (Fig. 4–11 B3, A1) to alkyne-modified uridines of eGFP mRNA required chemical modification of small molecules: To be available for copper catalyzed click-reaction, small molecules needed to be azide-functionalized. Therefore, Gardiquimod was equipped with an azido-ethylene glycol linker at the aliphatic amine and R848 was modified at its primary amine to yield Gardiquimod-diethylene-glycol-azide (GDA) and Resiquimod-polyethylene-glycol-azide (RPA), respectively (Fig. 4–11 B4, A2).

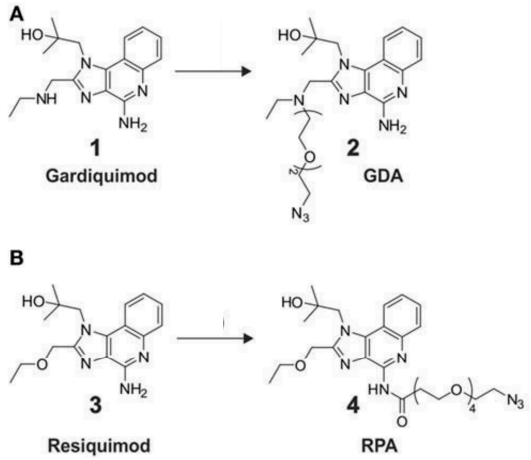

Fig. 4–11 Structure of small molecules and their respective azide-functionalized derivates. (A) Gardiquimod-diethylene-glycol-azide (GDA) (2) was synthetized from Gardiquimod (1) and (B) Resiquimod-polyethylene-glycol-azide (4) was created from Resiquimod (R848) (3)

The impact of azide-functionalisation on the immune stimulatory capacity of small molecules was examined by the stimulation of PBMCs at different concentrations of small molecules and the corresponding conjugated azide-derivates (Fig. 4–12 A). As a control, cells were stimulated with immune stimulatory eGFP mRNA. The activation of TLR7 within PBMCs was determined by the measurement of pDC dependent release of IFN-α. Of note, R848 induced similar IFN-α levels at a concentration of 1 µg/ml compared to eGFP mRNA and its azide-derivate RPA but at lower concentrations R848 was the most potent ligand to stimulate TLR7. Gardiquimod induced lower amounts of IFN-α in general, however, azide-functionalization abolished TLR7 activation completely (Fig. 4–12 A). In a second step, R848, GQI and azide-functionalized small molecules were added at a fixed concentration (0.1 µg/ml) to 0.01, 0.1 and 1 µg/ml eGFP mRNA to examine a possible synergistic effect of RNA and small molecules on TLR7 activation. Indeed, the addition of 0.1 µg/ml R848 to eGFP mRNA significantly increased IFN-α release at least at the two lower RNA concentrations. Of

note, the addition of RPA resulted in a minor increase of IFN-α secretion upon stimulation but GQI and GDA did not affect IFN-α release induced by eGFP mRNA alone (Fig. 4–12 B).

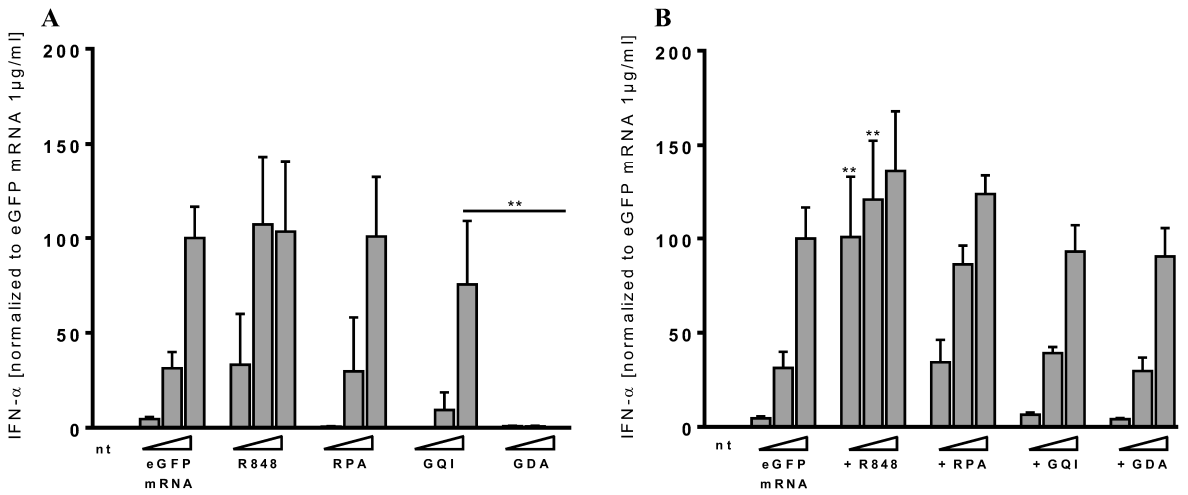

Fig. 4–12 Titration of small molecules and their corresponding azide-derivates. 400,000 human PBMCs were stimulated for 20 h with eGFP mRNA or small molecules at a total volume of 250 µl. Triangles indicate concentrations of 0.01, 0.1, and 1µg/ml. IFN-α release was measured in cell free supernatants by ELISA (A) IFN- α secretion induced by eGFP mRNA or the small molecules R848 and GQI and their respective azide-derivates RPA and GDA (B) Titration of eGFP mRNA with additional amount of small molecules. Triangles indicate concentrations of eGFP mRNA of 0.01, 0.1 and 1 µg/ml. Small molecules were added at a fixed concentration of 0.1 µg/ml. Data was normalized to cytokine production induced by 1.0 µg/ml eGFP mRNA alone to account for donor variation. All stimulations were performed in duplicate wells on three individual donors. Shown are mean + SEM

Interestingly, stimulation experiments of human PBMCs with high concentrations of unmodified small molecules always resulted in a drop of cytokine and IFN-α secretion. Furthermore, azide-functionalized small molecules demonstrated less TLR7 stimulation compared to their unmodified counterparts. To investigate the dose dependent effect of small molecules on PBMCs upon stimulation a cell viability assay was performed. Of note, IFN-α secretion induced by R848 was decreased at 1 and 10 µg/ml, whereby in case of the less stimulatory GQI no drop in IFN-α levels was detectable. In general, azide-functionalized small molecules were less stimulatory compared to unmodified R848 and GQI (Fig. 4–13 A). PBMCs were examined upon stimulation with small molecules and the azide-functionalized RPA and GDA to exclude toxic effects of the ligands. Indeed, stimulation with high concentrations of R848 decreased cell viability, whereby azide-functionalization did not affect the metabolic activity of PBMCs compared to non-treated control (Fig. 4–13 B). Of note, those samples with the strongest induction of IFN-α also demonstrated best vitality of cells.

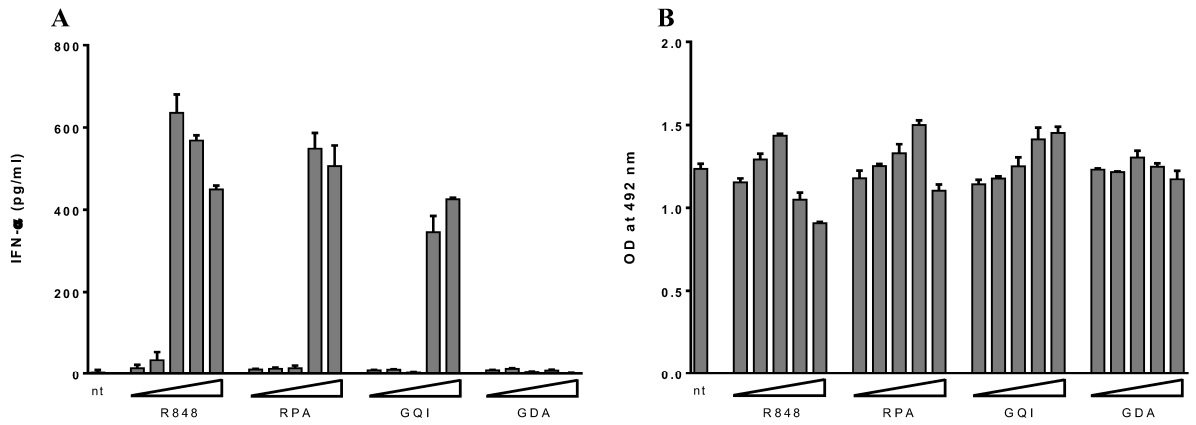

Fig. 4–13 Stimulation of human PBMCs and subsequent cell viability measurement. (A) 400,000 PBMCs per well were stimulated with indicated small molecules in 250 µl final volume. Triangles indicate concentrations of 0.001, 0.01, 0.1, 1 and 10 µg/ml. Cells were stimulated overnight and 150 µl cell free supernatant were taken for subsequent IFN-α quantification by ELISA. (B) PBMCs in remaining 100 µl media were supplemented with 20 µl of CellTiter solution and PBMCs were incubated for 3 h at 37°C in a humidified, 5% CO_2 atmosphere. Cell viability was assessed by measuring the absorbance of produced formazan at 492 nm in a Tecan sunrise photometer.

4.2.3.3 Covalent binding of small molecules to eGFP mRNA decreases immune stimulation

Previous experiments demonstrated an enhanced IFN-α secretion in case of co-transfection of R848 together with mRNA to PBMCs. Consequently, azide-functionalized small molecules were covalently bound at either 1% or 10% of total uridine to eGFP mRNA by copper-catalyzed click reaction. Activation of TLR7 was determined by IFN-α release measured by ELISA in cell-free supernatants. Of note, in contrast to former co-transfection results, physical coupling of small molecules to nucleobases of eGFP mRNA did not increase IFN-α release from PBMCs. In contrast, IFN levels were decreased by covalent bound small molecules (Fig. 4–14). The modification of 1% of overall uridines within eGFP mRNA with RPA did not decrease TLR7 activation, whereby 1% of GDA significantly reduced immune stimulation at higher mRNA concentration. Furthermore, modification of 10% of uridines significantly decreased TLR7 activation for both RPA and GTA at the two higher mRNA concentrations.

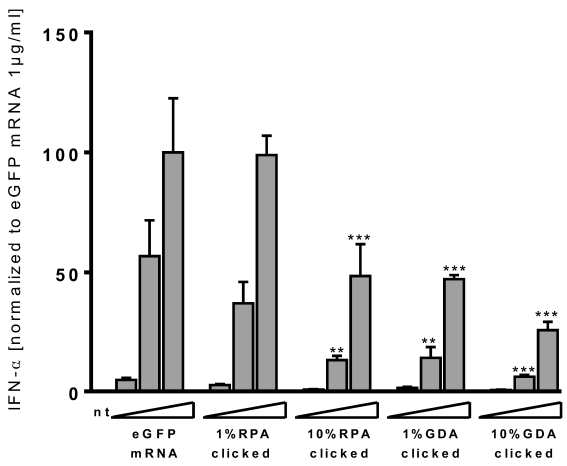

Fig. 4–14 Stimulation of PBMCs with clicked eGFP mRNA. PBMCs were transfected with DOTAP-encapsulated eGFP mRNA. Triangles indicate RNA concentrations of 0.01, 0.1 and 1 µg/ml. Absolute cytokine levels were detected in cell free supernatants 20 h after stimulation by ELISA. To account for donor variation, values were normalized to IFN-α levels induced by 1 µg/ml eGFP mRNA. All stimulations were performed in duplicate wells on three individual donors. Shown are mean + SEM

To elucidate if decreased IFN-α levels either resulted from an active competition between the two different binding sites of small molecules and RNA or a shielding effect of clicked mRNA to the receptor, sugar derivates were clicked to eGFP mRNA in a second step. The used azide-functionalized mono- (MMA) and tri-mannose (TMA) (Fig. 4–15 A, B) alone did not cause any cytokine release (data not shown). Modification of eGFP mRNA through MMA or TMA slightly decreased IFN-α release. Of note, 10% clicked mRNA showed a stronger decrease in cytokine release compared to 1% sugar clicked uridine (Fig. 4–15 C). However, decrease on immune stimulation based on clicked sugar derivates was less pronounced than IFN-α reduction caused by clicked small molecules.

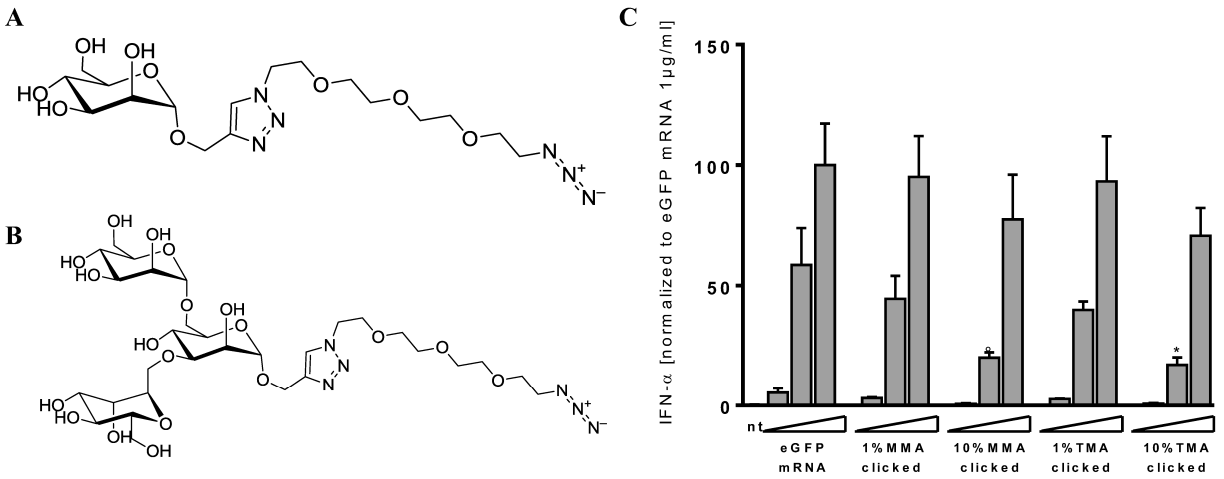

Fig. 4–15 Molecular structure of Mono-Mannose-N3 (MMA) Tri-Mannose-N3 (TMA) and IFN-α release induced by Mannose-clicked eGFP mRNA. Azide-functionalized mono- (A) and tri-mannose (B) and their respective immune stimulatory potential when clicked to eGFP mRNA (C). Human PBMCS were stimulated with mannose-clicked eGFP mRNA. Triangles indicate RNA concentrations of 0.01, 0.1 and 1 µg/ml. Cytokine release was detected in cell free supernatants 20 h after stimulation by ELISA. To account for donor variation, values were normalized to IFN-α levels induced by 1 µg/ml eGFP mRNA. All stimulations were performed in duplicate wells on three individual donors. Shown are mean + SEM ° p = 0.072

In summary, all introduced modifications within mRNA decreased the immunestimulatory potential. None of the otherwise immunestimulatory small molecules boosted immune stimulation when covalently bound to eGFP mRNA, but, in contrast, impeded TLR7 response. This effect was less pronounced for the tested sugar-derivates which were per se no TLR7 ligands. Of note, the classical TLR7 ligands R848 and GQI showed a stronger decrease of IFN-α level compared to mannose-derivates. A competition of small molecules and mRNA for the two different binding sites of TRL7 has to be considered.

4.2.3.4 A single modification within siRNA significantly reduces TLR7 activation

The incorporation of 1% or 10% alkyne-modified uridines necessary for click-reactions within long mRNAs happened randomly. As alkyne-modified uridines cannot be incorporated at defined positions within eGFP mRNA but were introduced stochastically, solely the overall content of modifications was predictable. To examine a more defined modified RNA species, an immune stimulatory siRNA was used for further experiments. The sense strand of anti-GFP siRNA (MH622) was already described as immune stimulatory and was alkyne-functionalized at cytosine at position 21. Copper-catalyzed click-reaction resulted in a siRNAs that only contained a single modification. Of note, the modification of siRNA by a single ligand significantly decreased TLR7 activation at RNA concentrations of 1µg/ml independent of the ligands structural origin (Fig. 4–16 A). While it is unclear, if the modification of a cytidine (siRNA) instead of uridine (eGFP mRNA) was affecting TLR7 recognition.

Significant decrease of immune stimulation of RNA by a single modification is a phenomenon known from the dominant inhibition of TLR7 by 2'-O-methylated guanosine. To distinguish an antagonising from a shielding effect of clicked small molecules, 1 µg/ml MH662 was co-transfected with different concentrations of MH662 clicked at position 21 with RPA, GDA or TMA. Gm8 modified MH662 served as positive control for dominant inhibition of TLR7. Of note, MH662 Gm8 obviously decreased activation of TLR7 by unmodified MH662 even though results were not statistically significant (Fig. 4–16 B). By contrast, co-transfection of unmodified and click-modified MH662 did not reduce IFN-α secretion compared to unmodified MH662 alone. The combination of both siRNAs rather increased IFN-α level due to residual stimulatory activity of clicked MH662.

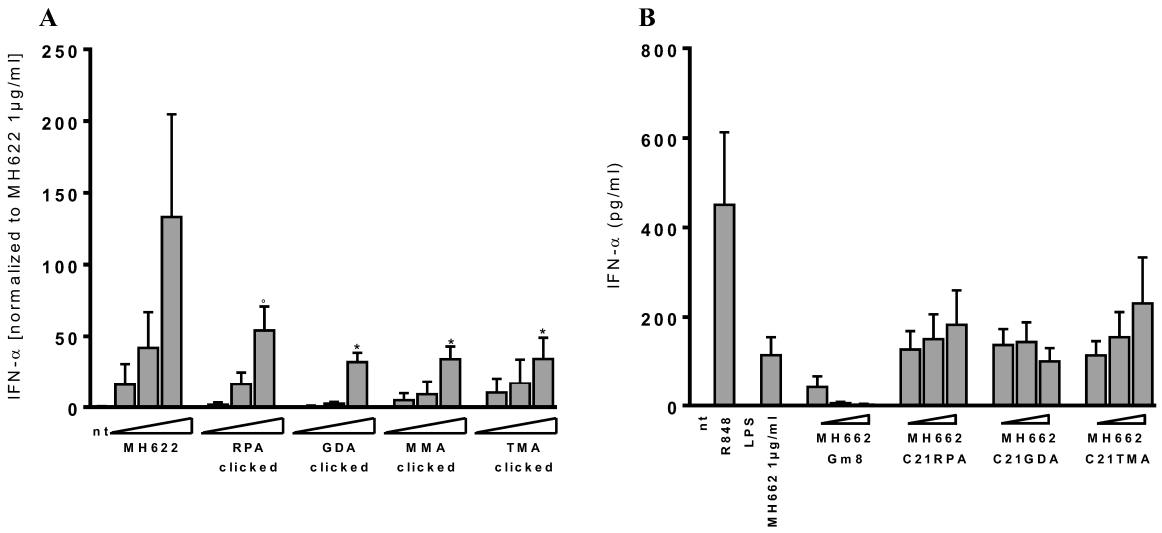

Fig. 4–16 Stimulation of PBMCs with clicked siRNA MH662. (A) PBMCs were transfected with DOTAP-encapsulated un-clicked or clicked sense strand of anti-GFP siRNA (MH622). Triangles indicate RNA concentrations of 0.01, 0.1 and 1 µg/ml. Absolute cytokine levels were detected in cell free supernatants 20 h after stimulation by ELISA. (B) Co-transfection of 1 µg/ml MH662 and either Gm modified siRNA or copper-clicked MH662 with indicated molecules. Triangles indicate concentrations of 0.01, 0.1 and 1 µg/ml of single clicked siRNA. To account for donor variation, values were normalized to IFN-α levels induced by 1 µg/ml MH662. All stimulations were performed in duplicate wells on three individual donors. Shown are mean + SEM
° p = 0.0618

Altogether, base modification of RNA with otherwise immune stimulatory or immunological inert molecules did not improve immune stimulation. By contrast, TLR7 activation was reduced by the tested RNA couplings. Within short siRNAs this effect was most prominent and a single modification decreased immune stimulation significantly. Of note, by comparing clicked and Gm modified MH662, no dominant inhibition of TLR7 was detectable.

4.3 Identification of a tri-nucleotide motif that inhibits recognition of RNA by TLR7 and TLR8

2'-O-methylation within different types of RNAs is known to antagonize TLR7 and TLR8 but whether the modification acts in a specific inhibitory sequence motif is poorly understood. A previous study identified a fundamental [DmR] motif (D= all but C; R= purine) within RNA required to avoid TLR7 stimulation [93]. Yet, a sequence motif inhibiting TLR8 was pending. To study especially the sequence dependency of the 2'-O-methylation induced antagonistic effect on TLR7 and TLR8 (that is inhibition of an otherwise stimulatory RNA by 2'-O-methylated RNA), a short 2'-O-methylated RNA fragment of *E. coli* $tRNA^{Tyr}$ was used. The sequence of the 26-mer oligoribonucleotide (ORN) corresponded to the native D-loop tRNA sequence which is naturally methylated at position 18 (Gm18). To investigate the dominant inhibitory effect of the single 2'-O-methylated ORNs, co-transfection experiments with otherwise stimulatory bacterial RNA (bRNA) were performed. To calculate the half maximal inhibitory concentration (IC_{50}) of the tested RNAs, methylated tRNA fragments and an unmodified specificity control ORN were titrated to a constant amount of stimulatory bRNA. Furthermore, by shortening the tRNA fragment containing the most efficient inhibitory motif, the minimal length of antagonistic 2'-O-methylated oligoribonucleotides was determined. Secretion of TNF-α served as readout for TLR8 activation in monocytes and IFN-α release indicated TLR7 stimulation in pDCs [38, 73].

4.3.1 Permutation of the nucleobase upstream of the methylated nucleotide is not affecting dominant inhibitory potential of RNA

To investigate the impact of the nucleobase at position 17 on the dominant inhibitory effect of Gm18 within tRNAs, the base upstream of the 2'-O-methylated guanosine was permutated. Upon co-stimulation of human PBMCs with indicated 26-mer ORNs and bRNA, secretion levels of TNF-α and IFN-α indicated similar antagonistic effects of all four sequence motifs (Fig. 4–17 A, B). Furthermore, IC_{50} of the methylated ORNs was quite similar for both TLR7 and TLR8 (Fig. 4–17 C). Of note, the native sequence motif 5'-CGm18GC-3' was not more efficient than other 2'-O-methylated ORNs.

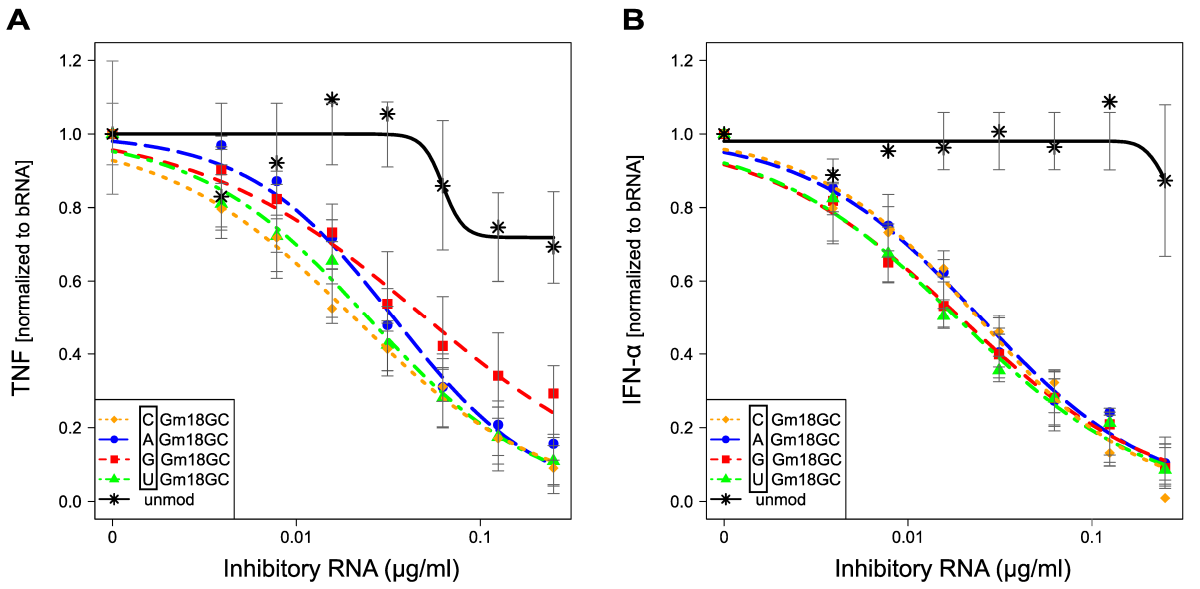

C

IC50 [µg/ml] (±Std. error)

	TNF	IFN-α
CGm18GC	0.020(±0.003)	0.024(±0.003)
AGm18GC	0.034(±0.003)	0.025(±0.003)
GGm18GC	0.048(±0.018)	0.019(±0.003)
UGm18GC	0.024(±0.005)	0.018(±0.003)
unmod	NA	NA

Fig. 4–17 Effect of base permutation at position 17 of *E. coli* tRNA^{Tyr} fragments on bRNA-dependant TLR7 and TLR8 activation. Human PBMCs (400,000/well) were stimulated overnight with a constant amount of bRNA (0.5 µg/ml) and different concentrations of 2'-O-methylated ORNs or an unmodified specificity control ORN (0.0039, 0.0078, 0.015, 0.031, 0.0625, 0.125, 0.25 µg/ml). The nucleobase at position 17 was permutated as indicated. TNF-α (A) as well as IFN-α (B) levels were quantified in cell-free supernatants by ELISA. To account for donor variation, cytokine secretion was normalized to values induced by bRNA alone. Each data point demonstrates the mean value of 3-6 individual donors and error bars indicate the confidence interval of the model. Curve fit and IC_{50} values (µg/ml) (C) were calculated with R software. Figure adapted from Schmitt *et al.* 2017

4.3.2 TLR7 and TLR8 activation is efficiently attenuated by all 2'-O-methylated nucleotides except cytidine at position 18

Since alteration of the base at position 17 did not affect the dominant inhibitory effect of any 2'-O-methylated ORN, subsequently the nucleobase carrying the methylated nucleotide (position 18) was permutated. Contrary to position 17, the exchange of the nucleobase at position 18 influenced dominant inhibitory effects of the tested ORNs and 2'-O-methylated cytidine failed to inhibit TLR7 and TLR8 activation by bRNA (Fig. 4–18 A-C). Guanosine, adenosine and uridine provided comparable IC_{50} values, whereby 2'-O-methylated cytidine showed similar results as the unmodified ORN.

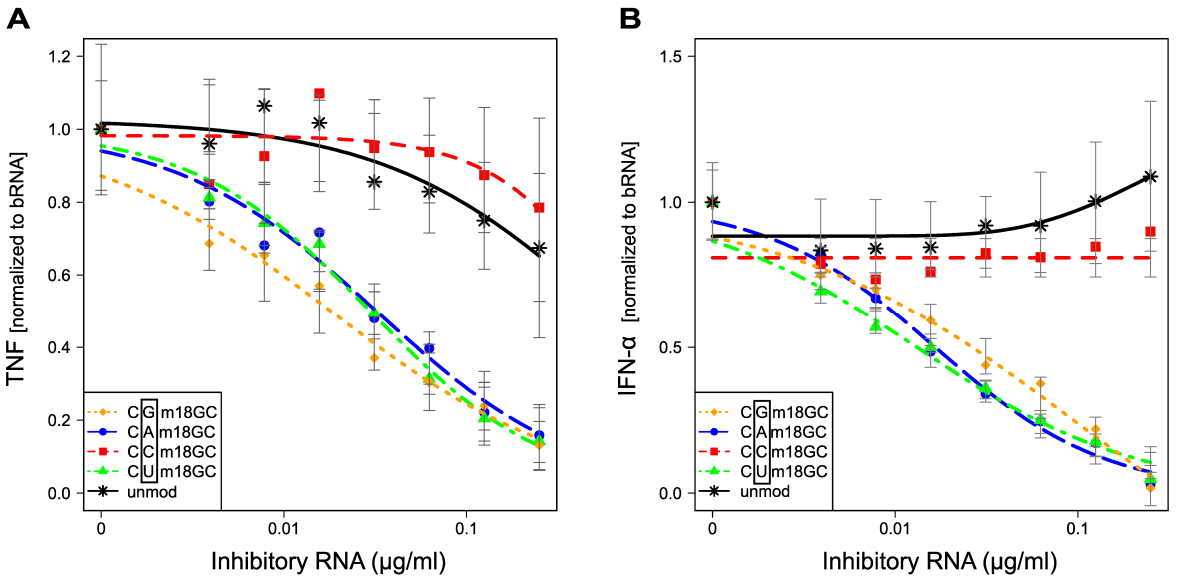

C

IC50 [µg/ml] (±Std. error)

	TNF	IFN-α
C**G**m18GC	0.018 (±0.004)	0.090 (±0.109)
C**A**m18GC	0.032 (±0.005)	0.016 (±0.001)
C**C**m18GC	NA	NA
C**U**m18GC	0.030 (±0.004)	0.013 (±0.001)
unmod	NA	NA

Fig. 4–18 Effect of nucleobase permutation at position 18 of tRNA fragments on TLR7 and TLR8 stimulation by bacterial RNA. Isolated PBMCs were stimulated overnight as described in Fig. 4–17 and TNF-α (A) and IFN-α (B) secretion was measured in cell-free supernatants as read-out for TLR8 and TLR7 stimulation, respectively. The nucleobase at position 18 was permutated as indicated. Data points represent the normalized mean value of five individual donors, except for the unmodified ORN (n=4) and the concentrations 0.0039 and 0.0078 µg/ml of inhibitory RNA for TNF (n=3). Curve fit and IC50 values (µg/ml) (C) were calculated with R software and error bars indicate the confidence interval of the method. Figure adapted from Schmitt *et al.* 2017

4.3.3 Permutation of the nucleobase at position 19 discriminates between TLR7 and TLR8 inhibition

In contrast to position 17 and 18, systematic permutation of the nucleobase at position 19 resulted in clear differences in immunosilencing capacities regarding TLR7 and TLR8 inhibition. For efficient antagonism of TLR8 within human PBMCs a purine base at position 19 (Gm18G or Gm18A) was mandatory (Fig. 4–19 A, C). The incorporation of a pyrimidine base at position 19 (Gm18U or Gm18C) was not sufficient to inhibit bacterial RNA induced TNF-α secretion compared to the unmodified control. However, all bases except cytidine (Gm18A, Gm18G and Gm18U) following the methylated guanosine were sufficient to antagonize TLR7 stimulation by bacterial RNA (Fig. 4–19 B, C).

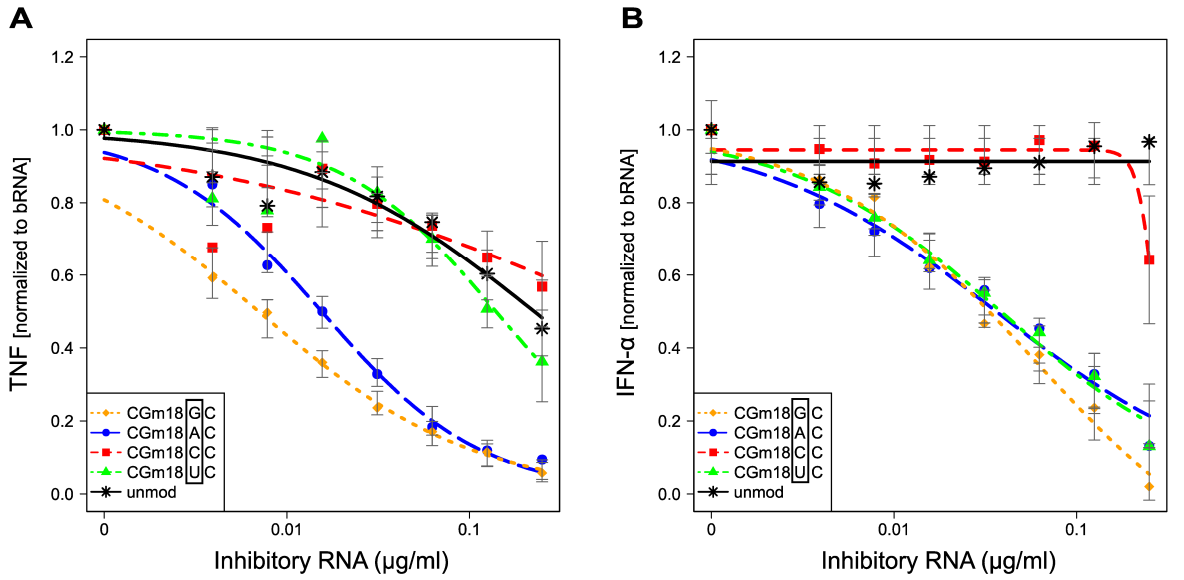

C

IC50 [µg/ml] (±Std. error)

	TNF	IFN-α
CGm18**G**C	0.007 (±0.001)	0.058 (±0.030)
CGm18**A**C	0.015 (±0.001)	0.036 (±0.007)
CGm18**C**C	NA	NA
CGm18**U**C	0.139 (±0.021)	0.038 (±0.005)
unmod	0.228 (±0.063)	NA

Fig. 4–19 Effect of base permutation at position 19 within *E. coli* derived tRNA^{Tyr} sequence on TLR7 and TLR8 antagonisation. Human PBMCs were stimulated as indicated in Fig. 4–17 and TNF-α (A) and IFN-α (B) secretion was measured in cell-free supernatants by ELISA. Permutation of position 19 was performed as indicated. For TNF, data points represent the normalized mean value of 7-8 individual donors, except for the concentration 0.0039 and 0.0078 µg/ml (n=3). In case of IFN-α, each data point demonstrates the average value of fife independent donors. Curve fit and IC50 values (µg/ml) (C) were calculated with R software and error bars indicate the confidence interval of the method. Figure adapted from Schmitt *et al.* 2017

4.3.4 The nucleobase at position 20 is the most discriminative one concerning TLR8 antagonisation

The nucleobase two positions downstream of Gm18 was consistently altered to analyse the effect of base permutation at position 20 regarding TLR7 and TLR8 antagonism. In case of bRNA-dependent TLR8 stimulation, all 2'-O-methylated nucleobases but cytidine within tRNA fragments showed only a minor inhibition of TNF-α release. Of note, the most potent antagonistic effect on TLR8 was observed for the naturally occurring sequence context CGm18GC (Fig. 4–20 A, C). In contrast, all four nucleobases at position 20 allowed the inhibition of TLR7 towards stimulatory bRNA whereby guanosine showed the weakest antagonistic effect on both, TLR7 and TLR8 (Fig. 4–20 A-C).

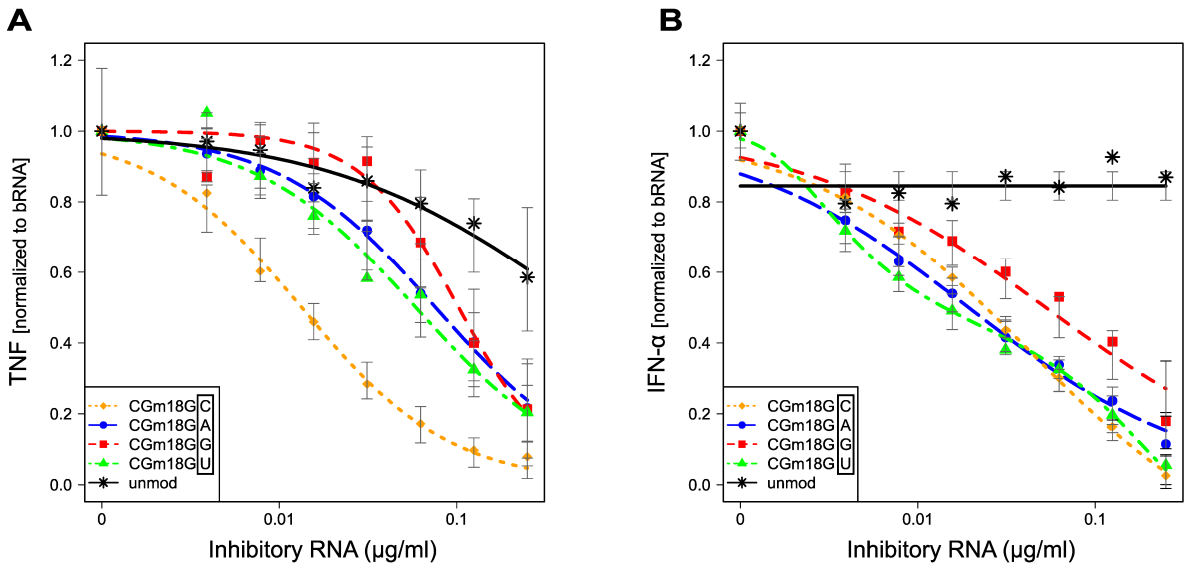

C

IC50 [µg/ml] (±Std. error)

	TNF	IFN-α
CGm18G**C**	0.013 (±0.001)	0.042 (±0.014)
CGm18G**A**	0.076 (±0.014)	0.019 (±0.002)
CGm18G**G**	0.102 (±0.016)	0.052 (±0.009)
CGm18G**U**	0.059 (±0.008)	0.023 (±0.008)
unmod	NA	NA

Fig. 4–20 Effect of nucleobase permutation at position 20 of tRNA fragments on TLR7 and TLR8 stimulation by bacterial RNA. Human PBMCs were stimulated and TNF-α (A) and IFN-α (B) secretion was analysed as described in Fig. 4–17. Nucleobase at position 20 was permutated as indicated. IC_{50} (µg/ml) (C) and curve fit were calculated using R software. Each data point for TNF and IFN represents mean values of 5-7 different donors. Figure adapted from Schmitt *et al.* 2017

4.3.5 The position of Dm motif and length of RNA fragments determines their dominant inhibitory capacity on TLR8

To define the minimal length of immunosilencing 2'-O-methylated RNAs, the initial 26-mer ORN according to the native $tRNA^{Tyr}$ sequence was shortened at both, the 5' and 3' end, up to a 5-mer ORN with central 2'-O-methylated guanosine. Of note, a nine nucleotide long 2'-O-methylated RNA fragment seemed to be most effective in TLR8 suppression. The analysed 15-mer ORN was slightly less efficient compared to the 9-mer ORN. Even weaker was the dominant inhibitory of the 7-mer and 26-mer ORN which showed quite similar results. Of note, a 2'-O-methylated 5-mer ORN was not sufficient to antagonize TLR8 response towards stimulatory bRNA (Fig. 4–21 A). In the next step, the identified optimal 2'-O-methylated 9-mer ORN was used for systemic shifting of the inhibitory GmGC motif from 5' to 3' end. Of note, localization of the Gm at position 2-7 did not affect the immunosilencing properties of the 9-mer ORN. Dominant inhibitory effects of the RNA were slightly decreased when Gm was placed at position 1. On the other hand the placement of 2'-O-methylated guanosine at position 8 or 9 (with concomitant disruption of above identified the tri-nucleotide motif) abrogated immunosilencing capacity of the 9-mer ORN (Fig. 4–21 B).

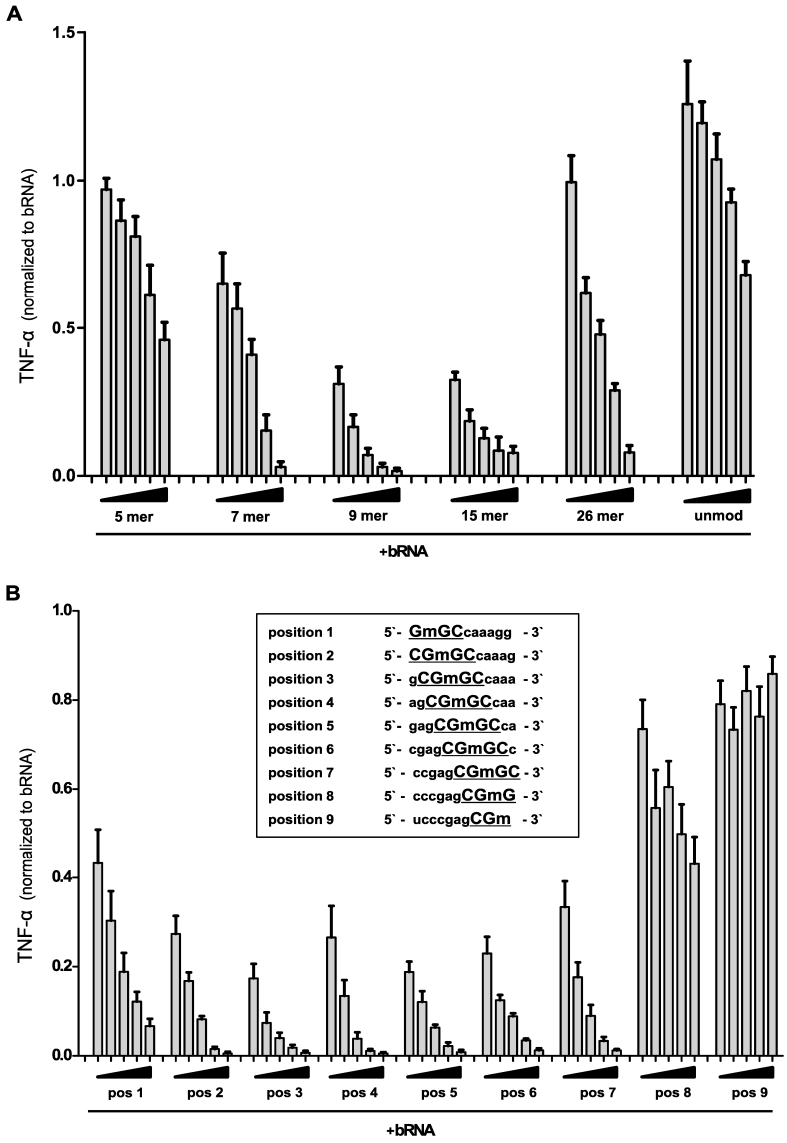

Fig. 4–21 Analysis of 2'-O-methylated ORN length and positional effects of Gm motif on TLR8 inhibition. Human PBMCs were co-transfected overnight with bRNA (0.5µg/ml) and 2'-O-metylated ORNs at different concentrations. Triangles indicate concentrations of 2'-O-methylated ORNs of 0.25, 0.125, 0.0625, 0.031 and 0.015 µg/ml. TNF was measured in cell free supernatants by ELISA. (A) 26-mer ORN with central Gm motif was shortened stepwise down to indicated length. (B) Inhibitory GmGC motif within a 9-mer tRNA fragment was permutated from 5' to 3' end as indicated. To account for donor variation, all cytokine values were normalized to cytokine production by 0.5µg/ml bRNA alone (n=2-3 + SEM). Figure adapted from Schmitt *et al.* 2017

In summary, two tri-nucleotide motifs were identified which effectively inhibit bRNA induced cytokine release up on activation of TLR7 and 8. Of note, the motif differed between TLR7 and TLR8, whereby the inhibitory sequence seemed to be more stringent for TLR8 compared to TLR7. We elucidated a [*D*m*R*C] motif (*D*= all but C, *R*= G, A) for inhibition of TLR8 and [*D*m*DN*] motif (*D*= all but C, *R*= G, A) for TLR7 antagonism. Furthermore, a length of 9 nucleotides was determined as most efficient ORN size to abrogate TLR8 activation. Moreover, permutation of the inhibitory tri-nucleotide motif showed that localization is less important as long as the inhibitory GmGC motif is preserved.

4.3.6 Immune silencing effects of 2'-O-methylated RNA requires co-delivery with immune stimulatory RNA

Considering the previously identified optimized tri-nucleotide motif inhibiting TLR7 and TLR8, we thought about a clinical application of modified RNA oligoribonucleotides to interrupt self-RNA-driven activation of TLR7 and TLR8. Of note, in former experiments stimulatory and inhibitory RNA were always mixed before encapsulation with DOTAP and therefore delivered to the same endolysosome. Under physiological or pathophysiological conditions self-RNA and inhibitory exogenous RNA likely end up in different endosomes. To mimic those conditions immune stimulatory RNA (ssRNA40) and immune inhibitory 2'-O-methylated 26-mer ORN (Gm18) were either packaged together or separately to stimulate BlaER1 cells. Of note, before stimulation BlaER1 cells were transdifferentiated to monocyte/macrophage-like cells as described in section 3.2.1.2. As a control BlaER1 cells were stimulated with ssRNA40 or Gm18 ORN alone to determine immune effects of the two different RNAs. 20 h after transfection BlaER1 cells were examined by FACS analysis. Upregulation of MHC-class II and CD86 were used as markers for TLR8 activation and immune stimulation. Of note, roughly 50% auf BlaER1 cells were MHC-class II positive and CD86 positive before stimulation (Fig. 4–22 A). The 2'-O-methylated Gm18 ORN did not induce a further upregulation of stimulation markers, whereas transfection of ssRNA resulted in almost 100% MHC-class II positive cells (Fig. 4–22 A-C). Of note, separately delivered ssRNA40 and Gm18 ORN resulted in a similar percentage of MHC-class II positive cells compared to ssRNA40 stimulation alone and mean fluorescence intensity (MFI) was only slightly decreased in case of MHC-class II surface expression (Fig. 4–22 A, B). However, when (stimulatory) ssRNA40 and (inhibitory) Gm18 ORN were packed together, surface activation markers decreased notably in expression (Fig. 4–22 A-C).To further examine the delivery of RNA, BlaER1 cells were transfected with atto-labeled ssRNA40 and atto-labeled Gm18 ORN. Transfected BlaER1 cells were examined by confocal microscopy. Indeed, when Gm18 ORN and ssRNA40 were packaged together, fluorescence signals of both atto-dyes were co-located in the cells, however in case of separately packaged RNAs, no co-localization was detectable (data not shown). Altogether, 2'-O-methylation within RNA was only sufficient to antagonize immune response towards stimulatory RNA when both, inhibitory and stimulatory RNA were delivered into the same endosome. Of note, preliminary experiments demonstrated at least equal amounts of inhibitory and stimulatory RNA of similar length were necessary to reduce immune stimulation. To abrogate immune stimulation completely, a higher proportion of inhibitory compared to stimulatory RNA was required.

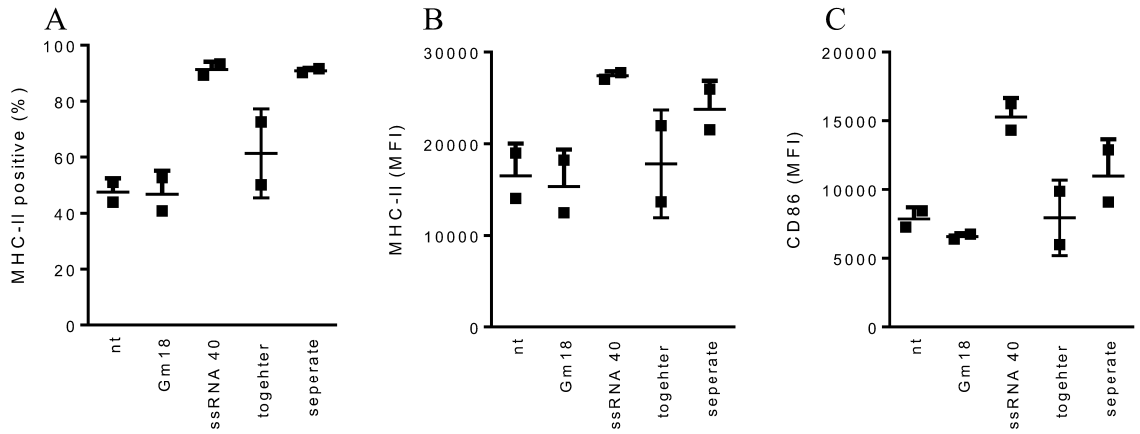

Fig. 4–22 Stimulation of BlaER1 cells with Gm18 26-mer ORN and ssRNA40. 500,000 BlaER1 cells were stimulated with 1.25 µg/ml ssRNA40 and Gm18 ORN as controls in a 6-well plate. Together and separately packaged RNA was added at a final concertation of 2.5 µg/ml RNA per ml to obtain comparable amounts of stimulatory ssRNA40. Cells were stimulated for 20 h at 37 °C, 5% CO_2. BlaER1 cells were stained with anti-human anti-MHC-class II antibody (APC) and anti-human anti-CD86 antibody (PE) for FACS analysis. (A) Number of MHC-II positive cells in%. (B) Mean fluorescence intensity (MFI) of MHC-class II (APC) positive cells (C) MFI of CD86 (PE) positive cells.

Altogether, co-delivery of inhibitory and stimulatory RNA was required to potentially antagonize TLR7 and TLR8 stimulation and to prevent immune cell activation and upregulation of costimulatory molecules.

4.4 Analysis of the importance of tRNA 2'-O-methylation for physiological modulation of immune stimulation

Dominant inhibitory characteristics of 2'-O-methylation were identified within bacterial tRNAs. Methylation of certain tRNAs within the whole tRNA fraction (composed of tRNAs carrying and not carrying a 2'-O-methylation modification) was sufficient to antagonize the immune response [70]. However, the relevance of 2'-O-methylation within tRNAs for immune stimulation of total RNA samples or whole organisms was pending. Furthermore, importance of 2'-O-methylation within eukaryotic tRNA was not elucidated. Therefore, tRNA, rRNA and total RNA samples of prokaryotic and eukaryotic origin were examined with regard to 2'-O-methylation of tRNAs. Moreover, immune stimulation of whole bacteria dependent on 2'-O-methylation of tRNA was investigated.

4.4.1 Verification of *E. coli* and *S. cerevisiae* wt strains and their corresponding methyltransferase deficient mutants

In further experiments wt strains and the tRNA-methyltransferase deficient mutants of *E. coli* (ΔtrmH) *and S. cerevisiae* (Δtrm3) were used to examine Gm18-dependant recognition of isolated RNA fractions and whole organisms. In order to verify G18 methylation of tRNAs of wt strains and methyltransferase deficient mutants, isolated tRNAs were examined by Prof. Dr. Yuri Motorin (Next-Generation Sequencing core facility, Biopole Lorraine University, Vandoeuvre-les-Nancy, France) for Illumina sequencing-based RiboMethSeq analysis. This approach allowed the site specific detection of 2'-O-methylated nucleotides within tRNAs. The method is based on alkaline hydrolysis of tRNA and subsequent Illumina sequencing. Of note, the 3' phosphodiester bond of 2'-O-methylated RNA is resistant to alkaline hydrolysis [130]. Thus, only a low number or even no RNA fragments starting or ending 3' to a 2'-O-methylation occurred within the RNA pool. Upon library preparation and sequencing, 5'-and 3'-end counting demonstrated a drop in the coverage of 2'-O-methyl protected sites. The sequencing data was further analysed and a heatmap depicting normalized mean methylation scores was created by Yuri Motorin (Fig. 4–23). Of note, the heatmaps represent all identified 2'-O-methylation sites within different tRNA isoacceptors. However, most prominent differences of 2'-O-methylation were identified for Gm18 of both, *E. coli* and *S. cerevisiae* tRNAs. High abundance of 2'-O-methylation was depicted in dark pink, whereas absence of Gm18 was demonstrated in dark blue. Of note, comparison of wt and methyltransferase

deficient mutants confirmed the absence of Gm18 in trmH and trm3 deficient mutants: certain isoacceptors of tRNAs were 2'-O-methylated in the wt (dark pink) but not in the methyltransferase deficient mutants (dark blue). Furthermore, 2'-O-methylation of other nucleotides than G18 were not affected by methyltransferase deficiency. For instance C34, U32 or U44 demonstrated a similar extend of 2'-O-methylation in wt and methyltransferase deficient strains.

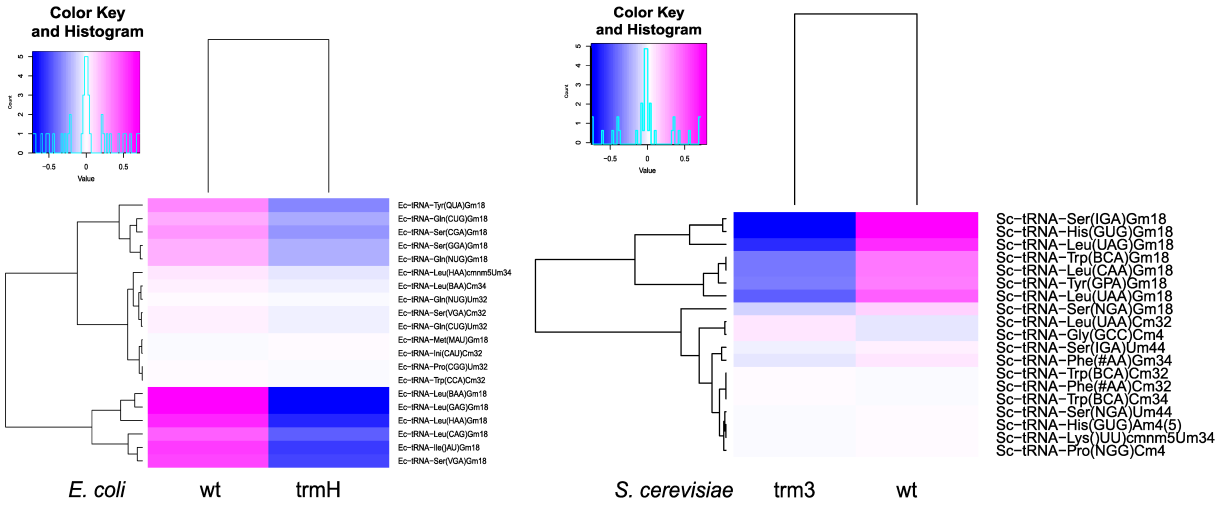

Fig. 4–23 Heatmap of analysed RiboMethSeq data. Clustering of tRNAs sites according to their 2′-O-methylation. Left: *E. coli* tRNA of wt and methyltransferase deficient mutant. Right: *S. cerevisiae* tRNA of methyltransferase deficient mutant and wt. Heatmap displayed normalized mean methylation scores. tRNA isoacceptors and modified nucleotide positions were indicated on the right. Colour key and histogram were depicted at the upper left part of the figure.

4.4.2 2'-O-methylated guanosine within tRNA fractions regulates their immunestimulatory potential

In cooperation with Prof. Dr. Mark Helm, Institute of Pharmacy and Biochemistry, Johannes Gutenberg-University of Mainz we got access to fractionated tRNAs of *Saccharomyces cerevisiae*. Those tRNAs were eluted in 24 different fractions by liquid chromatography, whereby each fraction contained different types of isoacceptors. Subsequent analysis of each fraction by LC-MS/MS approach (performed by Patrick Keller, Helm group, Mainz) identified the relative amount of various modified nucleotides within different fractions. Elution profiles of modifications among the different fractions were depicted by plotting the relative amount of modification against the fraction number. In addition, immune stimulation experiments were performed and human PBMCs were transfected with tRNAs of the 24 different fractions. Of note, the stimulation profile of IFN-α release of pDCs by TLR7 activation (Fig. 4–24 A) was inversely proportional to the relative amount of 2'-O-methylated guanosine (Gm) compared to total guanosine (G) within different tRNA fractions (Fig. 4–24 B). Those tRNA fractions which induced the highest levels of IFN-α showed the lowest amounts of Gm and vice versa. These results were in accordance with previous publications, which identified Gm as an immune inhibitory modification [70, 91, 92]. Of note, Kaiser *et al.* demonstrated an immune inhibitory effect not exclusively for Gm but also for 2'-O-methylated adenosine (Am) and uridine (Um) within tRNAs [93]. For this reason, fractions containing Am (Fig. 4–24 C) and Um (Fig. 4–24 D) were further examined. Interestingly, tRNAs with those modifications eluted in the same fractions as Gm, whereby fraction 11 and fractions 17-24 were the only fractions with low levels of Gm, Am and Um and therefore induced high amounts of IFN-α. An overlay of the relative amount of Gm, Am and Um of each fraction and the corresponding IFN-α release illustrated the context of 2'-O-methylated nucleotides and corresponding IFN-α levels (Fig. 4–24 E). Of note, the overall appearance of Um (yellow) was proportionally low compared to Gm (green) and Am (blue). A dose response model with R^2=0.9533 indicated a strong dependency of IFN-α release on the relative amount of Gm within tRNA fractions (Fig. 4–24 F).

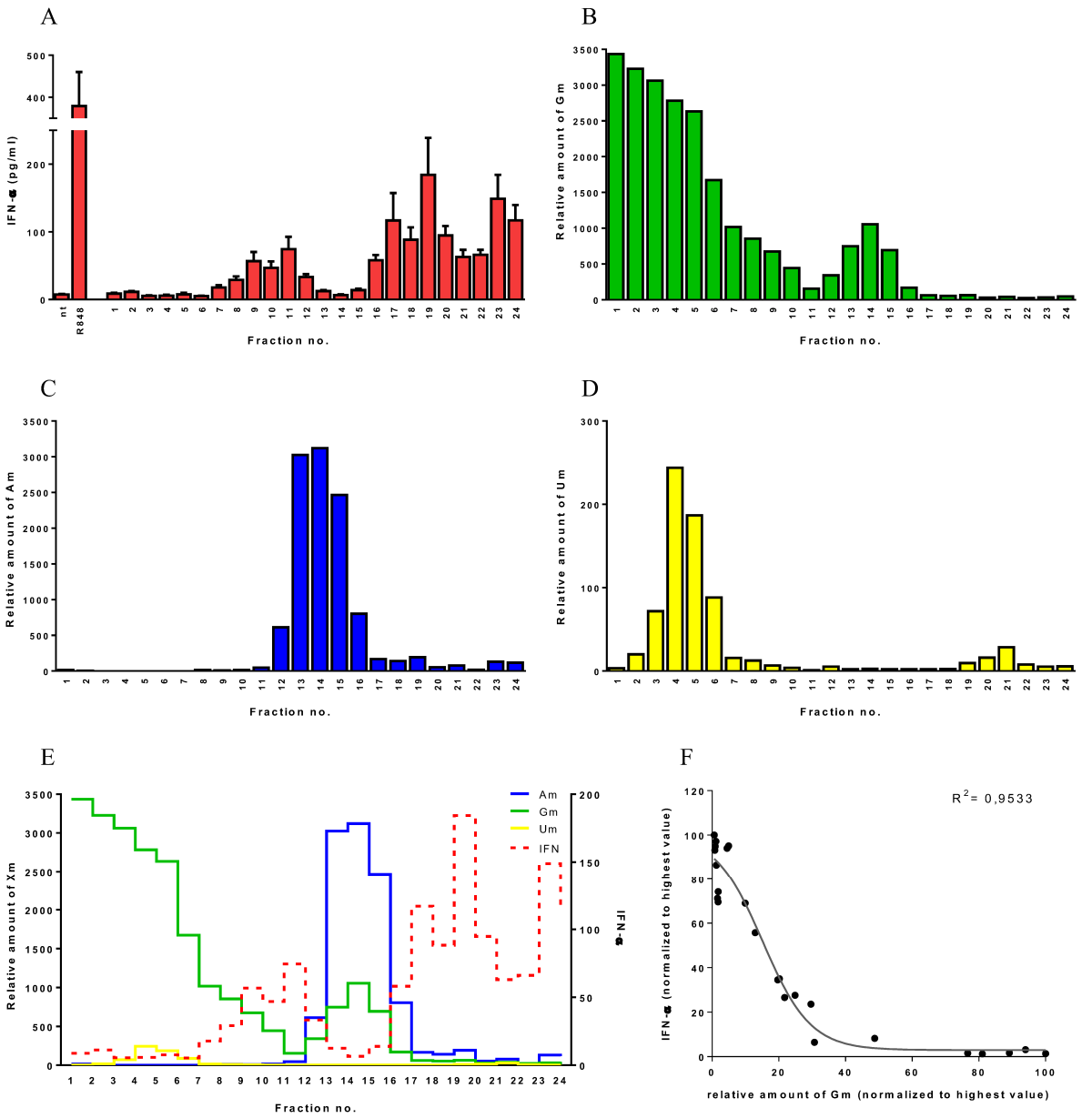

Fig. 4–24 IFN-α release of human PBMCs upon stimulation with *S. cerevisiae* tRNA fractions and corresponding elution profiles of 2'-O-methylated nucleotides. (A) Human PBMCs (400,000/well) were stimulated with 24 different DOTAP-encapsulated tRNA fractions. Stimulations were performed in duplicate wells and IFN-α was measured in cell-free supernatants by ELISA. Bars represent IFN-α value of 3 individual donors +SEM. (B-D) Relative amount of indicated 2'-O-methylated nucleotides measured by LC-MS/MS (Patrick Keller). (E) Overlay of IFN-α release and relative amount of Am, Gm and Um of the 24 tRNA fractions. Left Y-axis demonstrates relative amount of 2'-O-methylated nucleotides and right Y-axis displays release of IFN-α (F) Dose response model of IFN-α and relative amount of Gm was calculated by GraphPad Prism. R square indicated the goodness of fit for appropriated nonlinear dose response model.

To elucidate the effect of Gm within yeast tRNA, human PBMCs were next stimulated with whole tRNA fraction isolated from *S. cerevisiae* wt strains and corresponding trm3 deficient mutant (Fig. 4–25). Of note, isolated tRNAs of both, wt and trm3 deficient mutants induced IFN-α release. However, IFN-α secretion upon PBMC stimulation with tRNAs isolated from trm3 deficient mutants was slightly increased compared to wt tRNA. Immune stimulation

with total RNA preparations, however, induced only minor levels of IFN-α without considerable differences for RNAs derived from *S. cerevisiae* wt or trm3 deficient mutants.

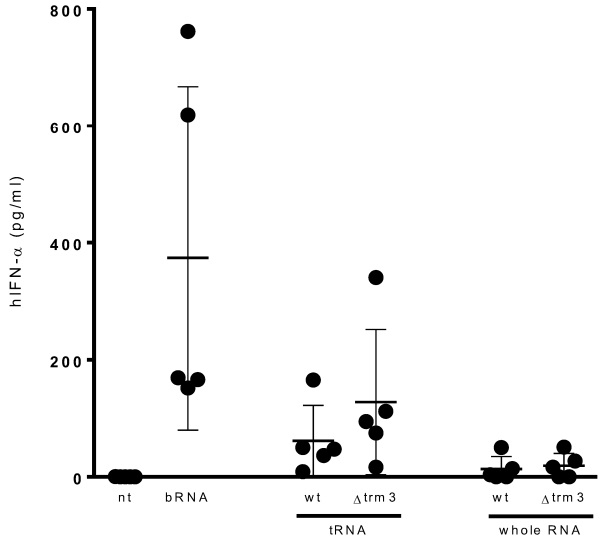

Fig. 4–25 Immune stimulation of isolated tRNAs and total RNA preparations isolated from *S. cerevisiae* wt strains and trm3 deficient mutant. 200,000 PBMCs were stimulated with 1 µg/ml encapsulated bRNA as stimulation control and indicated tRNAs. IFN-α release was measured in cell-free supernatants by ELISA. 5 independent donors were stimulated in duplicate wells and mean value of replicates were represented by one dot. Shown mean + SD

Altogether, the data confirmed the relevance of Gm18 for immune inhibition within isolated eukaryotic tRNA fractions. However, 2'-O-methylation of few yeast tRNA isoacceptors demonstrated only a minor effect on innate immune stimulation of total tRNA and no physiological relevance for lack of immunestimulation by whole RNA.

4.4.3 Immune stimulatory potential of bacterial tRNA depends on growth conditions of *E. coli*

Several studies investigated the relevance of Gm18 within tRNAs on immune stimulation [70, 74, 93]. Jöckel *et al.* demonstrated that tRNAs isolated from trmH deficient *E. coli* mutants were significantly more immune stimulatory compared to tRNAs isolated from wt *E. coli*. Furthermore, immunosilencing potential of tRNA fractions isolated from Gm18 deficient mutants could have been restored per *in vitro*-methylation of tRNAs by recombinant *T. thermophilus* trmH. To investigate the relevance of Gm18 within total RNA preparations including tRNA and rRNA we initially intended to reproduce those tRNA results using *E. coli* wt strain and trmH deficient mutant. Of note, as described in Jöckel *et al. E. coli* strains were cultured at 37°C in LB medium until mid-log phase to isolate bacterial RNA by TRIzol protocol and subsequently performed column based tRNA purification. However, the

obtained tRNA samples did not reflect the published results but demonstrated no or few differences in immune stimulation of *E. coli* wt and trmH deficient mutant. Initially, we considered contaminations with 5S rRNA within tRNA fractions masking immunosilencing effects of *E. coli* wt tRNAs (data not shown). To this end, different RNA isolation methods were examined and resulting RNA fractions were characterized. As described in section 4.1.1 column based RNA purification was replaced by an agarose gel based RNA isolation protocol. Subsequent immune stimulation experiments with isolated tRNAs demonstrated slightly increased TLR7 activation and therefore higher IFN-α levels for tRNAs isolated from trmH deficient mutants compared to *E. coli* wt (Fig. 4–26 A). Nevertheless, differences in immune stimulation of *E. coli* wt and trmH deficient mutant were not statistically significant. Interestingly, evidence from literature indicated a dependency of 2'-O-methylation of tRNA on the growth conditions of bacteria [84, 86, 90, 131]. For instance, several publications demonstrated an increase of 2'-O-methylation within tRNAs when bacteria grew at higher temperatures to stabilize tRNA secondary structures. Thus, regulation of 2'-O-methylation by other stress condition than high temperatures was considered to regulate Gm18 within tRNAs. Indeed, preliminary data of the cooperating working group of Prof. Dr. Yuri Motorin (Next-Generation Sequencing core facility, Biopole Lorraine University, Vandoeuvre-les-Nancy, France) indicated that 2'-O-methylation of G18 within tRNAs was upregulated by nutrient starvation or sub-lethal concentrations of antibiotics. Therefore, side by side comparison of immunestimulatory potential of isolated tRNA from starved and non-starved *E.coli* was performed. Of note, tRNAs isolated from *E. coli* wt and trmH deficient mutant grown under optimal growth conditions (37 °C, LB medium, 250 rpm) induced mostly similar levels of IFN-α (Fig. 4–26 A). However, isolated tRNAs from 24 h starved *E. coli* (37 °C, 1x PBS, 250 rpm, section 3.2.4.2) demonstrated significant differences in immune stimulation of wt strain or trmH deficient mutant at a tRNA concentration of 1 µg/ml (Fig. 4–26 B). Of note, immunestimulatory capacity of ribosomal and total RNA preparations was neither affected by trmH deficiency nor the growth conditions. All rRNA and total RNA preparations of *E. coli* wt and trmH deficient mutant induced a comparable IFN-α response (Fig. 4–26 A, B).

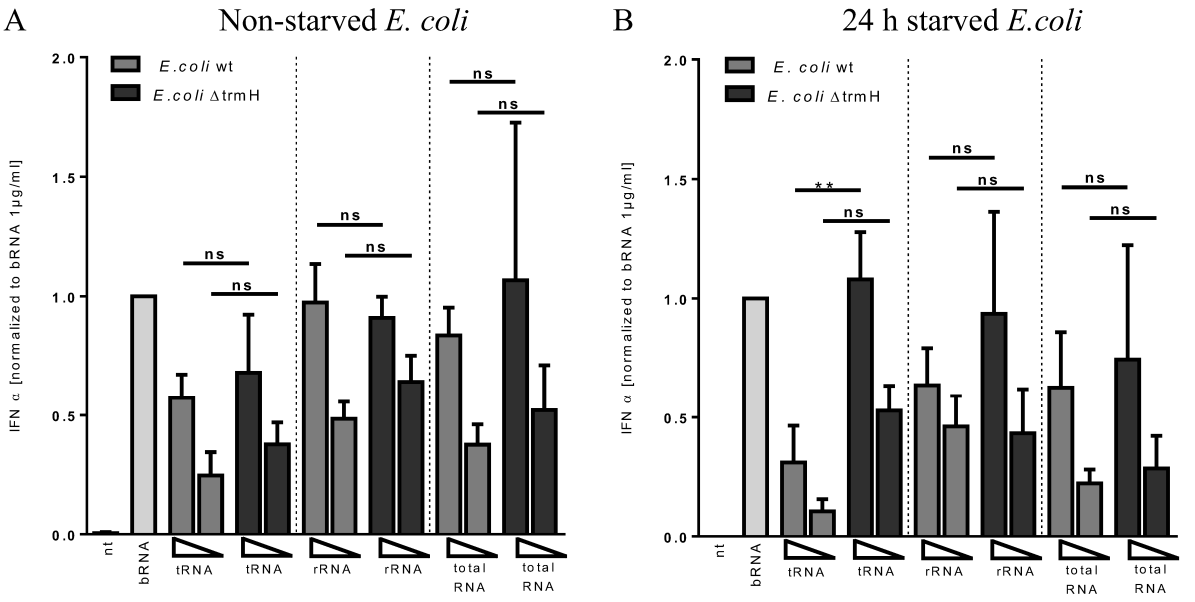

Fig. 4–26 Immune stimulation of isolated RNAs from differentially cultured *E. coli* wt strain and trmH deficient mutant. 200,000 human PBMCs/well were stimulated with DOTAP-encapsulated tRNA, rRNA and total RNA isolated from *E. coli* wt strain and trmH deficient mutant grown under (A) optimal growth conditions (37 °C, LB medium, 250 rpm) or (B) starvation conditions (37 °C, 1x PBS, 250 rpm). Triangles indicate RNA concentrations of 1 µg/ml and 0.5 µg/ml. After 20 h of stimulation at 37 °C, 5% CO_2, cell-free supernatants were collected and IFN-α secretion was measured by ELISA. Each bar represenst mean values (+ SEM) of 3 individual donors. To account for donor variation cytokine release of each donor was normalized to IFN-α levels induced by bRNA 1µg/ml.

Taken together, presence of Gm18 significantly reduced immune stimulation of tRNA samples of *E. coli*. However, this phenotype, previously described by Jöckel *et al.*, was only reproducible when *E. coli* were stressed before RNA isolation. However, immune stimulatory potential of total RNA preparations was not affected by 2'-O-methylation of tRNAs.

4.4.4 Gm18-deficiency within bacterial or fungal tRNAs is not affecting immuno-stimulation of living pathogens

2'-O-methylation within tRNAs of Gram-negative bacteria was discussed as a potential immune evasion mechanism of pathogens [70]. So far, the immune inhibitory effect of Gm18 within tRNAs on innate immune cells like pDCs and monocytes was only demonstrated for isolated tRNAs. However, there was no evidence that the methylation status of G18 within tRNAs of living bacteria could affect overall pathogen recognition. In order to investigate the relevance of Gm18 within tRNAs on the overall immunestimulatory potential of pathogens, *E. coli* wt and trmH deficient mutants were used to infect human PBMCs. Furthermore, human PBMCs were infected with different multiplicity of infections (MOIs) of *S. cerevisiae*

wt strain and trm3 deficient mutant to analyse the importance of Gm18 on immune activation by lower eukaryotes (Fig. 4–27). Bacterial RNA (bRNA) and R848 served as positive controls for TLR7 stimulation within pDCs or TLR8 activation of monocytes and subsequent secretion of IFN-α or TNF-α, respectively. LPS induced monocyte-dependent TLR4 response and subsequent secretion of proinflammatory cytokines like TNF-α.

Of note, the infection of PBMCs with *E. coli* and *S. cerevisiae* wt strains induced similar IFN-α and TNF-α levels compared to tRNA-methyltransferase deficient mutants (Fig. 4–27 A-D). Interestingly, *E. coli* induced a dose-dependent TLR-7 response but upon *S. cerevisiae* infection no IFN-α was detectable (Fig. 4–27 A, C). In case of TNF-α, no dose-dependency was detectable for infections with *E. coli*, whereby PBMC infection with *S. cerevisiae* induced overall lower cytokine levels (Fig. 4–27 B, D). Of note, sensing of *E. coli* by the innate immune system was described to be highly LPS-dependent. As the two main read-outs for immune stimulation were based on TLR7 activation of pDCs and TLR8 stimulation of monocytes it was important to consider other TLRs than TLR7 and TLR8 expressed by those immune cells. Besides TLR7, pDCs were described to express the DNA sensing TLR9 also inducing IFN-α secretion. Furthermore, monocytes were known to express TLR4 on their cell surface resulting in a robust secretion of proinflammatory cytokines like TNF-α upon LPS stimulation [7, 9]. Therefore, saturated TLR4 stimulation and LPS-dependent TNF-α secretion might have impeded MOI-dependent stimulation of PBMCs.

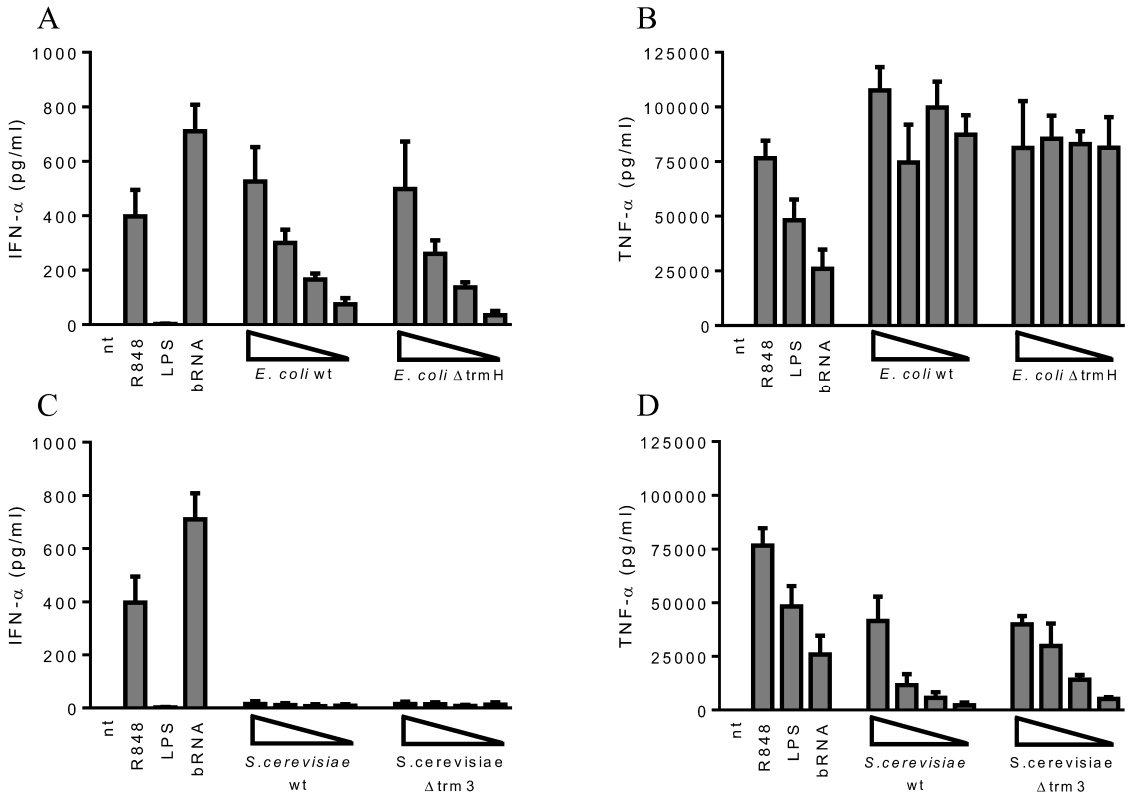

Fig. 4–27 Infection of human PBMCs with different MOI of *E. coli* and *S. cerevisiae.* Human PBMCs (200 000/well) were infected with MOI 1-0.03 of *E. coli* and *S. cerevisiae* wt strains and their corresponding trmH and trm3 deficient mutants, respectively. Microbes were killed after 1.5 h by addition of Antibiotic-Antimycotic 100x. Triangles indicate MOI of 1, 0.3, 0.1, 0.03. Cytokines were measured in cell-free supernatants by ELISA. (A) IFN-α release and (B) TNF-α release of PBMCs upon infection with *E. coli* wt and trmH deficient mutant. (C) IFN-α release of pDCs and (D) TNF-α release of monocytes within PBMCs upon infection with *S. cerevisiae* wt and trm3 deficient mutant. Results demonstrate stimulations of three individual donors in duplicate wells +SEM.

To further examine immune stimulation of living bacteria on human PBMCs, mRNA expression of IFN-α, IFN-β, IL-6 and TNF-α was also determined by qRT-PCR. Of note, mRNA based measuring of cytokine induction confirmed previous ELISA results. In general, *S. cerevisiae* induced lower levels of type I IFN and proinflammatory cytokines (Fig. 4–28 B) compared to *E. coli* (Fig. 4–28), whereby no differences between the wt strains and their corresponding methyltransferase deficient mutants were observed.

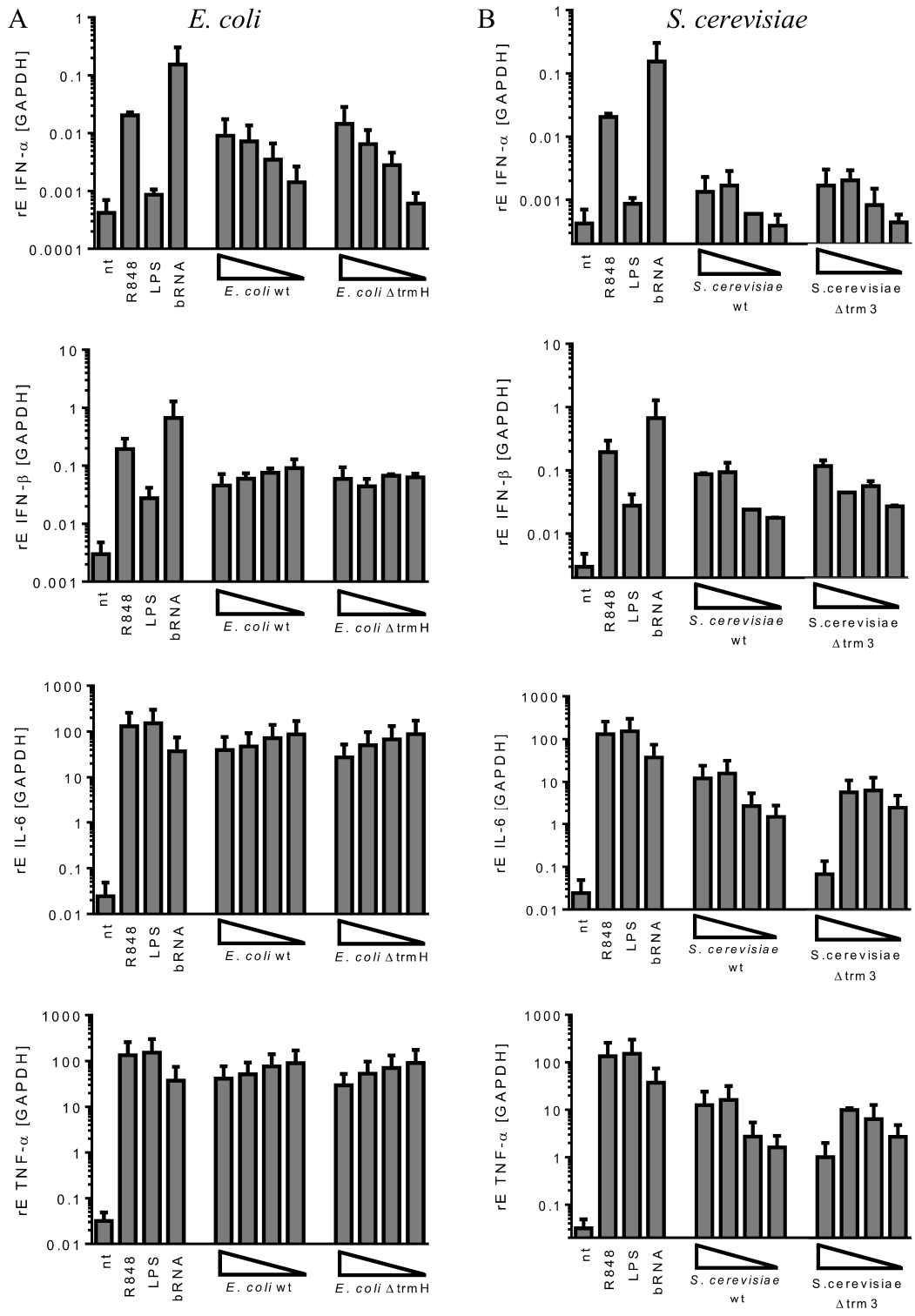

Fig. 4–28 mRNA expression of type I IFN and proinflammatory cytokines upon PBMC infection with *E. coli* and *S. cerevisiae*. 200, 000 human PBMCs were infected in a 96-well plate at a total volume of 100 µl. R848 (1 µg/ml), LPS (0.1 µg/ml) and bRNA (0.5 µg/ml) served as positive controls. Triangles indicate MOI of 1, 0.3, 0.1, 0.03 of *E. coli* (A) and *S. cerevisiae* (B). After 1.5 h, 1 µl 100x Antibiotic-Antimycotic were added per well and PBMCs were incubated for additional 3.5 h. Subsequently, cells were lysed and qRT-PCR was performed. Relative expression of target genes was calculated compare to GAPDH. n = 2 +SEM

Of note, bacteria and yeast used for these infection experiments were grown under optimal growth conditions (37 °C, LB medium, 250 rpm). However, extent of 2'-O-methylation and consequent immune stimulatory potential of tRNAs seemed to be regulated by growth conditions (section 4.4.3). Previous results indicated an upregulation of Gm18 by starvation of bacteria. In case of upregulation of Gm18 within tRNAs of 24 h starved *E. coli* wt strain, less immune stimulations compared to trmH deficient mutant and non-starved *E. coli* wt strain would have been expected. Consequently, human PBMCs were also infected with starved or non-starved *E. coli* wt strain and trmH deficient mutant (Fig. 4–29). As expected, PBMC infection with non-starved *E. coli* wt strain and trmH deficient mutants resulted in similar levels of IFN-α secretion (Fig. 4–29 A). Of note, *E. coli* starved for 24 h in 1x PBS also induced comparable amounts of IFN-α as non-starved *E. coli* and no differences between wt strain and trmH deficient mutant was detected (Fig. 4–29 B).

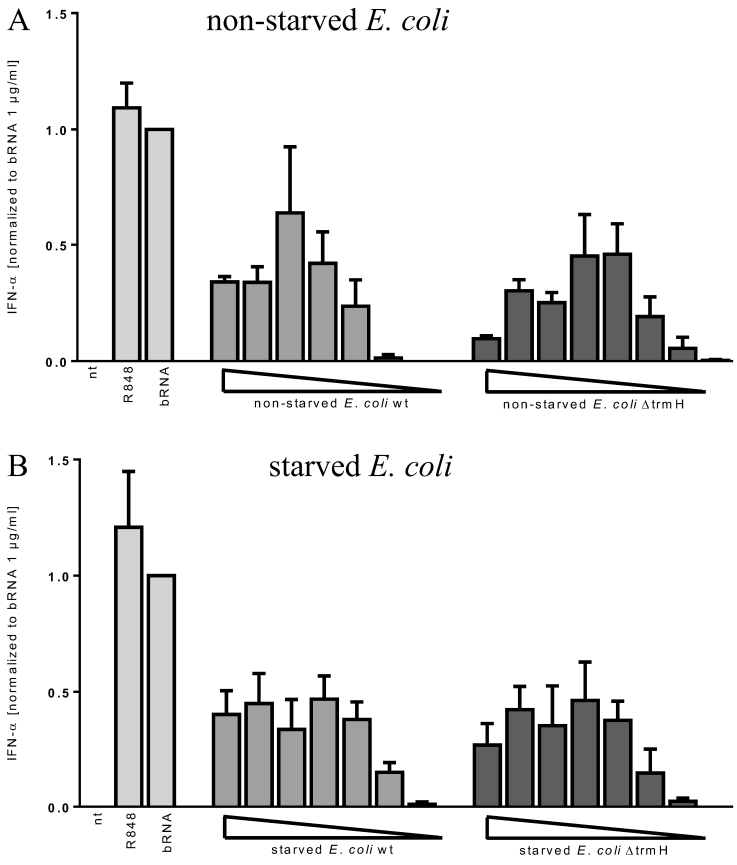

Fig. 4–29 Infection of human PBMCs with different MOI of *E. coli*. Human PBMCs (200,000/well) were infected with MOI 100-0.03 of non-starved (A) or starved (B) *E. coli* and wt strains and trmH deficient mutants. After 1.5 h Antibiotic-Antimycotic 100x was added. Triangles indicate MOI of 100, 30, 10, 3, 1, 0.3, 0.1 and 0.03. IFN-α was measured in cell-free supernatants by ELISA. To account for donor variation IFN-α release was normalized to IFN-α secretion induced by bacterial RNA. Results demonstrate stimulations of three individual donors in duplicate wells +SEM.

Altogether, we did not observe a relevance of Gm18 within tRNAs for the pathogenicity of *E.coli* or *S. cerevisiae* when PBMCs were infected with whole organisms. Furthermore, growth of bacteria under nutrient deficiency and associated upregulation of Gm18 within tRNAs did not trigger virulence of *E. coli* in this experiments.

4.4.5 Gene expression profiling of BlaER1 cells uncovers TLR8 dependent pathways upon infection with *E. coli*

The examination of a small subset of proinflammatory cytokines or type I IFNs by ELISA and qRT-PCR was not sufficient to display the overall regulation of the immune response within PBMCs towards *E. coli* wt strain and trmH deficient mutant. Regulation of other genes than examined proinflammatory cytokines and type I interferon might have been affected by Gm18 modification.

To investigate the entirety of regulated genes by infections with *E.coli*, a microarray expression analysis was performed. Of note, previous experiments demonstrated a high variability in the immune response of different donors. To examine a more defined infection model, we decided to make us of well described BlaER1 cells [132]. A further advantage of those cells was the availability of TLR8 knock-out BlaER1 cells to analyze TLR8 and therefore RNA dependent pathways upon infection with *E. coli.* All BlaER1 cells were kindly provided by Prof. Dr. Holger Heine, Research Center Borstel, Leibniz-Center for Medicine and Biosciences. Of note, macrophage-like BlaER1 cells were generated from B-cell like cells. According to the literature, transdifferentiated BlaER1 cells still showed residual TRL7 activity [133], whereas native monocytes and macrophages were known to exclusively express TLR8 [9]. Of note, monocyte/macrophage-like BlaER1 cells were sorted for $CD19^{+}$ B-cell like BlaER1 cells to exclude TLR7 response of this cell population, however, sorted BlaER1 cells were still responding to the TLR7 specific stimulus CL264. Therefore, TLR7 expression of transdifferentiated BlaER1 cells could not be excluded.

Of note, the microarray was set up to answer two different questions. First of all, the RNA dependent immune stimulation of *E. coli* wt strain should be examined by infecting transdifferentiated BlaER1 wt and TLR8 knock-out cells. In a second step, the relevance of Gm18 within bacterial tRNAs was investigated by infecting BlaER1 wt cells with *E. coli* wt strain and trmH deficient mutant. Interestingly, 482 genes were differentially regulated dependent on TLR8 within transdifferentiated BlaER1 cells when stimulated with *E. coli* wt (Fig. 4–30). The results for the first time show, that TLR8 (and thus presumably RNA recognition) plays an important role for the innate immune response against *E. coli*. Roughly half of the differentially regulated genes were upregulated in the BlaER1 wt compared to TLR8 KO cells. However, only 13 of those differentially regulated genes were upregulated with a Log2 fold change > 1.5 in the wt BlaER1 cells upon infection with *E. coli* (Table 4-1). Furthermore, none of the examined genes was upregulated in the BlaER1 TLR8 knockout with a Log2 fold change > 1.5 (data not shown). Remarkably, most of the upregulated genes

like *IFNB*, *IFNLR1* and *IL12A* and *CLCF1* or *CD40* were described to be involved in the antiviral response and in IL-6 or NFκB signalling. (according to www.genecards.org and www.uniprot.org). Differentially regulated genes between wt and TLR8 KO BlaER1 cells in response to whole bacteria proved the recognition of *E. coli* in a RNA-dependant manner.

To further investigate the impact of 2'-O-methylation of tRNA, BlaER1 cells were infected with *E. coli* wt and trmH deficient mutant and LPS as a control. Of note, no significantly differentially expressed genes were detected between the two *E. coli* strains. Comparison of gene expression upon infection of BlaER1 wt and TLR8 KO with *E. coli* trmH deficient mutant also demonstrated identical gene regulation as compared to *E. coli* wt considering upregulated genes with a log2 fold change >1.5 (data not shown).

Furthermore, gene expression profiles of BlaER1 cells stimulated with *E. coli* strains or LPS demonstrated highly similar gene expression patterns **(**Fig**.** 4–31). Interestingly, LPS stimulation of the three individual experiments clustered together based on the transcriptome. In case of infections with living *E. coli* the gene expression was more affected by interindividual variability of experiments than by the genotype of the pathogen. Consequently, LPS stimulation and *E. coli* infection formed one cluster, whereby LPS and each infection experiment represented one subgroup.

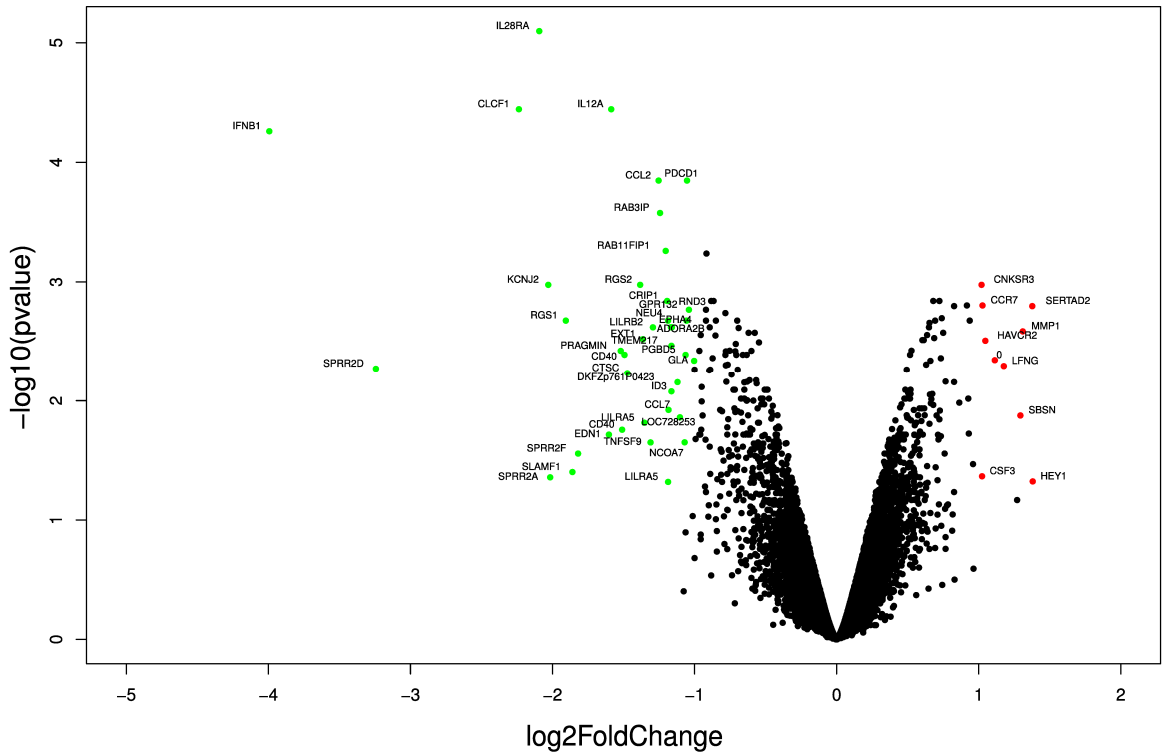

Fig. 4–30 Volcano plot of 482 regulated genes of BlaER wt compared to BlaER TLR8 KO cells examined by Illumina HT12 microarray. 200,000 transdifferentiated BlaER1 wt or TLR8 KO cells per well were seeded in a 48-well plate at a final volume of 300 µl. Cells were stimulated for 5 h in duplicate wells with *E. coli* wt strain. Infection with *E. coli* was performed at an MOI of 10. 1.5 h post infection Pen/Strep was added to kill bacteria. The three experiments represent individual sets of transdifferentiated BlaER1 cells. For mRNA isolation duplicate wells were pooled together and RNA was extracted with RNeasy Total RNA Kit. For further analysis samples were sent to DKFZ genomics and proteomics core facility. Data was analyzed using Chipster software [134]

Table 4-1: Top-list of upregulated genes demonstrating a Log2 fold change (FC) > 1.5 upon *E. coli* infection of BlaER1 wt cells compared to BlaER1 TLR8 KO cells

Gene name	Description	ID number	p value	Log2 FC
IFNB1	interferon, beta 1, fibroblast	1510669	5.5E-05	3.99
SPRR2D	small proline-rich protein 2D	1660521	5.3E-03	3.24
CLCF1	cardiotrophin-like cytokine factor 1	5290397	3.6E-05	2.24
IFNLR1	interferon, lambda receptor 1	3520398	8.0E-06	2.09
KCNJ2	potassium channel, inwardly rectifying subfamily J, member 2	60719	1.1E-03	2.03
SPRR2A	small proline-rich protein 2A	6770187	4.4E-02	2.02
RGS1	regulator of G-protein signalling 1	4490176	2.1E-03	1.91
SLAMF1	signalling lymphocytic activation molecule family member 1	5810136	4.0E-02	1.86
SPRR2F	small proline-rich protein 2F	2230500	2.8E-02	1.82
EDN1	endothelin 1	7040386	1.9E-02	1.60

IL12A	interleukin 12A	4120114	3.6E-05	1.59
PRAGMIN	homolog of rat pragma of Rnd2	2640441	3.8E-03	1.52
CD40	CD40 molecule, TNF receptor superfamily member 5	6420520	1.8E-02	1.51

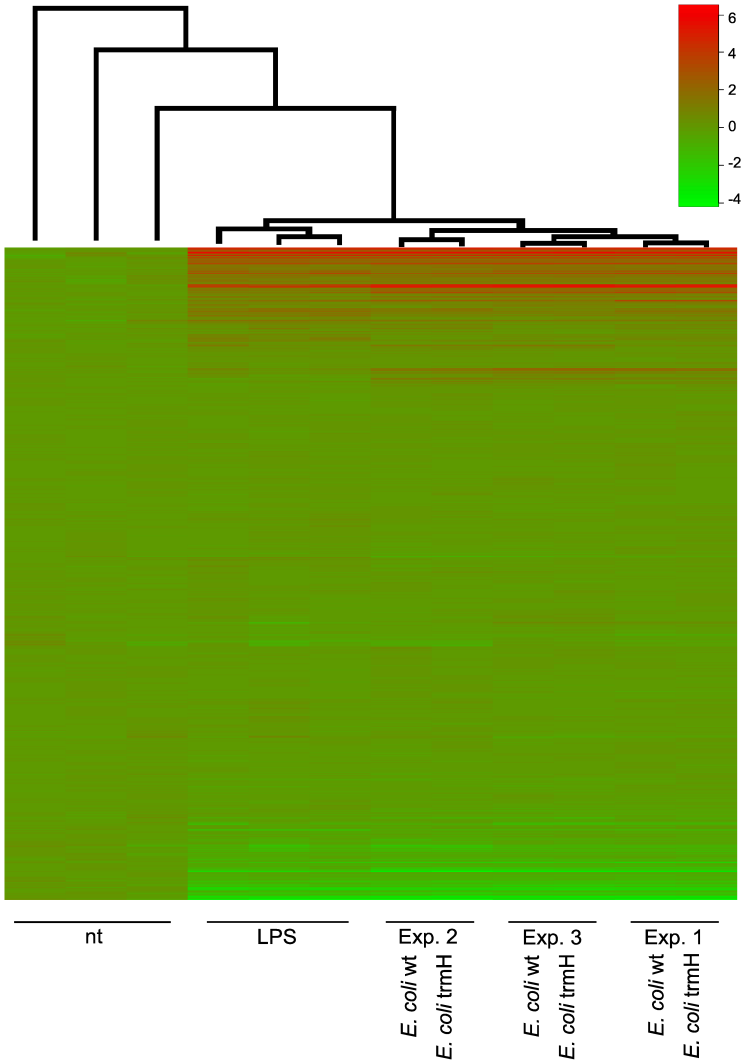

Fig. 4–31 Heatmap of all examined genes by Illumina HT12 microarray.
200,000 transdifferentiated wt BlaER1 cells per well were seeded in a 48-well plate at a final volume of 300 µl. Cells were stimulated in duplicates with 0.1 µg/ml LPS as a control and *E. coli* wt strain and trmH deficient mutant. Infection with *E. coli* was performed at an MOI of 10. The three experiments represent individual sets of transdifferentiated BlaER1 cells. For mRNA isolation duplicate wells were pooled together and RNA was extracted with RNeasy Total RNA Kit. For further analysis samples were sent to DKFZ genomics and proteomics core facility. Data was analyzed using Chipster software [134].

Similarity of gene expression of BlaER1 cells infected with *E. coli* wt and trmH deficient mutant was underlined by NMDS (non-metric multidimensional scaling) analysis depicting the differences of data by the distance within a matrix. Of note, expression data of *E. coli* infections with wt and trmH deficient mutant were located at the same position of NMDS, indicating no differences in transcriptome.

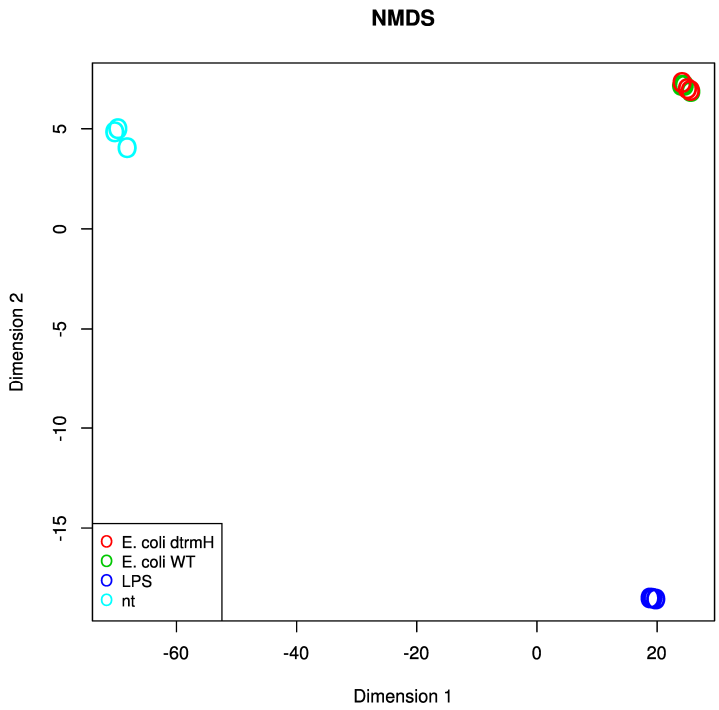

Fig. 4–32 NMDS of BlaER1 wt infected with *E. coli* wt and trmH deficient mutant. NMDS based on expression data previously depicted as heatmap (Fig. 4–31) was calculated using R software. The distance matrix demonstrated the relation of wt BlaER1 cells infected with *E. coli* wt and trmH deficient mutant (MOI 10) and non-treated and LPS (0.1 µg/ml) stimulated controls.

In summary, we impressively demonstrated Gm18-independent recognition of *E. coli* by the innate immune system. Indeed, in the case of isolated tRNAs, Gm18 was effecting immune stimulation but our data refuted an influence of 2'-O-methylation within tRNAs on the pathogenicity of *E. coli*. On the other hand, gene expression profiling identified a TLR8 dependency of the innate immune response towards *E. coli*, thus proving that LPS/TLR4 is not the only important PAMP but RNA/TLR8 is a significant contributer.

4.4.6 Generation of a tRNA (guanosine(18)-2'-O)-methyltransferase (TARBP1) deficient human cell line

To examine the relevance of 2'-O-methylation of guanosine at position 18 within human tRNAs, we planned to create a biallelic gene knock-out of the *trmH* homologue *TARBP1* in a human cell line by CRISPR/Cas9. To select a suitable cell line with a basal *TARBP1* expression, lysates of different cell lines were analysed by western blot. Of note, a first western blot did not show any TARBP1 signal for the alveolar basal epithelial cell line A549 and the bronchial epithelial cell line Beas2B. To confirm this first observation, another western blot was performed including primary human epithelial cell samples (Fig. 4–33 A #3, #4). Indeed, none of the cell lysates indicated a constitutive expression of TARBP1 within tested human lung epithelial cells. By contrast, human embryonic kidney cells (HEK293) and the human monocytic cell line THP-1 showed presence of TARBP1 protein by western blot (Fig. 4–33 A).

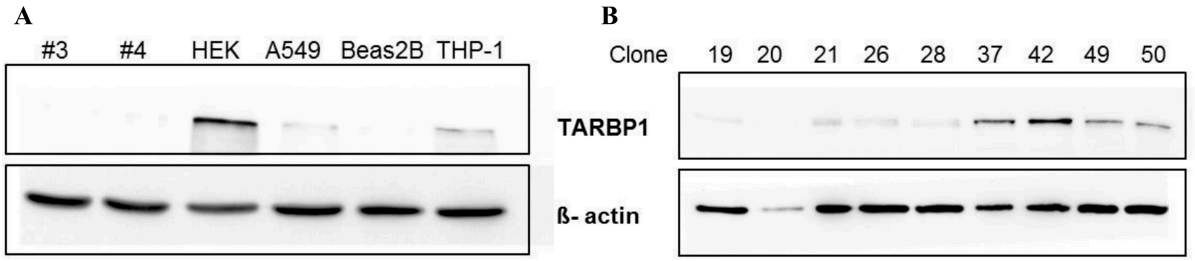

Fig. 4–33 Western blots of human primary bronchial epithelial cells, different human cell lines and CRISPR/Cas9 targeted HEK cell clones. 100,000 cells were lysed in 10 µl 1 x SDS sample buffer and loaded onto a 12% SDS-PAGE. β-actin was used as loading control. (A) Human primary bronchial epithelial cell lysates (#3, #4) kindly provided by Dr. Vedrana Mijosek and lysates of HEK, A549, Beas2B and THP-1 cells were analysed for TARBP1 expression. (B) HEK cell clones (clones numbers indicated above) were screened for TARBP1 expression.

4.4.7 *TARBP1* knock-out is confirmed in six HEK cell clones by western blot and Sanger sequencing

HEK cells are considered as an easy to handle and easy to transfect cell line. Furthermore, lysates of those cells gave a robust signal for TARBP1 protein on western blots. For those reasons, we decided to create the gene knock-out in HEK cells. Of note, it was not our intention to create a model to elucidate the effect of *TARBP1* within a cell line but we were interested in the immunestimulatory potential of isolated tRNAs. The gene disruption was induced by CRISPR/Cas9 as described in section 3.2.6. Ten days after sorting of GFP positive HEK cells by BD FACSMelody and subsequent limiting dilution into 96-well plates, 50 HEK clones were chosen for further analysis. Of note, clones were selected if only one colony was visible in the well. To preselect promising knock-out clones, those 50 clones were analyzed by western blot (Fig. 4–33 B). Of note, knock-out clones still exhibited a weak band on western blots at similar size like TARBP1. Personal communication with other working groups using the same antibody identified the band as unspecific. Prolonged running time of the gel should result in separation of weak unspecific bands and TARBP1 protein. Ultimately, six clones (clone 8, 19, 20, 21, 26, 28) which did not show any abnormalities in growth, size and shape were chosen for further sequencing analysis. Indeed, all six clones were confirmed as *TARBP1* knock-out clones by Sanger sequencing and subsequent analysis of sequencing data by CRISP-ID [135]. Clone 26 and 28 were used for further immune stimulation experiments. The mutated amino acid sequences of both clones were depicted in Fig. 4–34, whereby CRISPR/Cas9 either induced an altered amino acid sequence or a stop codon (Clone 26 allele 1).

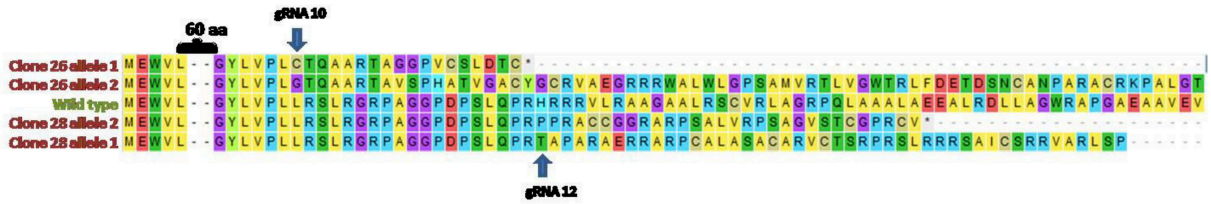

Fig. 4–34 CRISP-ID analysis of clone 26 and clone 28. Amino acid sequence of wild type TARBP1 (middle sequence) and CRISPR/Cas9 targeted clone 26 (upper two sequences) and clone 28 (lower two sequences). Arrows indicate binding region of guide RNA10 (clone 26) and guide RNA12 (clone28).

4.4.8 Analysis of isolated tRNA of *TARBP1* knock-out clone 26 and clone 28 by RiboMethSeq

TARBP1 was described as the human homologue of tRNA-methyltransferase trmH and trm3 of *E. coli* and *S. cerevisiae*, respectively. However, it was not known if TARBP1 was the only methyltransferase introducing 2'-O-methylation of guanosine at position 18 within tRNAs in humans. To ensure absence of Gm18 within tRNAs of clone 26 and clone 28, isolated tRNAs of three biological replicated were analyzed by Prof. Dr. Yuri Motorin (Next-Generation Sequencing core facility, Biopole Lorraine University, Vandoeuvre-les-Nancy, France) for Illumina sequencing-based RiboMethSeq analysis. Site specific detection of 2'-O-methylated nucleotides within tRNAs was based on alkaline hydrolysis of tRNA followed by library preparation and sequencing. 5'-and 3'-end counting demonstrated a drop in the coverage of 2'-O-methyl protected sites. Analysis of sequencing data of HEK wt tRNA compared to tRNAs isolated from clone 26 and clone 28 was performed by Prof. Dr. Yuri Motorin. The cleavage profile of HEK $tRNA^{Ser}$ of wt, clone 26 and clone 28 demonstrated a drop in cleavage at position 44 which was identified as Um (Fig. 4–35 A-C). Furthermore, $tRNA^{Ser}$ of wt HEK showed an additional drop at position G18, indicating a 2'O-methylation at that position (Fig. 4–35 A). Of note, this second drop was fully absent in tRNA samples of clone 26 and clone 28 confirming TARBP1 deficiency of those clones (Fig. 4–35 B, C).

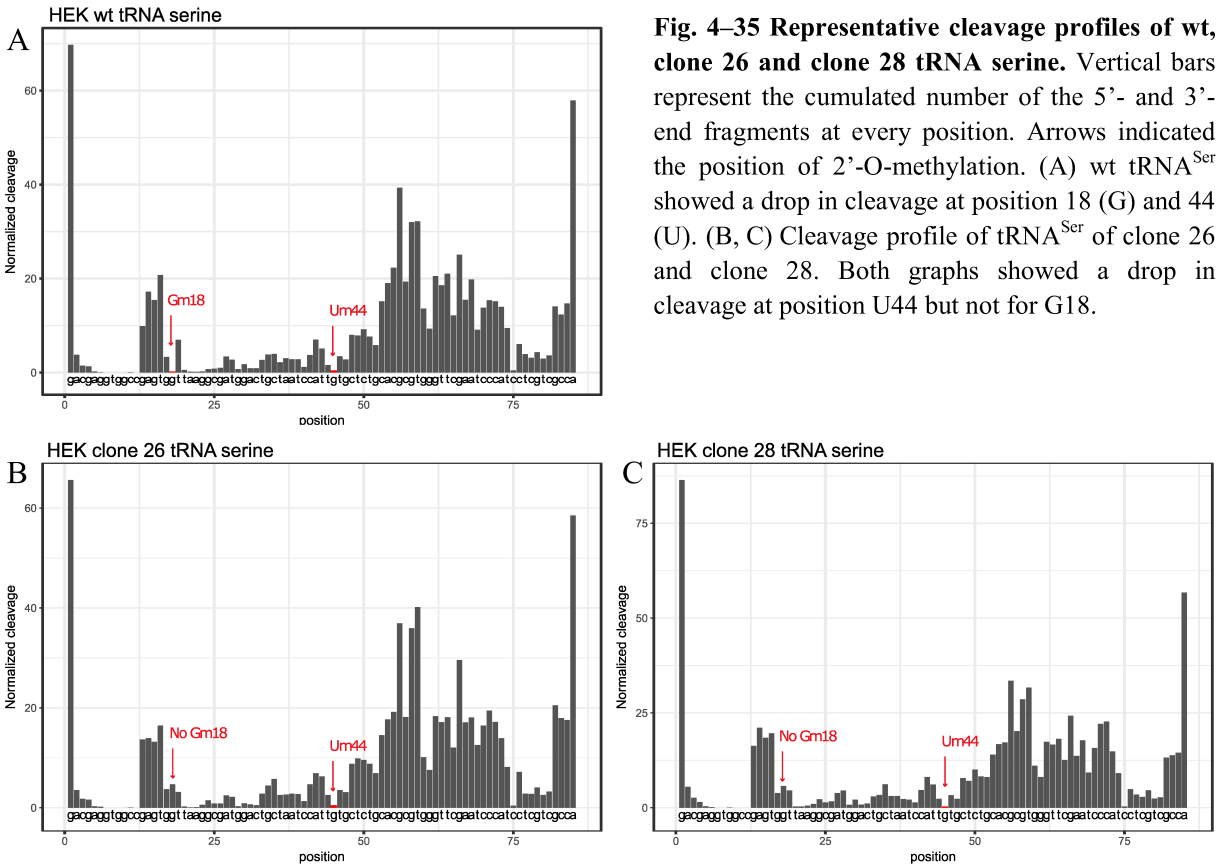

Fig. 4–35 Representative cleavage profiles of wt, clone 26 and clone 28 tRNA serine. Vertical bars represent the cumulated number of the 5'- and 3'-end fragments at every position. Arrows indicated the position of 2'-O-methylation. (A) wt tRNA^{Ser} showed a drop in cleavage at position 18 (G) and 44 (U). (B, C) Cleavage profile of tRNA^{Ser} of clone 26 and clone 28. Both graphs showed a drop in cleavage at position U44 but not for G18.

Beside the cleavage profiles of individual tRNAs, a heatmap with all 2'-O-methylation sites of different tRNA isoacceptors was provided by Prof. Dr. Yuri Motorin (Fig. 4–36). Three tRNA isoacceptors of total tRNA preparations were identified as 2'-O-methylated at position 18. Those isoacceptors, namely glutamine and two isoacceptors of serine were mapped in the upper part of the heatmap (pink square). According to the color key, strong pink color represented 2'-O-methylation of indicated nucleotides, whereas dark blue color implied absence of 2'-O-methylation. Of note, both *TARBP1* knock-out clones demonstrated no Gm18 for all three isoacceptors, whereas at least wt tRNAs isolated of two different cultures were highly modified but the third biological replicate of wt tRNAs showed less 2'-O-methylation at position 18. Interestingly, all other 2'-O-methylations than Gm18 were not affected by the deficiency of TARBP1. For example, clone 26 and 28 demonstrated similar 2'-O-methylation patterns of guanosine at position 34 or uridine at position 32, 44 and 54.

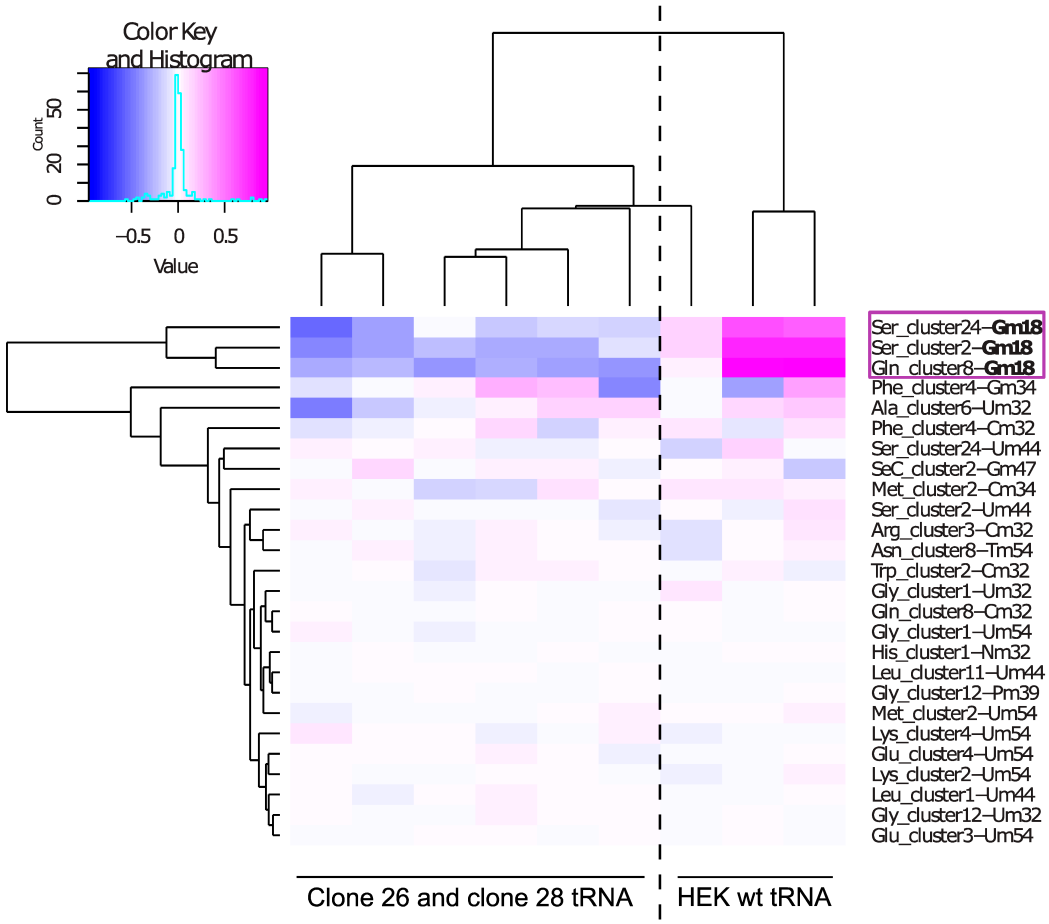

Fig. 4–36 Heatmap of analysed RiboMethSeq data. Clustering of human tRNAs sites according to their 2′-O-methylation. Heatmap displayed normalized mean methylation scores. tRNA isoacceptors and modified nucleotide positions were indicated on the right. Gm18 modified tRNAs were highlighted with a square. Colour key and histogram were depicted at the upper left part of the figure.

In summary, TARBP1 knock-out was successfully created in different HEK cell clones. Six putative knock-out clones were confirmed by Sanger sequencing, whereby two of those clones, namely clone 26 and clone 28, were further examined by RiboMethSeq analysis. Cleavage profiles created from cumulated 5'-and 3'-end extremity numbers and resulting heatmap confirmed the absence of 2'-O-methylation of guanosine at position 18 within clone 26 and clone 28. Of note, RiboMethSeq analysis of human tRNAs identified only three Gm18 modified isoacceptors.

4.4.9 Immune stimulatory potential of whole human tRNAs is independent of 2'-O-methylation at position 18

Human RNA and especially tRNAs were described as highly modified RNA species [82]. Therefore, human tRNAs were considered as non-stimulatory towards the human immune system. Of note, abrogation of immune stimulation of tRNAs was described for Gm18 modified bacterial tRNAs [70, 93], however relevance of Gm18 within human tRNAs remained to be investigated. Previously generated *TARBP1* knock-out clones exhibiting a lack of 2'-O-methylation at position 18 within tRNAs served a tool to isolate human G18-unmethylatd tRNAs. As human tRNAs were described as highly modified, at least for wt HEK tRNA no immune stimulation was expected. Remarkably, tRNAs isolated from wt and TARBP1 deficient HEK cells triggered the release of IFN-α within PBMCs (Fig. 4–37). However, unexpected immune stimulation by human tRNA was already observed in previous experiments (Fig. 4–4). Compared to tRNAs isolated from wt HEK, tRNAs isolated from TARBP1 deficient clones 26 and 28 induced slightly increased IFN-α levels, however differences in IFN-α secretion were never significant (Fig. 4–37 A, B). Of note, rRNA and total RNA preparations of both, wt and *TARBP* knock-out clones were not sufficient to induce IFN-α secretion within human PBMCs (Fig. 4–37 B). Consequently, absence of 2'-O-methylation at position 18 of previous identified $tRNA^{Ser}$ and $tRNA^{Gln}$ isoacceptors demonstrated only minor effects on immune stimulation of total tRNA preparations. Furthermore, non-stimulatory phenotype of ribosomal and total RNA was not affected by the lack of Gm18.

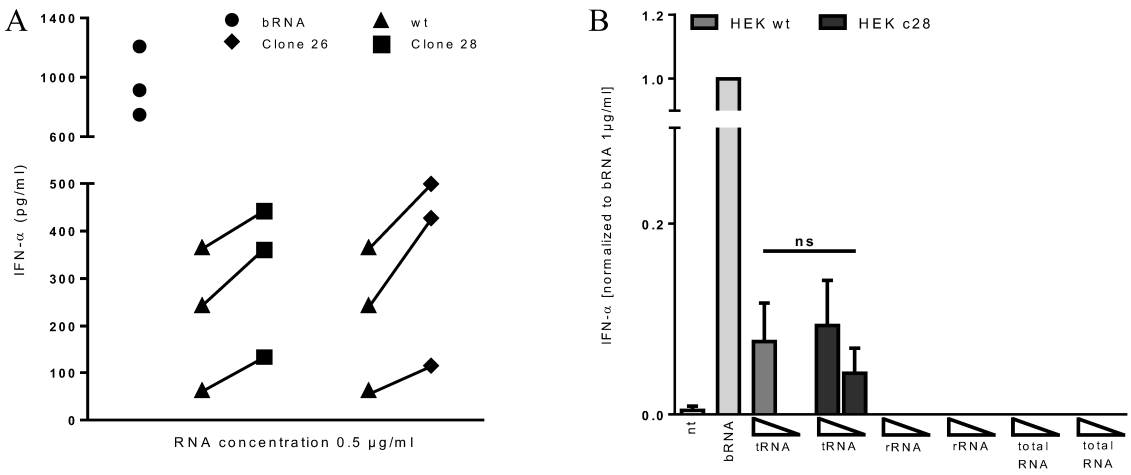

Fig. 4–37 Immune stimulation of isolated human tRNA, rRNA and total RNA. Human PBMCs (200,000/well) were stimulated for 20 h with human, DOTAP-encapsulated RNA samples. IFN-α release was measured in cell-free supernatants by ELISA. Data represented stimulations of three individual donors in duplicate wells. (A) tRNA samples of wt HEK cells and TARBP1 knock-out clones 26 and 28 (0.5 µg/ml) isolated by NucleoBond columns. (B) tRNA, rRNA and total RNA samples were purified via agarose gel electrophoresis. To account for donor variation, IFN-α levels were normalized to IFN-α values induced by bRNA.

In summary, importance of 2'-O-methylation at position 18 of tRNAs for immune inhibition was confirmed for bacterial tRNAs and fractionated yeast tRNA. However, Gm18 played a redundant role in the recognition of total RNA preparations of all examined organisms. Furthermore, 2'-O-methylation within tRNAs of *E. coli* did not affect the overall immune stimulation of bacteria.

5 DISCUSSION

Aim of this thesis was the examination of immune modulatory effects of RNA modifications. Besides, the identification of a new RNA modifications affecting TLR7 response, a shielding effect of bulky RNA modifications on TLR7 stimulation was demonstrated. Furthermore, an optimized dominant inhibitory sequence motif for TLR7 and TLR8 inhibition was elucidated and the relevance of 2'-O-methylation at position 18 of tRNAs for immune recognition was investigated. Indeed, Gm18 altered immune recognition of PBMCs towards isolated tRNAs but was not sufficient to modulate immune response upon infections with whole bacteria..

5.1 Method establishment

According to literature, various methods were described how to purify RNAs of different species and how to isolate and culture PBMC or to stimulate them. However, it was not outlined whether and how different isolation methods of RNA or PBMCs might affect the immune stimulation of different cell types. Of note, any of the recent publications discussed the used RNA isolation protocol with regard to their suitability. Some publication even did not demonstrate a quality control for isolated RNAs. To this end, we systematically reviewed our experimental setups to avoid the influence of methodological factors.

5.1.1 Column- and PAGE-based RNA purification can bias immune stimulation

Column-based RNA isolation is a very common, basic, rapid and simple method of RNA purification that has been used in the field of RNA immune stimulation. Ribosomal RNA purification and stimulation experiments mainly focused on the 23S and 16S, 25S and 18S and 28S and 18S rRNA subunits of *E. coli*, *S. cerevisiae* and human cells, respectively. Smaller subunits like the 5S rRNA subunit with a size of 120 nt were not specifically isolated but could have co-occurred in tRNA fractions (70-100 nt) [120]. Of note, dependent on the extraction kit used, different species of RNA are eluted. For example, columns of the RNeasy Total RNA Kit from Qiagen show an RNA size cut-off < 200 nt. Therefore, purified total RNA samples do not contain tRNAs and 5S rRNA anymore. Furthermore, NucleoBond RNA/DNA columns promise a RNA species specific purification along a KCl gradient. RNA separation is based on anion-exchange chromatography and by increasing salt concentrations

lager RNA species are eluted. However, we observed frequently DNA and RNA contaminations by agarose gel based quality controls (Fig. 4–1). Of note, as we were interested in the immunestimulatory capacity of defined RNAs, those contaminations might have masked modification-dependent effects or could have led to false-positive results. Besides column-based RNA purification, gel-based RNA isolation methods are quite common. A PAGE-based protocol was provided by Patrick Keller, Helm Group (see section 3.2.4.4). Indeed, this protocol resulted in tRNA preparations without visible nucleic acid contaminations but stimulation experiments with those RNAs induced higher amounts of proinflammatory cytokines compared to tRNAs isolated from agarose gel. Proinflammatory cytokines possibly indicated activation of the NFκB-pathway by chemical residues (Fig. 4–4). In line with this observation, Zhao *et al.* described the induction of ROS and NFκB-pathway due to acrylamide in astrocytes [136]. Since chemical impurities of tRNA samples were not easily preventable and not detectable, reproducible and pure tRNA isolation from PAA gels was not guaranteed. In conclusion we decided to prepare all RNA species from agarose gels. This procedure possessed two clear advantages: i) we could not identify any impurities within isolated RNA fractions and ii) all RNA species were purified in the same manner, thereby immune stimulation results of tRNA, rRNA and total RNA should be comparable.

5.2 Identification of double methylation of uridine as new RNA modification inhibiting Toll-like receptor 7 response

The human $tRNA^{Lys}_3$ was previously determined as a non-stimulatory tRNA which lacks Gm18 [73]. So far, only 2'-O-methylation was described as a natural immune inhibitory modification. Hence, we assumed other post-transcriptional modifications than 2'-O-methylation can alter innate immune responses towards RNA. To identify this unknown modification Patrick Keller, Helm group, provided several modivariants of human $tRNA^{Lys}_3$.

5.2.1 Native $tRNA^{Lys}_3$ is not activating immune response but is not efficient to antagonize TLR7

First, the non-stimulatory characteristics of human $tRNA^{Lys}_3$ was demonstrated and subsequently its dominant inhibitory potential was examined (Fig. 4–8 A, B). In contrast to previously described bacterial $tRNA^{Tyr}$ which contained Gm18, human $tRNA^{Lys}_3$ was not dominant inhibitory. Of note, the unmodified $tRNA^{Lys}_3$ ORN efficiently stimulated TLR7 excluding a sequence dependent non-stimulatory effect. This indicated a modification-based immonosilencing mechanism of $tRNA^{Lys}_3$. In a further study, we identified steric shielding of RNA by various bulky modifications which masked the RNA and prevented from immune stimulation (section 4.2.3.1). As human $tRNA^{Lys}_3$ contained in total 14 modifications (Fig. 4–7), whereby 2-methylthio-N6-threonylcarbamoyladenosine and 5-methoxycarbony-l-methyl-2-thiouridine within the anticodon were quite bulky, a steric shielding of the $tRNA^{Lys}_3$ could have been considered. Of note, the incorporation of shielding but not antagonizing modifications might be a crucial feature for self/non-self discrimination by silencing the host RNA without blocking RNA sensing receptors to ensure a fast immune response towards foreign RNA. To further analyse the modifications abrogating TLR7 activation, human $tRNA^{Lys}_3$ was digested by Colicin D to facilitate a splint ligation of a native tRNA fragment and an unmodified ORN. Of note, Colicin D cut the native $tRNA^{Lys}_3$ between position 38 and 39, whereby the bulky modifications of the anticodon stem remained within the 5'-part of the tRNA. Interestingly, modivariant 1 (mv#1) exhibiting native 5'-part induced significantly higher IFN-α levels compared to native $tRNA^{Lys}_3$, whereas mv#2 containing native 3'-part showed no significant differences to native $tRNA^{Lys}_3$. Indeed, this contradictory results suggested a dominant modification within the 3'-fragment of human $tRNA^{Lys}_3$ inducing the immunosilencing phenotype.

5.2.2 Double methylation of U54 to 2′-O-methylthymidine (Tm) is the major determinant of immunosilencing

Considering the posttranscriptional modifications within the 3'-fragment Tm at position 54 of native $tRNA^{Lys}_3$ was further investigate for immunomodulatory properties. 2'-O-methylation of nucleotides within a certain sequence context were already described as immune inhibitory and therefore Tm was the most promising candidate altering TLR7 activation. Indeed, a single Tm at position 54 of otherwise unmodified tRNA significantly decreased TLR7 stimulation (Fig. 4–10). In contrast to native $tRNA^{Lys}_3$ Tm did not abolish TLR7 activation completely but reduced IFN-α release by roughly 50%. This implies that some other modifications than Tm were necessary to completely silence TLR7 activation by $tRNA^{Lys}_3$. Of note, Kaiser *et al.* identified a di-nucleotide motif silencing TLR7 [93]. In this study the authors demonstrated that the nucleobase downstream the 2'-O-methylation determines immunosilencing properties of tRNAs. In case of Xm modified $tRNA^{Lys}_3$, Tm was followed by uridine, whereas native $tRNA^{Lys}_3$ exhibited a pseudouridine downstream of Tm. Former studies demonstrated a decrease in immune activation when pseudouridine was incorporated randomly into RNA [39, 137]. A defined sequence context of the two modifications (2'-O-methylation followed by pseudouridine) might have synergistic effects on immonosilencing potential of native $tRNA^{Lys}_3$. Of note, a purine base (adenine or guanine) at position 54 significantly decreased TLR7 activation compared to unmodified control and detected IFN-α levels were comparable with those induced by native $tRNA^{Lys}_3$. Considering the two nucleobases downstream of the 2'-O-methylation the following sequence motif was identified: *R*mUC (R= A, G). This sequence context was in line with the previously identified tri-nucleotide motif antagonizing TLR7 and TLR8 (section 4.3). Altogether, the data suggested an important structural effect of the 2'-O-methylated nucleobase. Of note, immune stimulation decreased from Cm to Gm, indicating that the binding site of TLR7 was preferentially recognizing purine residues in combination with a methylation at the ribose. The additional methylation of U to T and concomitant increase of the hydrophobic surface of the nucleobase significantly impaired TLR7 activation compared to unmodified control (Fig. 4–9). C5-methylation of uridine seemed to shift the molecular structure of the pyrimidine base toward a purine base and thereby induced the immunosilencing effect of Tm. To prove this theory, the hydrophobic surface of thymidine could be increased by additional methyl groups until the size of a purine base is reached. By increasing size of the nucleobase, a drop in the immune response would be expected. With regard to biological functions, Tm might be an important modification for self/non-self discrimination. In contrast to Gm18, Tm54 was not dominant inhibitory but

silenced the recognition of $tRNA^{Lys}_3$ by TLR7. As a consequence, TLR7 was still capable to recognize foreign stimulatory RNA to ensure a fast immune response against invading pathogens.

5.2.2.1 Base modification of mRNA with small molecules impedes recognition by TLR7

mRNA based vaccines represent a promising alternative to conventionally produced vaccine approaches. A high potency, low-cost manufacture and safe administration are decisive aspects of mRNA vaccine development [122]. mRNA can not only encode for the desired immunogenic antigens but possesses adjuvant activity at the same time and therefore provides signal 1 and signal 2 for T-cell activation. However, recognition of antigen-mRNA by the innate immune system has been associated with impeded antigen expression. Activation of pDCs results in a robust type I interferon expression and upregulation of OAS and degradation of mRNA lead to a decrease in translation of the encoded immunogenic antigen. Therefore, mRNA recognition by TLR7 could be modified by immune inhibitory modifications like 2'-O-methylation of certain nucleotides to enhance antigen expression [122-124]. Based on these studies, the idea arose to bind imidazoquinolines to mRNA to boost TLR7 response of mRNA while retaining translational competence. Of note, the conjugation of up to three different TLR ligands to one single molecule was already possible. Innate immune cells were successfully stimulated with covalent linked TLR4, TLR7 and TLR9 ligands [138]. Indeed, the tri-agonist construct stimulated the innate immune system and facilitated production of a broader spectrum of antibodies compared to the single ligands. Of note, co-transfection of small molecules and eGFP mRNA demonstrated additive effects on immune stimulation without detectable cell toxic effect based on azide-functionalization of small molecules. However, decrease of immune stimulation of chemically modified R848 and GQI (RPA and GDA) might be explained by impeded binding to the first binding site of TLR7 [64]. Interestingly, covalent binding of the small molecules decreased immune stimulation by eGFP mRNA. The reduced TLR7 activation might be based on a steric shielding of mRNA by the covalently bound ligands. To further investigate this assumed shielding effect, non-stimulatory mono- and tri-Mannose were clicked to eGFP mRNA. Interestingly, those bulky modifications affected IFN-α secretion much less than clicked classical TLR7 ligands. Altogether, these results indicated, beside a shielding effect, a competition of covalently bound small molecule and mRNA for the first and the second binding site of TLR7, respectively. The combined stimuli were less effective compared to co-transfection of

unbound small molecule and mRNA. Furthermore, eGFP expression data in HeLa cells provided by Isabell Hellmuth demonstrated complete ablation of translation by a single modified uridine [139]. Taken together, a covalent binding of immune stimulatory small molecules with protein encoding mRNA to boost immune response towards the encoded protein and to facilitate robust T-cell response did not provide requested results. Neither mRNA gained immunestimulatory capacity nor the encoded protein was translated.

5.2.2.2 Immune stimulation of siRNA is decreased by a single base modification of cytosine

As bioconjugation of chemical molecules to eGFP mRNA decreased immune stimulation, other application possibilities than mRNA vaccination were discussed for those modifications. For instance, in case of knock-down experiments by siRNA, activation of TLR7 and TLR8 were undesired side-effects. Of note, 2'-O-methylation which was known to antagonize TLR7/8 response has been used to circumvent immune stimulation by siRNA [92]. Conjugation of siRNA with sugar derivates or small molecules might be a new option to avoid immune stimulation. Indeed, both sugar molecules as well as GDA significantly decreased immune stimulation by siRNA at a concentration of 1 µg/ml (Fig. 4–16 A). Of note, Isabell Hellmuth demonstrated in further experiments the functionality of clicked siRNA [139]. To confirm siRNA was only shielded by clicked molecules without antagonizing TLR7, co-stimulation experiments with MH662 and 2'-O-methylated or clicked siRNA were performed. As expected, only 2'-O-methylation of siRNA was sufficient to antagonize TLR7 response (Fig. 4–16). Immune indifferent sugar derivates might be a useful tool to modify siRNA. The sugar might prevent siRNA from immune recognition without inhibiting the immune response as 2'-O-methylation. Of note, siRNA conjugated with trimeric sugar moiety similar to described tri-mannose were already involved in preclinical trials [140]. The authors described a robust gene silencing by siRNA *in vivo* without reporting adverse immunological effects.

5.3 Identification of an optimal 2'-O-methylated RNA tri-nucleotide motif inhibiting TLR7 and TLR8

In a previous study, Kaiser *et al*. identified a DmR (2'-O-methylated D= all but C; R= purine) di-nucleotide motif which rendered tRNA non-stimulatory with respect of TLR7 activation [93]. Yet, the impact of the DmR motif on TLR8 activation was not investigated in that study. Furthermore, the publication focused on the lack of immune stimulation based on 2'-O-methylation but did not consider dominant inhibitory effects of RNA. To answer these outstanding issues a systematic permutation study based on the previously identified DmR motif was performed and an optimal tri-nucleotide motif was identified antagonizing TLR7 and TLR8.

5.3.1 The two nucleobases downstream of the 2'-O-methylation discriminate between TLR7 and TLR8 inhibition

To systematically evaluate the sequence context of 2'-O-methylation facilitating the dominant inhibitory effects on TLR7 and TLR8, a 26-mer ORN according to the Gm18 modified *E. coli* $tRNA^{Tyr}$ sequence was used. The 2'-O-methylated 26-mer ORN was co-transfected with otherwise immune stimulatory bacterial RNA to investigate antagonisation of TLR7 and TLR8. At first, the nucleobase upstream of Gm18 was permutated without affecting dominant inhibitory capacity of Gm18 (Fig. 4–17). Consequently, the nucleobase at position 18 was permutated and the results confirmed the initial conclusion of Kaiser *et al*.: all 2'-O-methylated nucleobases but cytidine efficiently silenced TLR7 and TLR8 response towards RNA (Fig. 4–18). Interestingly, the two nucleobases downstream the 2'-O-methylation were discriminative for TLR7 and TLR8 inhibition. In case of position 19, all nucleobases but cytidine were effective to antagonize TLR7, whereby TLR8 antagonism required a purine base following Gm18 (Gm18A or Gm18G) (Fig. 4–19). Of note, TLR7 made no demands on the nucleobase at position 20, whereby TLR8 was only inhabitable by a cytidine two nucleotides downstream of Gm18. Consequently, we elucidated a [DmRC] motif (D= all but C, R= G, A) for inhibition of TLR8 and [DmDN] motif (D= all but C, R= G, A) for TLR7 antagonism. However, the study did not consider all 64 possible sequence motives resulting from simultaneous permutation of the nucleobases of position 18-20. Nevertheless, a former study of Jung *et al.* supports described results [91]. The authors investigated a GmGU motif within a 18s rRNA-derived RNA sequence and demonstrated a robust TLR8 activation by the detection of IL-6 within PBMC supernatants, whereby no IFN-α upon TLR7 stimulation was

detectable. Jung *et al.* concluded a shift from a TLR7/TLR8 ligand towards a specific TLR8 ligand by 2'-O-methylation. Of note, the identified inhibitory tri-nucleotide motif predicted the investigated GmGU motif as a TLR7 but not as a TLR8 antagonist explaining the detection of IL-6 and the absence of IFN-α within PBMC. In the literature, TLR7 and TLR8 were described to be closely related in sequence and function [141]. With regard to the two different identified inhibitory motifs for TLR7 and TLR8 inhibition, at least the binding sites for 2'-O-methylated RNA appear to be different. Crystal structures of the RNA binding sites of TLR7 and TLR8 give a hint of differential recognition of RNA by both receptors [64, 65]. Of note, the first binding site of TLR7 and TLR8 is involved in sensing chemical components and seems to be conserved among the receptors. However, upon RNA binding a single guanosine or uridine is detected at the first site of TLR7 or TLR8, respectively. In contrast, the second binding site of TLR7, localized at the dimerization interface, was identified to bind a poly-U 3-mer, whereas an UUG oligoribonucleotide was found to bind to the second binding site outside the dimerization interface of TLR8. Of note, the identification of a minimal inhibitory tri-nucleotide motif might indicate recognition and inhibition towards 2'-O-methylated RNA at the second binding site of TLR7 and TLR8. This assumption is further supported by the systemic shifting of the inhibitory GmGC motif from 5'- to 3'-end of a 9-mer ORN. Of note, GmGC motif at position 1-7 efficiently antagonized TLR8, whereas disruption of the inhibitory motif by placing Gm at position 8 and 9 abrogated antagonizing effects (Fig. 4–21). However, there was no clear evidence that 2'-O-methylated RNA was occupying the same binding sites as unmethylated RNA. A crystal structure of a 2'-O-methylated 9-mer ORN and TLR7/TLR8 would have been essential to answer the question of site specific RNA binding. Another option would have been an in silico modelling of the inhibitory GmGC motif and TLR7/TLR8 to identify potential binding sites of 2'-O-methylated RNA.

Understanding of binding of methylated and unmethylated RNA to TLR7 and TLR8 might be useful to design RNA-based TLR7 and TLR8 antagonists to treat certain autoimmune diseases like systemic lupus erythematosus (SLE) which were known to be linked to inappropriate TLR activation by endogenous RNA. Furthermore, psoriasis was associated with TLR7 and TLR8 activation by RNA [142, 143]. Formulation of inhibitory oligoribonucleotides as pharmaceuticals to treat RNA-driven autoimmune disease might be an important advantage for therapeutic methods. Systemic application of inhibitory RNA packed in liposomes might be a successful treatment of rheumatic diseases. Small negatively charged nanocarriers were described as optimal delivery systems to target monocytes and

macrophages, however, positively charged larger liposomes are known to induce proinflammatory cytokines, cell toxicity and ROS production [144, 145]. Elimination of conventional liposomes by the reticuloendothelial system resulted in short blood circulation of 1-2 hours. Inclusion of polyethylene glycol (PEG) chains extended liposome stability and lifetime in the blood stream by the reduction of non-specific interactions with immune cells to 1-2 days [146]. So called immunoliposomes combine previous described stealth technology (PEGylated liposomes) with specific antibodies directing the nanocarriers to the target cell. Beside specific cell surface markers, lectins recognizing for example mannose were promising targets to direct liposomes to certain cell types. Of note, most immune cells like macrophages and dendritic cells were described to express high levels of mannose receptor, providing a potential target to direct stealth liposomes loaded with immune inhibitory 2'-O-methylated ORNs to supress immune response towards self RNA [146-150]. Type I interferon producing pDCs could be selectively targeted by antibodies directed against a specific surface marker like BDCA-4 to interrupt interferon-driven SLE [151]. Pathogenesis of psoriasis was linked to LL37 dependant RNA recognition of certain immune cells and keratinocytes [152, 153]. Therefore, cutaneous treatment of psoriasis with previous described immune inhibitory oligoribonucleotides might be a therapeutic option. Topical delivery of liposomal packaged drugs has been widely discussed in the literature. However, a recent study demonstrated that intact liposomes were not able to cross the skin barrier [154]. Other cutaneous drug delivery systems are based on chemical penetration enhancers like DMSO. However, concentrations > 60% of DMSO were required to efficiently mediate drug delivery through the skin causing skin irritations. Oxazolidinones were a new class of chemical penetrations enhancers with low systemic permeation and better tolerance [155, 156]. RNase protected phosphothioate (PTO) modified 2'-O-methylated 9-mer ORNs in combination with a chemical penetration enhancer might be an effective treatment of cutaneous psoriasis, however, tolerance and penetration efficiency needed to be evaluated.

5.3.2 Naturally occurring Gm18 motif within tRNAs is most efficient in antagonizing TLR7 and TLR8

Interestingly, TLR7 seemed to be less stringent regarding the inhibitory sequence motif compared to TLR8. Of note, TLR8 inhibition tolerated only a cytidine at position 20, whereby antagonisation of TLR7 depended in particular on position 18 and 19. In case of TLR8, the naturally occurring CGmGC motif (yellow curve Fig. 4–17, Fig. 4–18, Fig. 4–19, Fig. 4–20) was most efficient in suppressing TLR response towards stimulatory RNA. Of note, this sequence context was highly conserved among prokaryotic and even more frequent within eukaryotic tRNAs [120]. While reviewing various tRNA sequences, an even more frequent dihydrouridine (D) at position 20 within prokaryotic as well as eukaryotic tRNAs was observed [120]. Based on the striking effect of position 20 on dominant inhibition of TLR8, the antagonizing potential of a GmGD motif remains to be analysed. As this highly conserved immune inhibitory motif was also present within prokaryotic tRNA of Gram-negative bacteria, it was discussed that 2'-O-methylation within bacterial tRNA might serve as an immune evasion mechanism [70]. Although tRNA constitutes only 10% of total bacterial RNA, tRNAs are not bound to proteins like ribosomal RNA but freely accessible in the cytosol of bacteria. Therefore, tRNAs might represent the most relevant immune stimulatory RNA species despite their lower abundance. Interestingly, Gm18 modified tRNAs were detected with higher abundancy in prokaryotes and low eukaryotes. According to modomics database, 15 out of 47 isoacceptors of *E. coli* tRNAs were described to be 2'-O-methylated at position 18. Of note, in a recent publication we identified tRNA isoacceptor for methionine was false-positive annotated for Gm18 [157]. Stimulation experiments with isolated $tRNA^{Met}$ elucidated immune stimulatory characteristics of the isoacceptors and corresponding RiboMethSeq data confirmed the absence of Gm18. Therefore, 14 out of 47 *E. coli* and 12 out of 35 described *S. cerevisiae* tRNA isoacceptors exhibit guanosine 2'-O-methylation at position 18. Yet RiboMethSeq analysis of human HEK tRNAs only identified three 2'-O-methylated isoacceptors (section 4.4.8). Contrary to expectations, prokaryotic tRNAs were more heavily Gm18 modified compared to eukaryotic tRNAs. As tRNA modifications where described to stabilize the translation of mRNA, one explanation might be the higher cell division rate of bacteria compared to eukaryotic cells [84]. The fast cell turnover might demand a robust protein synthesis and therefore a stabilized interaction of ribosome, tRNA and mRNA [158]. However Gm18 was identified as the sole 2'-O-methylation present in prokaryotic tRNA [120]. Therefore, other modifications than Gm18 within eukaryotic tRNAs might compensate decreased Gm18 appearance to stabilize secondary tRNA structures. For instance, pseudouridine in RNA

double helices stabilizes 3D-interactions by enhancing hydrogen bonds or m^5C and m^5U promotes tRNA stability [82, 83, 159].

5.3.3 Antagonisation of TLR7 and TLR8 stimulation by stimulatory RNA requires co-delivery with inhibitory RNA to the same endosome.

Unpublished stimulation experiments with differentially packaged inhibitory and stimulatory RNA revealed delivery-dependant inhibition of TLR7 and TLR8. Of note, neither pre-treatment of PBMCs with inhibitory ORNs nor transfection with separately packaged inhibitory and stimulatory RNA at the same time point abrogated immune stimulation. Furthermore, upregulation of co-stimulatory molecules like MHC-class II and CD86 was only impaired when both RNAs were delivered within one liposome (Fig. 4–22). Interestingly, Yasuda *et al.* demonstrated delivery of DOTAP encapsulated RNA was based on endocytosis [160]. Therefore, RNA containing vesicles were shuttled to early endosomes within immune cells. Of note, maturation of human persistent early endosomes was based on the uptake of vesicles, sorting of internalized material and recycling of certain proteins and lipids like cell surface receptors for instance. Remaining extracellular material was described to be shuttled by multi vesicular bodies or endosomal carrier vesicles to the late endosome where recognition of nucleic acids by endosomal TLRs takes place [161, 162]. However, DOTAP-encapsulated RNA was delivered to the late endosome in multiple steps (endocytosis, sorting, multi vesicular body, late endosome). Therefore, delivery of separate packaged inhibitory and immune stimulatory RNA was not predictable. Targeting of RNA sensing late endosomes happened randomly and chance of co-delivery of separately packed RNA was rather low. Thus, application of inhibitory RNA as therapeutic agent might fail due to insufficient delivery of 2'-O-methylated ORNs to activated endolysosomes.

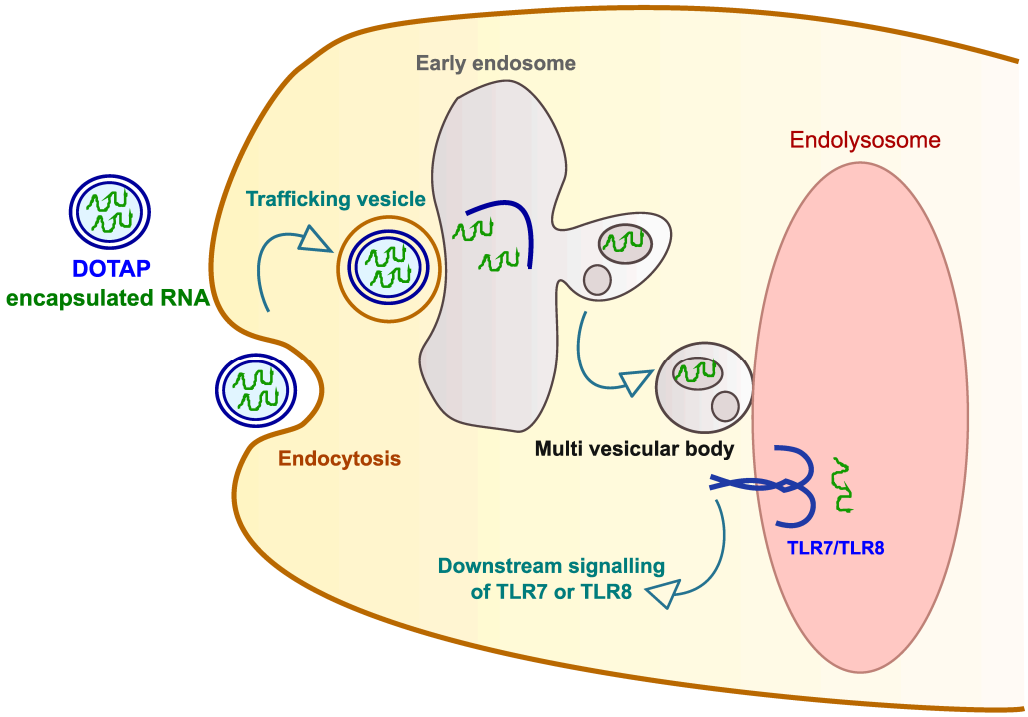

Fig. 5–1 Schematic overview of RNA trafficking. DOTAP encapsulated RNA is taken up by endocytosis and vesicles are trafficked to the early endosome. After sorting of extracellular components, RNA is shuttled via multi vesicular bodies (MVBs) to an endolysosome. MVBs fuse with endolysosomes, shuttled RNA is released and can activate TLR7 or TLR8.

5.4 2'-O-methylation at position 18 of tRNAs plays a minor role within the human immune system

Gm18 was discussed as a critical feature of tRNAs for self/non-self discrimination by the innate immune system or as an immune escape mechanism of Gram-negative bacteria. However, our data now suggest a minor role of Gm18 within tRNAs for overall immune responses.

5.4.1 2'-O-methylation of guanosine at position 18 determines immune stimulatory potential of isolated tRNAs

Examination of yeast fractions and isolated tRNAs of *E. coli* (section 4.4) confirmed previous studies demonstrating that immune stimulation is affected by the presence of Gm18. Of note, isolated fractions of yeast RNA varied in their immune stimulatory potential strongly and this correlated with 2'-O-methylated guanosine within different fractions. However, stimulation experiments with isolated total tRNA samples demonstrated weak differences in IFN-α secretion for *S. cerevisiae* wt and trm3 deficient mutant, implying redundant immunosilencing

modifications within yeast tRNAs. Indeed, *S. cerevisiae* tRNAs possessed besides Gm18, 2'-O-methylated adenosine and uridine which were also identified as immune inhibitory and not affected by trm3 deficiency. Of note, total RNA preparations of both, wt and trm3 deficient *S. cerevisiae* induced negligible amounts of IFN-α compared to bacterial RNA, indicating important immunosilencing modifications within ribosomal RNA of budding yeast. According to the literature, rRNA of *S. cerevisiae* is more heavily 2'-O-methylated as compared to bacterial RNA by the rRNA 2'-O-methyltransferase NOP1 [120, 163]. Hence, the discriminative overall stimulatory potential of bacterial compared to yeast RNA is possibly not driven by Gm18 within tRNAs but enhanced 2'-O-mehylation within ribosomal RNA of *S. cerevisiae.* Consequently, NOP1 and 2'-O-methylation of rRNA would have been interesting targets to examine modification dependent immune responses. However, NOP1 was described as crucial for cell viability and biallelic permanent *S. cerevisiae* knock-out strains were not available [163, 164]. Of note, fibrillarin, a highly conserved nucleolar protein involved in RNA processing, was identified as the human homologue of NOP1 [164]. Interestingly, anti-fibrillarin antibodies are detected in the serum of patients suffering from rheumatic autoimmune diseases like systemic sclerosis (SSc), systemic lupus erythematosus (SLE), primary Raynaud's phenomenon and myositis [165-168]. Of note, rheumatic diseases and associated inflammatory response have been linked to self-recognition of endogenous nucleic acids like RNA [169, 170]. So far, the impact of anti-fibrillarin antibodies on the methylation status of rRNA was not investigated. However, a decrease in 2'-O-methylation might affect rRNA sensing by TRL7 and TLR8 and therefore facilitate self-recognition and prime type I IFN levels within patients. Unlike transient IFN-α induction in case of viral infections, sustained increased type I IFN levels lead to a so called 'IFN signature' in SLE patients. This long-term expression of a panel of type I IFN-responsive genes in the peripheral blood of SLE patients drives disease progression [171, 172]. Initial type I interferon secretion and a steady re-stimulation of TLR7 by weakly modified self RNA might promote induction of interferon-stimulated response elements.

5.4.2 Gm18 within human tRNAs is not a key-factor of self/non-self-discrimination

Mutations in nucleic acid modifying genes were described to cause severe diseases like cancer, asthma and mitochondrial dysfunctions [173]. For instance, deaminase ADAR1 converts adenosine to inosine within double-stranded RNA and protects host RNA from MDA5 recognition. Mutations in the *ADAR* gene were linked to Aicardi-Goutières syndrome (AGS) which was associated with increased levels of IFN-α [75, 174]. Furthermore, mutations in the

human *FTSJ1* gene were described to cause non-syndromic X-linked intellectual disability. In this disease, loss-of-function mutations of *FTSJ1* caused lack of 2'-O-methylation of C32 and G34 of human tRNAs [175]. However, deficiency of TARBP1 within described HEK cells clones did not cause abnormalities in cell growth or cell division rate indicating no crucial requirement of Gm18 for cell proliferation. Furthermore, absence of 2'-O-methylation at position 18 of tRNAs was not significantly affecting immune stimulation of total tRNA preparation questioning the relevance for self/non-self discrimination (section 4.4.6). Remarkably, recent publications demonstrated a prognostic significance of the upregulation of *TARBP1* in human hepatocellular carcinoma and human non-small-cell lung cancer [176, 177] and an association with psoriasis [178]. A common characteristic of those diseases was cell hyper proliferation. Of note, 2'-O-methylation at position 18 within tRNAs was described to stabilize tRNAs secondary structures and translation of proteins [84]. Rapid cell proliferation might have requested stable translation machinery achieved by robust 2'-O-methylation of tRNAs at position 18. Furthermore, HIV replication requires TARBP1 protein for binding of trans-activating response (TAR) RNA to RNA polymerase II [179]. Yet, no cases of TARBP1 deficiency within humans were described in literature and loss-of-function mutations were not examined. Perhaps, mutations of the *TARBP1* gene were not associated with severe diseases and therefore not recognized yet.

5.4.3 2'-O-methylation of guanosine at position 18 within tRNA depends on growth conditions

tRNAs isolated from *E. coli* wt strain and trmH deficient mutant cultured for 24 h in PBS demonstrated significant differences in immune stimulations as compared to strains grown under nutrient rich conditions. However, immunosilencing capacity of 2'-O-methylated tRNAs was based on culture conditions indicating a stress response of *E. coli* towards suboptimal growth conditions. Those results were encouraged by RiboMethSeq data provided by Prof. Dr. Yuri Motorin, indicating upregulation of 2'-O-methylation due to stress conditions triggered by starvation or sub-lethal amount of antibiotics. So far, experiments were missing explaining the mechanism of Gm18 upregulation. Of note, bacteria for RNA extraction were harvested in the mid-log phase indicating a maximal cell division rate at the time of RNA isolation. One hypothesis was time-dependent insufficient 2'-O-methylation of tRNAs at position 18 due to fast cell growth and 2'-O-methyltransferase was lagging behind. However, data of *in vivo* RNA methylation kinetics are still missing. 2'-O-methylation of

tRNA by trmH is dependent on S-adenosyl-L-methionine as methyl donor [180, 181]. However, besides the methyltransferase the methyl source might be a limiting factor of 2'-O-methylation in the mid-log phase of bacterial growth. Interestingly, extent of posttranscriptional modifications has been linked to available nutrients and their metabolites [182]. For instance, pyruvate derived from glycolysis was identified as the source of carbons forming the imidazoline ring of 4-demethylwyosine of tRNAs [183]. Moreover, 2'-O-methylation of tRNAs as stress response was a second hypothesis. Gm18 was described to stabilize tRNA secondary structure and translation of mRNA under thermic stress [84, 184, 185]. Of note, beside Gm18, other posttranscriptional modifications like pseudouridine have been proposed to facilitate temperature resistance in *E. coli* [186, 187]. Ishida *et al.* described an increase in Gm18, m5s2U54, and m1A58 when pseudouridine at position 55 was absent, indicating compensatory modification patterns dependent on the environment and modification status of other nucleotides within tRNAs. Hence, the growth milieu of bacteria *in vitro* as well as *in vivo* might affect metabolic pathways and therefore availability of substrates for posttranscriptional modifications. Starvation or sub-lethal concentrations of antibiotics might have also affected other modifications than Gm18 directly and upregulation of 2'-O-methylation was an indirect compensatory mechanism to ensure stability of tRNA structures. However, as posttranscriptional RNA modification could be influenced by several aspects an exact modification pattern under certain growth conditions was hard to predict. Therefore, immune stimulation experiments based on naturally occurring RNA modifications might be poorly reproducible under different growth conditions. Of note, former studies of Jöckel *et al.* demonstrated nearly complete absence of IFN-α secretion when PBMCs were stimulated with *E. coli* wt tRNAs, however cells were grown under optimal growth conditions (37°C in LB medium, shaking was not defined) [70]. As indicated in figure Fig. 4–26, a similar phenotype was only reproducible when bacteria were starved before RNA isolation. However, other unknown stress conditions like residues of detergents after cleaning of flasks or antibiotic residues of former experiments might have affected bacterial growth and 2'-O-methylation of tRNAs. Of note, trmH is described as part of the stringent response operon of *E. coli.* This operon is triggered by stress conditions like nutrient starvation [188, 189]. Therefore, upregulation of the methyltransferase trmH and an increase of 2'-O-methylation of tRNA during altered growth conditions might be possible.

5.4.4 2'-O-methylation of bacterial tRNA does not serve as immune escape mechanisms of *E. coli*

To investigate a potential immune escape mechanism of *E.coli* linked to 2'-O-methylated guanosine at position 18 of tRNAs, immune stimulation of *E.coli* wt strain and the corresponding methyltransferase deficient mutant on PBMCs and BlaER1 cells was examined. Interestingly, microarray data of infected BlaER1 cells did not elucidate any compensatory pathways of RNA recognition in the absence of TLR8 (Fig. 4–30). Indeed, no relevant pathways for RNA signalling upregulated in TLR8 knock-out BlaER1 cells were detected. Of note, stimulation of PBMCs with starved and non-starved bacteria as well as microarray data of BlaER1 cells contradicted an immune escape mechanism of *E. coli* based on Gm18. Although starved *E. coli* showed a higher degree of Gm18 modified tRNAs, the overall immune-stimulation was similar to *E. coli* grown under rich conditions. Also, although BlaER1 cells clearly showed dependency of total *E. coli* recognition on TLR8 (indicating RNA recognition), no differences were observed between stimulation of wt and trmH deficient bacteria. An immune evasion theory was suggested by Jöckel *et al.* demonstrating an immune silencing effect of isolated tRNA of *E. coli* wt strain and even more for *E. coli Nissle 1917* (EcN). The authors claimed an immune escape mechanism based on a decreased in RNA recognition and therefore a delay of adequate immune response against invading pathogens. An immune silencing effect of EcN based on 2'-O-methylation of tRNA was discussed. However, *E. coli Nissle 1917* demonstrated a defect in LPS biosynthesis leading to a semi-rough phenotype facilitating complement-mediated bacterial killing [190]. Furthermore, genome analysis of EcN elucidated the lack of several virulence factors like alpha-hemolysin and P-fimbrial adhesins [191]. EcN-dependent secretion of high amounts of anti-inflammatory IL-10 was linked to TLR4 stimulation by soluble factors of cell extracts but not to components of cell pellets [192, 193]. Immune modulatory properties of *E. coli Nissle* in case of bowl disease were associated with induction of AP-1 and NFκB-dependent secretion of the antimicrobial peptide human beta defensing-2 [194, 195]. Immune modulatory abilities of EcN were associated with induced beta defensin-2 but not with an altered immune response. Furthermore, Jöckel *et al.* only investigated immune stimulation of isolated tRNAs but experiments with whole bacteria were pending. Altogether, major differences in gene expression of virulence factors of non-pathogenic *E. coli Nissle 1917* and facultative pathogen *E. coli* strains cannot allow conclusions on immune escape mechanism or immune modulation capacities of EcN linked to Gm18.

5.5 Structure dependent recognition of RNA by TLR7 – a controversial discussion

tRNAs are known to contain internal complementarity sequences forming cloverleaf like secondary structures following the rules of Watson-Crick base pairing [196]. Of note, these secondary double stranded structures of tRNA provoked several discussions about the RNA recognition of TLR7. Some authors proposed recognition of not only ssRNA by TLR7 but also dsRNA species [6]. As a result the question arose if the secondary tRNA structure was necessary to activate TLR7 response. Moreover, posttranscriptional modifications involved in formation of secondary structures were discussed to be mandatory but unmodified tRNA was shown to form similar secondary structures as their modified counterparts [197]. Of note, isolated tRNAs used for TLR7 and TLR8 stimulation in the present study were purified and dissolved in RNase free deionized water. Nucleic acids are known to be highly negatively charged and metal ions are critical for folding into native structures [198]. Hence, folding of isolated native tRNAs or their corresponding unmodified counterparts is not predictable. Furthermore, at an acidic pH < 5 within the endolysosome unfolding of secondary and tertiary structures of tRNAs is expected [199, 200]. Interestingly, recent studies postulated the recognition of RNA degradation products by TLR7 and TLR8 [64, 65]. Of note, the phosphodiester bound of RNA is described to be highly stable at an acid pH < 5. In contrast to alkaline hydrolysis for which RNA is known to be highly susceptible, acidic hydrolysis of RNA is only possible at a pH < 2 [201, 202]. Consequently, other mechanisms than hydrolysis needs to be responsible for degradation of RNA within the endolysosome. The contribution of an endosomal RNase upstream of TLR7 and TLR8 was discussed to process longer RNA fragments for TLR recognition [65]. Furthermore, processing of endosomal DNA by DNase II was described to be essential for TLR9 activation by unmethylated CpG DNA [68]. Little is known about endosomal ribonucleases but RNase T2 might have been one candidate for RNA processing within the lysosome. This endosomal RNase was described to cleave single-stranded RNA into mono- or oligo-nucleotides with a pH optimum consistent with the endolysosomal pH of 5 [203]. Additionally, RNase 6 expressed in neutrophils and monocytes was reported to be involved in innate immunity and RNase 2 was described to occur within the endolysosome † [204]. With respect to the relevance of an upstream endo- or exonuclease to activate TLR7 and TLR8, gene knock-outs of described RNases are necessary to investigate the effect of RNA processing on immune activation. So far, no diseases were associated to loss of function

† https://www.uniprot.org/

mutations of those RNases. However, insufficient RNA processing might reduce TLR7 and TLR8 response towards invading pathogens. By decreased type I interferon and IL-12 secretion, living bacteria might not be detected as viable anymore and no adequate immune response is initiated [44]. On the other hand, non-degraded RNA might overload the endosome as described for DNA [68] and leak to the cytosol. Dependent on the initial source of RNA, leaked RNA might activate cytosolic RNA sensors and facilitate undesired immune responses.

5.6 Conclusion and Outlook

In summary, this work demonstrated the importance of 2'-O-methylation for the innate immune recognition of RNA. A new immune modulatory posttranscriptional modification based on 2'-O-methylation was characterized in human tRNA. Tm was the first naturally occurring RNA modification identified as immune silencing but not dominant inhibitory on the innate immune system. This kind of posttranscriptional modification could be applied to functional RNA molecules like siRNA for *in vivo* application to on the one hand avoid unwanted immune stimulation without affecting TLR7 and TLR8 response towards nucleic acids derived from pathogens.

The identification of an optimized inhibitory 2'-O-methylated RNA motif in our study could aid the rational design of TLR7/8 antagonistic ORNs for therapeutic application. A possible application of such small immunomodulatory ORNs are auto immune diseases like SLE or psoriasis which are linked to the pathological recognition of self or foreign nucleic acids. To this end, suitable delivery systems for RNA based pharmaceutical ingredients need to be established and distribution of inhibitory ORNs in the body requires close monitoring.

Furthermore, the physiological relevance of previous described 2'-O-methylation at position 18 of tRNA (Gm18) was examined in the context of prokaryotic and eukaryotic RNA preparations. Gm18 mediated antagonism of RNA-dependent immune responses via TLR7 and TLR8 was relevant within tRNA fractions of both prokaryotic and eukaryotic origin. However, Gm18 within tRNAs was not sufficient to modulate immune responses towards total RNA preparations or whole organisms. Given its high abundance, it is conceivable that immune responses towards total RNA preparations and most likely towards whole organisms is mainly driven by ribosomal RNA and its modifications. Unlike bacterial RNA, eukaryotic

rRNA is highly 2'-O-methylated by the methyltransferase fibrillarin. Of note, the auto immune disease SLE is associated with anti-fibrillarin antibodies and might therefore cause a decreased methylation status of host rRNA and therefore facilitate self-RNA recognition and pathogenesis. Yet, this hypothesis requires verification in future experiments. Extend of 2'-O-methylation of rRNA of SLE patients needs to be examined by quantitative LC/MS analysis and immune stimulation experiments with isolated rRNA fractions of patients and healthy controls should be performed.

Moreover, microarray analysis revealed three different small proline-rich proteins to be involved in RNA-dependent recognition of *E. coli*. However, the function of this protein family during bacterial infections is unknown. After verification of microarray data in human PBMCs as a more physiological system by RT-qPCR, the role of proline-rich proteins during infections might be elucidated by knock-out or knock-down experiments in human cell lines or primary cells, respectively. Furthermore, as small proline-rich proteins are also described in mice, an infection model could be applied to small proline-rich protein deficient mice to examine the physiological relevance *in vivo*.

As recent findings indicate a critical impact of growth conditions on the 2'-O-methylation status, acidic pH and altered oxygen content as found at bacterial infection sites might influence the RNA modification patterns of bacteria and thus alter immune recognition under pathophysiological conditions. It would be therefore interesting to examine the bacterial RNA methylation status *in situ* during infection, although the analysis might be technically demanding due to low abundancy of bacterial tRNA at the site of infection.

Altogether, investigation of posttranscriptional RNA modifications illuminates novel approaches to design new immunomodulatory drugs. Moreover, pathogenesis of certain diseases might be explained by altered modification patterns of self RNA. Furthermore, microarray analysis might reveal new pathways involved in immune signalling and recognition of RNA by the innate immune system.

6 BIBLIOGRAPHY

1. Medzhitov R, Janeway CA. Innate immunity: impact on the adaptive immune response. Current Opinion in Immunology. 1997;9(1):4-9.
2. Akira S, Uematsu S, Takeuchi O. Pathogen recognition and innate immunity. Cell. 2006;124(4):783-801.
3. Janeway CA. The immune system evolved to discriminate infectious nonself from noninfectious self. Immunology Today. 1992;13(1):11-6.
4. Medzhitov R, Janeway C, Jr. Innate immune recognition: mechanisms and pathways. Immunological Reviews. 2000;173(1):89-97.
5. Gourbeyre P, Berri M, Lippi Y, Meurens F, Vincent-Naulleau S, Laffitte J, et al. Pattern recognition receptors in the gut: analysis of their expression along the intestinal tract and the crypt/villus axis. Physiol Rep. 2015;3(2).
6. Hartmann G. Nucleic Acid Immunity. Adv Immunol. 2017;133:121-69.
7. Brubaker SW, Bonham KS, Zanoni I, Kagan JC. Innate immune pattern recognition: a cell biological perspective. Annu Rev Immunol. 2015;33:257-90.
8. Lebedev KA, Ponyakina ID. Immunophysiology of epithelial cells and pattern-recognition receptors. Human Physiology. 2006;32(2):224-34.
9. Hornung V, Rothenfusser S, Britsch S, Krug A, Jahrsdorfer B, Giese T, et al. Quantitative Expression of Toll-Like Receptor 1-10 mRNA in Cellular Subsets of Human Peripheral Blood Mononuclear Cells and Sensitivity to CpG Oligodeoxynucleotides. The Journal of Immunology. 2002;168(9):4531-7.
10. Takeuchi O, Akira S. Pattern recognition receptors and inflammation. Cell. 2010;140(6):805-20.
11. Geijtenbeek TB, Gringhuis SI. Signalling through C-type lectin receptors: shaping immune responses. Nat Rev Immunol. 2009;9(7):465-79.
12. Kato H, Takeuchi O, Sato S, Yoneyama M, Yamamoto M, Matsui K, et al. Differential roles of MDA5 and RIG-I helicases in the recognition of RNA viruses. Nature. 2006;441(7089):101-5.
13. Ablasser A, Goldeck M, Cavlar T, Deimling T, Witte G, Rohl I, et al. cGAS produces a 2'-5'-linked cyclic dinucleotide second messenger that activates STING. Nature. 2013;498(7454):380-4.
14. Wu J, Chen ZJ. Innate immune sensing and signaling of cytosolic nucleic acids. Annu Rev Immunol. 2014;32:461-88.
15. Brencicova E, Diebold SS. Nucleic acids and endosomal pattern recognition: how to tell friend from foe? Front Cell Infect Microbiol. 2013;3:37.
16. Dalpke A, Helm M. RNA mediated Toll-like receptor stimulation in health and disease. RNA Biol. 2012;9(6):828-42.
17. Ferwerda G, Meyer-Wentrup F, Kullberg BJ, Netea MG, Adema GJ. Dectin-1 synergizes with TLR2 and TLR4 for cytokine production in human primary monocytes and macrophages. Cell Microbiol. 2008;10(10):2058-66.
18. Karumuthil-Melethil S, Sofi MH, Gudi R, Johnson BM, Perez N, Vasu C. TLR2- and Dectin 1-associated innate immune response modulates T-cell response to pancreatic beta-cell antigen and prevents type 1 diabetes. Diabetes. 2015;64(4):1341-57.
19. Farhat K, Riekenberg S, Heine H, Debarry J, Lang R, Mages J, et al. Heterodimerization of TLR2 with TLR1 or TLR6 expands the ligand spectrum but does not lead to differential signaling. J Leukoc Biol. 2008;83(3):692-701.

20. Oliveira-Nascimento L, Massari P, Wetzler LM. The Role of TLR2 in Infection and Immunity. Front Immunol. 2012;3:79.
21. Bäckhed F, Normark S, Schweda EKH, Oscarson S, Richter-Dahlfors A. Structural requirements for TLR4-mediated LPS signalling: a biological role for LPS modifications. Microbes and Infection. 2003;5(12):1057-63.
22. Park BS, Song DH, Kim HM, Choi BS, Lee H, Lee JO. The structural basis of lipopolysaccharide recognition by the TLR4-MD-2 complex. Nature. 2009;458(7242):1191-5.
23. Maldonado RF, Sa-Correia I, Valvano MA. Lipopolysaccharide modification in Gram-negative bacteria during chronic infection. FEMS Microbiol Rev. 2016;40(4):480-93.
24. Tan Y, Kagan JC. A cross-disciplinary perspective on the innate immune responses to bacterial lipopolysaccharide. Mol Cell. 2014;54(2):212-23.
25. Song WS, Jeon YJ, Namgung B, Hong M, Yoon SI. A conserved TLR5 binding and activation hot spot on flagellin. Sci Rep. 2017;7:40878.
26. Matusiak M, Van Opdenbosch N, Vande Walle L, Sirard JC, Kanneganti TD, Lamkanfi M. Flagellin-induced NLRC4 phosphorylation primes the inflammasome for activation by NAIP5. Proc Natl Acad Sci U S A. 2015;112(5):1541-6.
27. Dolasia K, Bisht MK, Pradhan G, Udgata A, Mukhopadhyay S. TLRs/NLRs: Shaping the landscape of host immunity. Int Rev Immunol. 2018;37(1):3-19.
28. Gaidt MM, Hornung V. The NLRP3 Inflammasome Renders Cell Death Pro-inflammatory. J Mol Biol. 2018;430(2):133-41.
29. Nielsen AE, Hantho JD, Mancini RJ. Synthetic agonists of NOD-like, RIG-I-like, and C-type lectin receptors for probing the inflammatory immune response. Future Med Chem. 2017;9(12):1345-60.
30. Schlee M. Master sensors of pathogenic RNA - RIG-I like receptors. Immunobiology. 2013;218(11):1322-35.
31. Sasaki O, Yoshizumi T, Kuboyama M, Ishihara T, Suzuki E, Kawabata S, et al. A structural perspective of the MAVS-regulatory mechanism on the mitochondrial outer membrane using bioluminescence resonance energy transfer. Biochim Biophys Acta. 2013;1833(5):1017-27.
32. Broquet AH, Hirata Y, McAllister CS, Kagnoff MF. RIG-I/MDA5/MAVS are required to signal a protective IFN response in rotavirus-infected intestinal epithelium. J Immunol. 2011;186(3):1618-26.
33. Herzner AM, Hagmann CA, Goldeck M, Wolter S, Kubler K, Wittmann S, et al. Sequence-specific activation of the DNA sensor cGAS by Y-form DNA structures as found in primary HIV-1 cDNA. Nat Immunol. 2015;16(10):1025-33.
34. Kanneganti T-D, Özören N, Body-Malapel M, Amer A, Park J-H, Franchi L, et al. Bacterial RNA and small antiviral compounds activate caspase-1 through cryopyrin/Nalp3. Nature. 2006;440(7081):233-6.
35. Sha W, Mitoma H, Hanabuchi S, Bao M, Weng L, Sugimoto N, et al. Human NLRP3 inflammasome senses multiple types of bacterial RNAs. Proc Natl Acad Sci U S A. 2014;111(45):16059-64.
36. Eigenbrod T, Dalpke AH. Bacterial RNA: An Underestimated Stimulus for Innate Immune Responses. J Immunol. 2015;195(2):411-8.
37. Sander LE, Davis MJ, Boekschoten MV, Amsen D, Dascher CC, Ryffel B, et al. Detection of prokaryotic mRNA signifies microbial viability and promotes immunity. Nature. 2011;474(7351):385-9.
38. Eberle F, Sirin M, Binder M, Dalpke AH. Bacterial RNA is recognized by different sets of immunoreceptors. Eur J Immunol. 2009;39(9):2537-47.
39. Kariko K, Buckstein M, Ni H, Weissman D. Suppression of RNA recognition by Toll-like receptors: the impact of nucleoside modification and the evolutionary origin of RNA. Immunity. 2005;23(2):165-75.

40. Gratz N, Hartweger H, Matt U, Kratochvill F, Janos M, Sigel S, et al. Type I interferon production induced by Streptococcus pyogenes-derived nucleic acids is required for host protection. PLoS Pathog. 2011;7(5):e1001345.
41. Gratz N, Siller M, Schaljo B, Pirzada ZA, Gattermeier I, Vojtek I, et al. Group A streptococcus activates type I interferon production and MyD88-dependent signaling without involvement of TLR2, TLR4, and TLR9. J Biol Chem. 2008;283(29):19879-87.
42. Loof TG, Goldmann O, Medina E. Immune recognition of Streptococcus pyogenes by dendritic cells. Infect Immun. 2008;76(6):2785-92.
43. Eigenbrod T, Pelka K, Latz E, Kreikemeyer B, Dalpke AH. TLR8 Senses Bacterial RNA in Human Monocytes and Plays a Nonredundant Role for Recognition of Streptococcus pyogenes. J Immunol. 2015;195(3):1092-9.
44. Ugolini M, Gerhard J, Burkert S, Jensen KJ, Georg P, Ebner F, et al. Recognition of microbial viability via TLR8 drives TFH cell differentiation and vaccine responses. Nat Immunol. 2018;19(4):386-96.
45. Lee BL, Barton GM. Trafficking of endosomal Toll-like receptors. Trends Cell Biol. 2014;24(6):360-9.
46. Park B, Brinkmann MM, Spooner E, Lee CC, Kim YM, Ploegh HL. Proteolytic cleavage in an endolysosomal compartment is required for activation of Toll-like receptor 9. Nat Immunol. 2008;9(12):1407-14.
47. Petes C, Odoardi N, Gee K. The Toll for Trafficking: Toll-Like Receptor 7 Delivery to the Endosome. Front Immunol. 2017;8:1075.
48. Kumagai Y, Takeuchi O, Akira S. TLR9 as a key receptor for the recognition of DNA. Adv Drug Deliv Rev. 2008;60(7):795-804.
49. Tao Y, Zhang X, Markovic-Plese S. Toll-like receptor (TLR)7 and TLR9 agonists enhance interferon (IFN) beta-1a's immunoregulatory effects on B cells in patients with relapsing-remitting multiple sclerosis (RRMS). J Neuroimmunol. 2016;298:181-8.
50. Rutz M, Metzger J, Gellert T, Luppa P, Lipford GB, Wagner H, et al. Toll-like receptor 9 binds single-stranded CpG-DNA in a sequence- and pH-dependent manner. Eur J Immunol. 2004;34(9):2541-50.
51. Ablasser A, Poeck H, Anz D, Berger M, Schlee M, Kim S, et al. Selection of molecular structure and delivery of RNA oligonucleotides to activate TLR7 versus TLR8 and to induce high amounts of IL-12p70 in primary human monocytes. J Immunol. 2009;182(11):6824-33.
52. Kawai T, Akira S. The role of pattern-recognition receptors in innate immunity: update on Toll-like receptors. Nat Immunol. 2010;11(5):373-84.
53. Li XD, Chen ZJ. Sequence specific detection of bacterial 23S ribosomal RNA by TLR13. Elife. 2012;1:e00102.
54. Oldenburg M, Kruger A, Ferstl R, Kaufmann A, Nees G, Sigmund A, et al. TLR13 recognizes bacterial 23S rRNA devoid of erythromycin resistance-forming modification. Science. 2012;337(6098):1111-5.
55. Song W, Wang J, Han Z, Zhang Y, Zhang H, Wang W, et al. Structural basis for specific recognition of single-stranded RNA by Toll-like receptor 13. Nat Struct Mol Biol. 2015;22(10):782-7.
56. Schroder M, Bowie AG. TLR3 in antiviral immunity: key player or bystander? Trends Immunol. 2005;26(9):462-8.
57. Barrat FJ, Meeker T, Gregorio J, Chan JH, Uematsu S, Akira S, et al. Nucleic acids of mammalian origin can act as endogenous ligands for Toll-like receptors and may promote systemic lupus erythematosus. J Exp Med. 2005;202(8):1131-9.
58. Gitlin L, Barchet W, Gilfillan S, Cella M, Beutler B, Flavell RA, et al. Essential role of mda-5 in type I IFN responses to polyriboinosinic:polyribocytidylic acid and encephalomyocarditis picornavirus. Proc Natl Acad Sci U S A. 2006;103(22):8459-64.

59. Lee SM, Yip TF, Yan S, Jin DY, Wei HL, Guo RT, et al. Recognition of Double-Stranded RNA and Regulation of Interferon Pathway by Toll-Like Receptor 10. Front Immunol. 2018;9:516.
60. Barbet G, Sander LE, Geswell M, Leonardi I, Cerutti A, Iliev I, et al. Sensing Microbial Viability through Bacterial RNA Augments T Follicular Helper Cell and Antibody Responses. Immunity. 2018;48(3):584-98 e5.
61. Saitoh SI, Abe F, Kanno A, Tanimura N, Mori Saitoh Y, Fukui R, et al. TLR7 mediated viral recognition results in focal type I interferon secretion by dendritic cells. Nat Commun. 2017;8(1):1592.
62. Diebold SS, Kaisho T, Hemmi H, Akira S, Reis e Sousa C. Innate antiviral responses by means of TLR7-mediated recognition of single-stranded RNA. Science. 2004;303(5663):1529-31.
63. Heil F, Hemmi H, Hochrein H, Ampenberger F, Kirschning C, Akira S, et al. Species-specific recognition of single-stranded RNA via toll-like receptor 7 and 8. Science. 2004;303(5663):1526-9.
64. Zhang Z, Ohto U, Shibata T, Krayukhina E, Taoka M, Yamauchi Y, et al. Structural Analysis Reveals that Toll-like Receptor 7 Is a Dual Receptor for Guanosine and Single-Stranded RNA. Immunity. 2016;45(4):737-48.
65. Tanji H, Ohto U, Shibata T, Taoka M, Yamauchi Y, Isobe T, et al. Toll-like receptor 8 senses degradation products of single-stranded RNA. Nat Struct Mol Biol. 2015;22(2):109-15.
66. Schlee M, Hartmann G. Discriminating self from non-self in nucleic acid sensing. Nat Rev Immunol. 2016;16(9):566-80.
67. Holm CK, Paludan SR, Fitzgerald KA. DNA recognition in immunity and disease. Curr Opin Immunol. 2013;25(1):13-8.
68. Chan MP, Onji M, Fukui R, Kawane K, Shibata T, Saitoh S, et al. DNase II-dependent DNA digestion is required for DNA sensing by TLR9. Nat Commun. 2015;6:5853.
69. Pawaria S, Moody K, Busto P, Nundel K, Choi CH, Ghayur T, et al. Cutting Edge: DNase II deficiency prevents activation of autoreactive B cells by double-stranded DNA endogenous ligands. J Immunol. 2015;194(4):1403-7.
70. Jockel S, Nees G, Sommer R, Zhao Y, Cherkasov D, Hori H, et al. The 2'-O-methylation status of a single guanosine controls transfer RNA-mediated Toll-like receptor 7 activation or inhibition. J Exp Med. 2012;209(2):235-41.
71. Gantier MP, Tong S, Behlke MA, Xu D, Phipps S, Foster PS, et al. TLR7 Is Involved in Sequence-Specific Sensing of Single-Stranded RNAs in Human Macrophages. The Journal of Immunology. 2008;180(4):2117-24.
72. Eigenbrod T, Keller P, Kaiser S, Rimbach K, Dalpke AH, Helm M. Recognition of Specified RNA Modifications by the Innate Immune System. Methods Enzymol. 2015;560:73-89.
73. Gehrig S, Eberle ME, Botschen F, Rimbach K, Eberle F, Eigenbrod T, et al. Identification of modifications in microbial, native tRNA that suppress immunostimulatory activity. J Exp Med. 2012;209(2):225-33.
74. Rimbach K, Kaiser S, Helm M, Dalpke AH, Eigenbrod T. 2'-O-Methylation within Bacterial RNA Acts as Suppressor of TLR7/TLR8 Activation in Human Innate Immune Cells. J Innate Immun. 2015;7(5):482-93.
75. Mannion NM, Greenwood SM, Young R, Cox S, Brindle J, Read D, et al. The RNA-editing enzyme ADAR1 controls innate immune responses to RNA. Cell Rep. 2014;9(4):1482-94.
76. Liddicoat BJ, Piskol R, Chalk AM, Ramaswami G, Higuchi M, Hartner JC, et al. RNA editing by ADAR1 prevents MDA5 sensing of endogenous dsRNA as nonself. Science. 2015;349(6252):1115-20.

77. Hornung V, Ellegast J, Kim S, Brzozka K, Jung A, Kato H, et al. 5'-Triphosphate RNA is the ligand for RIG-I. Science. 2006;314(5801):994-7.
78. Schuberth-Wagner C, Ludwig J, Bruder AK, Herzner AM, Zillinger T, Goldeck M, et al. A Conserved Histidine in the RNA Sensor RIG-I Controls Immune Tolerance to N1-2'O-Methylated Self RNA. Immunity. 2015;43(1):41-51.
79. Werner M, Purta E, Kaminska KH, Cymerman IA, Campbell DA, Mittra B, et al. 2'-O-ribose methylation of cap2 in human: function and evolution in a horizontally mobile family. Nucleic Acids Res. 2011;39(11):4756-68.
80. Hyde JL, Diamond MS. Innate immune restriction and antagonism of viral RNA lacking 2-O methylation. Virology. 2015;479-480:66-74.
81. Zhao Y, Soh TS, Lim SP, Chung KY, Swaminathan K, Vasudevan SG, et al. Molecular basis for specific viral RNA recognition and 2'-O-ribose methylation by the dengue virus nonstructural protein 5 (NS5). Proc Natl Acad Sci U S A. 2015;112(48):14834-9.
82. Motorin Y, Grosjean H. Transfer RNA Modification. Encyclopedia of Life Sciences2005.
83. Motorin Y. RNA Modification. eLS2015. p. 1-18.
84. Hori H. Methylated nucleosides in tRNA and tRNA methyltransferases. Front Genet. 2014;5:144.
85. Lorenz C, Lunse CE, Morl M. tRNA Modifications: Impact on Structure and Thermal Adaptation. Biomolecules. 2017;7(2).
86. Hori H, Terui Y, Nakamoto C, Iwashita C, Ochi A, Watanabe K, et al. Effects of polyamines from Thermus thermophilus, an extreme-thermophilic eubacterium, on tRNA methylation by tRNA (Gm18) methyltransferase (TrmH). J Biochem. 2016;159(5):509-17.
87. Subramanian M, Srinivasan T, Sudarsanam D. Examining the Gm18 and m(1)G Modification Positions in tRNA Sequences. Genomics Inform. 2014;12(2):71-5.
88. Ochi A, Makabe K, Yamagami R, Hirata A, Sakaguchi R, Hou YM, et al. The catalytic domain of topological knot tRNA methyltransferase (TrmH) discriminates between substrate tRNA and nonsubstrate tRNA via an induced-fit process. J Biol Chem. 2013;288(35):25562-74.
89. Ochi A, Makabe K, Kuwajima K, Hori H. Flexible recognition of the tRNA G18 methylation target site by TrmH methyltransferase through first binding and induced fit processes. J Biol Chem. 2010;285(12):9018-29.
90. Noon KR, Guymon R, Crain PF, McCloskey JA, Thomm M, Lim J, et al. Influence of Temperature on tRNA Modification in Archaea: Methanococcoides burtonii (Optimum Growth Temperature [Topt], 23 C) and Stetteria hydrogenophila (Topt, 95 C). Journal of Bacteriology. 2003;185(18):5483-90.
91. Jung S, von Thulen T, Laukemper V, Pigisch S, Hangel D, Wagner H, et al. A single naturally occurring 2'-O-methylation converts a TLR7- and TLR8-activating RNA into a TLR8-specific ligand. PLoS One. 2015;10(3):e0120498.
92. Hamm S, Latz E, Hangel D, Muller T, Yu P, Golenbock D, et al. Alternating 2'-O-ribose methylation is a universal approach for generating non-stimulatory siRNA by acting as TLR7 antagonist. Immunobiology. 2010;215(7):559-69.
93. Kaiser S, Rimbach K, Eigenbrod T, Dalpke AH, Helm M. A modified dinucleotide motif specifies tRNA recognition by TLR7. RNA. 2014;20(9):1351-5.
94. Tollervey D, Lehtonen H, Carmo-Fonseca M, Hurt EC. The small nucleolar RNP protein NOP1 (fibrillarin) is required for pre-rRNA processing in yeast. The EMBO Journal. 1991;10(3):573-83.
95. Sharma S, Lafontaine DLJ. 'View From A Bridge': A New Perspective on Eukaryotic rRNA Base Modification. Trends Biochem Sci. 2015;40(10):560-75.

96. Amin MA, Matsunaga S, Ma N, Takata H, Yokoyama M, Uchiyama S, et al. Fibrillarin, a nucleolar protein, is required for normal nuclear morphology and cellular growth in HeLa cells. Biochem Biophys Res Commun. 2007;360(2):320-6.
97. Newton K, Petfalski E, Tollervey D, Caceres JF. Fibrillarin Is Essential for Early Development and Required for Accumulation of an Intron-Encoded Small Nucleolar RNA in the Mouse. Molecular and Cellular Biology. 2003;23(23):8519-27.
98. Polikanov YS, Melnikov SV, Soll D, Steitz TA. Structural insights into the role of rRNA modifications in protein synthesis and ribosome assembly. Nat Struct Mol Biol. 2015;22(4):342-4.
99. International Human Genome Sequencing C. Initial sequencing and analysis of the human genome. Nature. 2001;409:860.
100. Boettcher M, McManus MT. Choosing the Right Tool for the Job: RNAi, TALEN, or CRISPR. Mol Cell. 2015;58(4):575-85.
101. Elbashir SM, Harborth J, Lendeckel W, Yalcin A, Weber K, Tuschl T. Duplexes of 21-nucleotide RNAs mediate RNA interference in cultured mammalian cells. Nature. 2001;411:494.
102. Moore CB, Guthrie EH, Huang MT, Taxman DJ. Short hairpin RNA (shRNA): design, delivery, and assessment of gene knockdown. Methods Mol Biol. 2010;629:141-58.
103. Bibikova M, Carroll D, Segal DJ, Trautman JK, Smith J, Kim YG, et al. Stimulation of homologous recombination through targeted cleavage by chimeric nucleases. Mol Cell Biol. 2001;21(1):289-97.
104. Yang-Gyun K, Jooyeun C, Srinivasan C. Hybrid restriction enzymes: Zinc finger fusions to Fok I cleavage domain. Proc Natl Acad Sci. 1996;Vol. 93:1156-60.
105. Urnov FD, Rebar EJ, Holmes MC, Zhang HS, Gregory PD. Genome editing with engineered zinc finger nucleases. Nat Rev Genet. 2010;11(9):636-46.
106. Miller JC, Tan S, Qiao G, Barlow KA, Wang J, Xia DF, et al. A TALE nuclease architecture for efficient genome editing. Nat Biotechnol. 2011;29(2):143-8.
107. Wade M. High-Throughput Silencing Using the CRISPR-Cas9 System: A Review of the Benefits and Challenges. J Biomol Screen. 2015;20(8):1027-39.
108. Wang H, La Russa M, Qi LS. CRISPR/Cas9 in Genome Editing and Beyond. Annu Rev Biochem. 2016;85:227-64.
109. Jinek M, Chylinski K, Fonfara I, Hauer M, Doudna JA, Charpentier E. A programmable dual-RNA-guided DNA endonuclease in adaptive bacterial immunity. Science. 2012;337(6096):816-21.
110. Cong L, Ran FA, Cox D, Lin S, Barretto R, Habib N, et al. Multiplex genome engineering using CRISPR/Cas systems. Science. 2013;339(6121):819-23.
111. Chen B, Gilbert LA, Cimini BA, Schnitzbauer J, Zhang W, Li GW, et al. Dynamic imaging of genomic loci in living human cells by an optimized CRISPR/Cas system. Cell. 2013;155(7):1479-91.
112. Sorek R, Lawrence CM, Wiedenheft B. CRISPR-mediated adaptive immune systems in bacteria and archaea. Annu Rev Biochem. 2013;82:237-66.
113. Sternberg SH, Redding S, Jinek M, Greene EC, Doudna JA. DNA interrogation by the CRISPR RNA-guided endonuclease Cas9. Nature. 2014;507(7490):62-7.
114. Gasiunas G, Barrangou R, Horvath P, Siksnys V. Cas9-crRNA ribonucleoprotein complex mediates specific DNA cleavage for adaptive immunity in bacteria. Proc Natl Acad Sci U S A. 2012;109(39):E2579-86.
115. Yumlu S, Stumm J, Bashir S, Dreyer AK, Lisowski P, Danner E, et al. Gene editing and clonal isolation of human induced pluripotent stem cells using CRISPR/Cas9. Methods. 2017;121-122:29-44.

116. Jacobi AM, Rettig GR, Turk R, Collingwood MA, Zeiner SA, Quadros RM, et al. Simplified CRISPR tools for efficient genome editing and streamlined protocols for their delivery into mammalian cells and mouse zygotes. Methods. 2017;121-122:16-28.
117. Concordet JP, Giovannangeli C. CRISPR-Cas systems for genome engineering and investigation. Methods. 2017;121-122:1-2.
118. Klonowska-Szymczyk A, Wolska A, Robak T, Cebula-Obrzut B, Smolewski P, Robak E. Expression of toll-like receptors 3, 7, and 9 in peripheral blood mononuclear cells from patients with systemic lupus erythematosus. Mediators Inflamm. 2014;2014:381418.
119. Tomita K, Ogawa T, Uozumi T, Watanabe K, Masaki H. A cytotoxic ribonuclease which specifically cleaves four isoaccepting arginine tRNAs at their anticodon loops. Proc Natl Acad Sci U S A. 2000;97(15):8278-83.
120. Boccaletto P, Machnicka MA, Purta E, Piatkowski P, Baginski B, Wirecki TK, et al. MODOMICS: a database of RNA modification pathways. 2017 update. Nucleic Acids Res. 2018;46(D1):D303-D7.
121. Hengesbach M, Meusburger M, Lyko F, Helm M. Use of DNAzymes for site-specific analysis of ribonucleotide modifications. RNA. 2008;14(1):180-7.
122. Iavarone C, O'Hagan D T, Yu D, Delahaye NF, Ulmer JB. Mechanism of action of mRNA-based vaccines. Expert Rev Vaccines. 2017;16(9):871-81.
123. Pardi N, Hogan MJ, Porter FW, Weissman D. mRNA vaccines - a new era in vaccinology. Nat Rev Drug Discov. 2018;17(4):261-79.
124. Schlake T, Thess A, Fotin-Mleczek M, Kallen KJ. Developing mRNA-vaccine technologies. RNA Biol. 2012;9(11):1319-30.
125. Van Hoeven N, Fox CB, Granger B, Evers T, Joshi SW, Nana GI, et al. A Formulated TLR7/8 Agonist is a Flexible, Highly Potent and Effective Adjuvant for Pandemic Influenza Vaccines. Sci Rep. 2017;7:46426.
126. Lynn GM, Laga R, Darrah PA, Ishizuka AS, Balaci AJ, Dulcey AE, et al. In vivo characterization of the physicochemical properties of polymer-linked TLR agonists that enhance vaccine immunogenicity. Nat Biotechnol. 2015;33(11):1201-10.
127. Holbrook BC, Kim JR, Blevins LK, Jorgensen MJ, Kock ND, D'Agostino RB, Jr., et al. A Novel R848-Conjugated Inactivated Influenza Virus Vaccine Is Efficacious and Safe in a Neonate Nonhuman Primate Model. J Immunol. 2016;197(2):555-64.
128. Heidenreich R, Jasny E, Kowalczyk A, Lutz J, Probst J, Baumhof P, et al. A novel RNA-based adjuvant combines strong immunostimulatory capacities with a favorable safety profile. Int J Cancer. 2015;137(2):372-84.
129. Ziegler A, Soldner C, Lienenklaus S, Spanier J, Trittel S, Riese P, et al. A New RNA-Based Adjuvant Enhances Virus-Specific Vaccine Responses by Locally Triggering TLR- and RLH-Dependent Effects. J Immunol. 2017;198(4):1595-605.
130. Maden BE. Mapping 2'-O-methyl groups in ribosomal RNA. Methods. 2001;25(3):374-82.
131. McCloskey JA, Liu XH, Crain PF, Bruenger E, Guymon R, Hashizume T, et al. Posttranscriptional modification of transfer RNA in the submarine hyperthermophile Pyrolobus fumarii. Nucleic Acids Symp Ser. 2000(44):267-8.
132. Rapino F, Robles EF, Richter-Larrea JA, Kallin EM, Martinez-Climent JA, Graf T. C/EBPalpha induces highly efficient macrophage transdifferentiation of B lymphoma and leukemia cell lines and impairs their tumorigenicity. Cell Rep. 2013;3(4):1153-63.
133. Vierbuchen T, Bang C, Rosigkeit H, Schmitz RA, Heine H. The Human-Associated Archaeon Methanosphaera stadtmanae Is Recognized through Its RNA and Induces TLR8-Dependent NLRP3 Inflammasome Activation. Front Immunol. 2017;8:1535.
134. Kallio MA, Tuimala JT, Hupponen T, Klemela P, Gentile M, Scheinin I, et al. Chipster: user-friendly analysis software for microarray and other high-throughput data. BMC Genomics. 2011;12:507.

135. Dehairs J, Talebi A, Cherifi Y, Swinnen JV. CRISP-ID: decoding CRISPR mediated indels by Sanger sequencing. Sci Rep. 2016;6:28973.
136. Zhao M, Lewis Wang FS, Hu X, Chen F, Chan HM. Acrylamide-induced neurotoxicity in primary astrocytes and microglia: Roles of the Nrf2-ARE and NF-kappaB pathways. Food Chem Toxicol. 2017;106(Pt A):25-35.
137. Kariko K, Muramatsu H, Welsh FA, Ludwig J, Kato H, Akira S, et al. Incorporation of pseudouridine into mRNA yields superior nonimmunogenic vector with increased translational capacity and biological stability. Mol Ther. 2008;16(11):1833-40.
138. Tom JK, Dotsey EY, Wong HY, Stutts L, Moore T, Davies DH, et al. Modulation of Innate Immune Responses via Covalently Linked TLR Agonists. ACS Cent Sci. 2015;1(8):439-48.
139. Hellmuth I, Freund I, Schloder J, Seidu-Larry S, Thuring K, Slama K, et al. Bioconjugation of Small Molecules to RNA Impedes Its Recognition by Toll-Like Receptor 7. Front Immunol. 2017;8:312.
140. Nair JK, Willoughby JL, Chan A, Charisse K, Alam MR, Wang Q, et al. Multivalent N-acetylgalactosamine-conjugated siRNA localizes in hepatocytes and elicits robust RNAi-mediated gene silencing. J Am Chem Soc. 2014;136(49):16958-61.
141. Colak E, Leslie A, Zausmer K, Khatamzas E, Kubarenko AV, Pichulik T, et al. RNA and imidazoquinolines are sensed by distinct TLR7/8 ectodomain sites resulting in functionally disparate signaling events. J Immunol. 2014;192(12):5963-73.
142. Lai CY, Yeh DW, Lu CH, Liu YL, Huang LR, Kao CY, et al. Identification of Thiostrepton as a Novel Inhibitor for Psoriasis-like Inflammation Induced by TLR7-9. J Immunol. 2015;195(8):3912-21.
143. Gilliet M, Conrad C, Geiges M, Cozzio A, Thurlimann W, Burg G, et al. Psoriasis triggered by toll-like receptor 7 agonist imiquimod in the presence of dermal plasmacytoid dendritic cell precursors. Arch Dermatol. 2004;140(12):1490-5.
144. Takano S, Aramaki Y, Tsuchiya S. Physicochemical properties of liposomes affecting apoptosis induced by cationic liposomes in macrophages. Pharm Res. 2003;20(7):962-8.
145. Epstein-Barash H, Gutman D, Markovsky E, Mishan-Eisenberg G, Koroukhov N, Szebeni J, et al. Physicochemical parameters affecting liposomal bisphosphonates bioactivity for restenosis therapy: internalization, cell inhibition, activation of cytokines and complement, and mechanism of cell death. J Control Release. 2010;146(2):182-95.
146. Altin JG, van Broekhoven CL, Parish CR. Targeting dendritic cells with antigen-containing liposomes: antitumour immunity. Expert Opin Biol Ther. 2004;4(11):1735-47.
147. Bozzuto G, Molinari A. Liposomes as nanomedical devices. Int J Nanomedicine. 2015;10:975-99.
148. Garnier B, Tan S, Gounou C, Brisson AR, Laroche-Traineau J, Jacobin-Valat MJ, et al. Development of a platform of antibody-presenting liposomes. Biointerphases. 2012;7(1-4):11.
149. Kelly C, Jefferies C, Cryan SA. Targeted liposomal drug delivery to monocytes and macrophages. J Drug Deliv. 2011;2011:727241.
150. van Broekhoven CL, Parish CR, Demangel C, Britton WJ, Altin JG. Targeting dendritic cells with antigen-containing liposomes: a highly effective procedure for induction of antitumor immunity and for tumor immunotherapy. Cancer Res. 2004;64(12):4357-65.
151. Crow MK. Interferon-alpha: a therapeutic target in systemic lupus erythematosus. Rheum Dis Clin North Am. 2010;36(1):173-86, x.
152. Ganguly D, Chamilos G, Lande R, Gregorio J, Meller S, Facchinetti V, et al. Self-RNA-antimicrobial peptide complexes activate human dendritic cells through TLR7 and TLR8. J Exp Med. 2009;206(9):1983-94.

153. Morizane S, Yamasaki K, Muhleisen B, Kotol PF, Murakami M, Aoyama Y, et al. Cathelicidin antimicrobial peptide LL-37 in psoriasis enables keratinocyte reactivity against TLR9 ligands. J Invest Dermatol. 2012;132(1):135-43.
154. Dreier J, Sorensen JA, Brewer JR. Superresolution and Fluorescence Dynamics Evidence Reveal That Intact Liposomes Do Not Cross the Human Skin Barrier. PLoS One. 2016;11(1):e0146514.
155. Tran TN. Cutaneous drug delivery: an update. J Investig Dermatol Symp Proc. 2013;16(1):S67-9.
156. Marren K. Dimethyl sulfoxide: an effective penetration enhancer for topical administration of NSAIDs. Phys Sportsmed. 2011;39(3):75-82.
157. Marchand V, Pichot F, Thuring K, Ayadi L, Freund I, Dalpke A, et al. Next-Generation Sequencing-Based RiboMethSeq Protocol for Analysis of tRNA 2'-O-Methylation. Biomolecules. 2017;7(1).
158. Demeshkina N, Jenner L, Yusupova G, Yusupov M. Interactions of the ribosome with mRNA and tRNA. Curr Opin Struct Biol. 2010;20(3):325-32.
159. Vare VY, Eruysal ER, Narendran A, Sarachan KL, Agris PF. Chemical and Conformational Diversity of Modified Nucleosides Affects tRNA Structure and Function. Biomolecules. 2017;7(1).
160. Yasuda K, Yu P, Kirschning CJ, Schlatter B, Schmitz F, Heit A, et al. Endosomal Translocation of Vertebrate DNA Activates Dendritic Cells via TLR9-Dependent and -Independent Pathways. The Journal of Immunology. 2005;174(10):6129-36.
161. Scott CC, Vacca F, Gruenberg J. Endosome maturation, transport and functions. Semin Cell Dev Biol. 2014;31:2-10.
162. Woodman PG. Biogenesis of the Sorting Endosome: The Role of Rab5. Traffic. 2000;1(9):695-701.
163. Tollervey D, Lehtonen H, Carmo-Fonseca M, Hurt EC. The small nucleolar RNP protein NOP1 (fibrillarin) is required for pre-rRNA processing in yeast. EMBO J. 1991;10(3):573-83.
164. Jansen RP, Hurt EC, Kern H, Lehtonen H, Carmo-Fonseca M, Lapeyre B, et al. Evolutionary conservation of the human nucleolar protein fibrillarin and its functional expression in yeast. J Cell Biol. 1991;113(4):715-29.
165. Tormey VJ, Bunn CC, Denton CP, Black CM. Anti-fibrillarin antibodies in systemic sclerosis. Rheumatology. 2001;40(10):1157-62.
166. Van Eenennaam H, Vogelzangs JHP, Bisschops L, Te Boome LCJ, Seelig HP, Renz M, et al. Autoantibodies against small nucleolar ribonucleoprotein complexes and their clinical associations. Clinical and Experimental Immunology. 2002;130(3):532-40.
167. Pollard KM, Hultman P, Kono DH. Toxicology of autoimmune diseases. Chem Res Toxicol. 2010;23(3):455-66.
168. Lafyatis R, York M. Innate immunity and inflammation in systemic sclerosis. Curr Opin Rheumatol. 2009;21(6):617-22.
169. Guiducci C, Gong M, Cepika AM, Xu Z, Tripodo C, Bennett L, et al. RNA recognition by human TLR8 can lead to autoimmune inflammation. J Exp Med. 2013;210(13):2903-19.
170. Crowl JT, Gray EE, Pestal K, Volkman HE, Stetson DB. Intracellular Nucleic Acid Detection in Autoimmunity. Annu Rev Immunol. 2017;35:313-36.
171. Banchereau J, Pascual V. Type I interferon in systemic lupus erythematosus and other autoimmune diseases. Immunity. 2006;25(3):383-92.
172. Pascual V, Farkas L, Banchereau J. Systemic lupus erythematosus: all roads lead to type I interferons. Curr Opin Immunol. 2006;18(6):676-82.
173. Jonkhout N, Tran J, Smith MA, Schonrock N, Mattick JS, Novoa EM. The RNA modification landscape in human disease. RNA. 2017;23(12):1754-69.

174. Fisher AJ, Beal PA. Effects of Aicardi-Goutieres syndrome mutations predicted from ADAR-RNA structures. RNA Biol. 2017;14(2):164-70.
175. Guy MP, Shaw M, Weiner CL, Hobson L, Stark Z, Rose K, et al. Defects in tRNA Anticodon Loop 2'-O-Methylation Are Implicated in Nonsyndromic X-Linked Intellectual Disability due to Mutations in FTSJ1. Hum Mutat. 2015;36(12):1176-87.
176. Ye J, Wang J, Tan L, Yang S, Xu L, Wu X, et al. Expression of protein TARBP1 in human hepatocellular carcinoma and its prognostic significance. Int J Clin Exp Pathol. 2015;8(8):9089-96.
177. Ye J, Wang J, Zhang N, Liu Y, Tan L, Xu L. Expression of TARBP1 protein in human non-small-cell lung cancer and its prognostic significance. Oncol Lett. 2018;15(5):7182-90.
178. Tang H, Jin X, Li Y, Jiang H, Tang X, Yang X, et al. A large-scale screen for coding variants predisposing to psoriasis. Nat Genet. 2014;46(1):45-50.
179. Wu-Baer F, Lane WS, Gaynor RB. The cellular factor TRP-185 regulates RNA polymerase II binding to HIV-1 TAR RNA. EMBO J. 1995;14(23):5995-6009.
180. Kumagai I, Watanabe K, Oshima T. A thermostable tRNA (guanosine-2')-methyltransferase from Thermus thermophilus HB27 and the effect of ribose methylation on the conformational stability of tRNA. J Biol Chem. 1982;257(13):7388-95.
181. Kumagai I, Watanabe K, Oshima T. Thermally induced biosynthesis of 2'-O-methylguanosine in tRNA from an extreme thermophile, Thermus thermophilus HB27. Proc Natl Acad Sci U S A. 1980;77(4):1922-6.
182. Helm M, Alfonzo JD. Posttranscriptional RNA Modifications: playing metabolic games in a cell's chemical Legoland. Chem Biol. 2014;21(2):174-85.
183. Young AP, Bandarian V. Pyruvate is the source of the two carbons that are required for formation of the imidazoline ring of 4-demethylwyosine. Biochemistry. 2011;50(49):10573-5.
184. Robertus JD, Ladner JE, Finch JT, Rhodes D, Brown RS, Clark BFC, et al. Structure of yeast phenylalanine tRNA at 3 Å resolution. Nature. 1974;250(5467):546-51.
185. Hori H. Transfer RNA methyltransferases with a SpoU-TrmD (SPOUT) fold and their modified nucleosides in tRNA. Biomolecules. 2017;7(1).
186. Ishida K, Kunibayashi T, Tomikawa C, Ochi A, Kanai T, Hirata A, et al. Pseudouridine at position 55 in tRNA controls the contents of other modified nucleotides for low-temperature adaptation in the extreme-thermophilic eubacterium Thermus thermophilus. Nucleic Acids Res. 2011;39(6):2304-18.
187. Kinghorn SM, O'Byrne CP, Booth IR, Stansfield I. Physiological analysis of the role of truB in Escherichia coli: a role for tRNA modification in extreme temperature resistance. Microbiology. 2002;148(Pt 11):3511-20.
188. Jain V, Kumar M, Chatterji D. ppGpp: stringent response and survival. J Microbiol. 2006;44(1):1-10.
189. Persson BC, Jager G, Gustafsson C. The spoU gene of Escherichia coli, the fourth gene of the spoT operon, is essential for tRNA (Gm18) 2'-O-methyltransferase activity. Nucleic Acids Res. 1997;25(20):4093-7.
190. Grozdanov L, Zahringer U, Blum-Oehler G, Brade L, Henne A, Knirel YA, et al. A Single Nucleotide Exchange in the wzy Gene Is Responsible for the Semirough O6 Lipopolysaccharide Phenotype and Serum Sensitivity of Escherichia coli Strain Nissle 1917. Journal of Bacteriology. 2002;184(21):5912-25.
191. Grozdanov L, Raasch C, Schulze J, Sonnenborn U, Gottschalk G, Hacker J, et al. Analysis of the genome structure of the nonpathogenic probiotic Escherichia coli strain Nissle 1917. J Bacteriol. 2004;186(16):5432-41.
192. Adam E, Delbrassine L, Bouillot C, Reynders V, Mailleux AC, Muraille E, et al. Probiotic Escherichia coli Nissle 1917 activates DC and prevents house dust mite allergy through a TLR4-dependent pathway. Eur J Immunol. 2010;40(7):1995-2005.

193. Helwig U, Lammers KM, Rizzello F, Brigidi P, Rohleder V, Caramelli E, et al. Lactobacilli, bifidobacteria and E. coli nissle induce pro- and anti-inflammatory cytokines in peripheral blood mononuclear cells. World J Gastroenterol. 2006;12(37):5978-86.
194. Schlee M, Wehkamp J, Altenhoefer A, Oelschlaeger TA, Stange EF, Fellermann K. Induction of human beta-defensin 2 by the probiotic Escherichia coli Nissle 1917 is mediated through flagellin. Infect Immun. 2007;75(5):2399-407.
195. Wehkamp J, Harder J, Wehkamp K, Wehkamp-von Meissner B, Schlee M, Enders C, et al. NF-kappaB- and AP-1-mediated induction of human beta defensin-2 in intestinal epithelial cells by Escherichia coli Nissle 1917: a novel effect of a probiotic bacterium. Infect Immun. 2004;72(10):5750-8.
196. Schimmel P, Tamura K. tRNA Structure Goes from L to λ. Cell. 2003;113(3):276-8.
197. Jackman JE, Alfonzo JD. Transfer RNA modifications: nature's combinatorial chemistry playground. Wiley Interdiscip Rev RNA. 2013;4(1):35-48.
198. Tan ZJ, Chen SJ. Salt contribution to RNA tertiary structure folding stability. Biophys J. 2011;101(1):176-87.
199. Mindell JA. Lysosomal acidification mechanisms. Annu Rev Physiol. 2012;74:69-86.
200. Thaplyal P, Bevilacqua PC. Experimental approaches for measuring pKa's in RNA and DNA. Methods Enzymol. 2014;549:189-219.
201. Bernhardt HS, Tate WP. Primordial soup or vinaigrette: did the RNA world evolve at acidic pH? Biol Direct. 2012;7:4.
202. Oivanen M, Kuusela S, Lönnberg H. Kinetics and Mechanisms for the Cleavage and Isomerization of the Phosphodiester Bonds of RNA by Brønsted Acids and Bases. Chemical Reviews. 1998;98(3):961-90.
203. Fujiwara Y, Wada K, Kabuta T. Lysosomal degradation of intracellular nucleic acids-multiple autophagic pathways. J Biochem. 2017;161(2):145-54.
204. Prats-Ejarque G, Arranz-Trullen J, Blanco JA, Pulido D, Nogues MV, Moussaoui M, et al. The first crystal structure of human RNase 6 reveals a novel substrate-binding and cleavage site arrangement. Biochem J. 2016;473(11):1523-36.

7 PUBLICATIONS AND CONFERENCES

7.1 Publication

The following publications are based on different chapters of this thesis:

Chapter 4.2

Double methylation of tRNA-U54 to 2'-O-methylthymidine (Tm) synergistically decreases immune response by Toll-like receptor 7.

Keller P [#], **Freund I** [#], Marchand V, Bec G, Huang R, Motorin Y, Eigenbrod T, Dalpke A, and Helm M.

Nucleic Acids Res. 2018 Aug 8. doi: 10.1093/nar/gky644. [Epub ahead of print]

[#] equal contribution

Chapter 4.3

Identification of an optimized 2'-O-methylated trinucleotide RNA motif inhibiting Toll-like receptors 7 and 8

Schmitt FCF [#], **Freund I** [#], Weigand MA, Helm M, Dalpke AH, Eigenbrod T

RNA. 2017 Sep;23(9):1344-1351. Doi: 10.1261/rna.061952.117

[#] equal contribution

Chapter 4.3.2.1

Bioconjugation of Small Molecules to RNA Impedes Its Recognition by Toll-Like Receptor 7

Hellmuth I, **Freund I**, Schloder J, Seidu-Larry S, Thuring K, Slama K, Langhanki J, Kaloyanova S, Eigenbrod T, Krumb M, Rohm S, Peneva K, Opatz T, Jonuleit H, Dalpke AH and Helm M.

Front Immunol. 2017 Mar 24;8:312. Doi: 10.3389/fimmu.2017.00312.

Chapter 4.4

Next-Generation Sequencing-Based RiboMethSeq Protocol for Analysis of tRNA 2'-O-Methylation.

Marchand V, Pichot F, Thuring K, Ayadi L, **Freund I**, Dalpke AH, Helm M and Motorin Y

Biomolecules. 2017 Feb 9;7(1). pii: E13. doi: 10.3390/biom7010013

Crucial role of nucleic acid sensing via endosomal Toll-like receptors for the defense of Streptococcus pyogenes *in vitro* and *in vivo*

Hafner A, Kolbe U, **Freund I**, Castiglia C, Kovarik P, Poth T, Herster F, Weigand MA, Weber ANR, Dalpke AH, Eigenbrod T

Manuscript submitted

7.2 Conferences

Poster: Nucleic acid dependent recognition of S. pyogenes by the innate immune system

Isabel Freund, Anna Hafner, Virginia Castiglia, Pavel Kovarik, Tanja Poth, Alexander Dalpke, Tatjana Eigenbrod

5th Joint Conference of the DGHM & VAAM

VAAM Annual Meeting 2017

69th Annual Meeting of the DGHM

Würzburg, March 2017

Poster: Context effects of ribose 2'-O-methylation as a modification in RNA that suppresses recognition by Toll-like receptor 7 and 8

Isabel Freund, Felix Schmitt, Patrick Keller, Mark Helm, Alexander Dalpke, Tatjana Eigenbrod

Keystone Symposia meeting on Nucleic Acid Sensing Pathways: Innate Immunity, Immunobiology and Therapeutics

Dresden, May 2016

8 ACKNOWLEDGEMENT

Mein besonderer Dank gilt Prof. Dr. Alexander Dalpke für die Möglichkeit, meine Doktorarbeit in seiner Arbeitsgruppe zu schreiben, sowie für seine herausragende wissenschaftliche Betreuung, hilfreiche Diskussionen, wertvolle Ratschläge und immer neue Ideen. Zudem möchte ich mich für die Möglichkeit bedanken an, Kongressen und Fortbildungen teilzunehmen.

Ganz herzlich möchte ich mich bei PD Dr. Tatjana Eigenbrod bedanken für die vielen interessanten Diskussionen weit über den Tellerrand hinaus und ganz besonders dafür, dass sie auch den deprimierendsten Ergebnissen etwas Positives abgewinnen konnte und mich immer ermutigt und motiviert hat weiterzumachen.

Herrn Prof. Dr. Ralf Bartenschlager danke ich für die Begutachtung meiner Arbeit, sowie seine Funktion als Erstgutachter und Mitglied meines TAC Komitees und für neue Ideen und Impulse im Rahmen meine Doktorarbeit.

Herrn Prof. Dr. Gert Fricker und Frau PD Dr. Odilia Popanda möchte ich für Ihre Funktion als Prüfer im Rahmen meiner Disputation danken.

Für die hervorragende wissenschaftliche Kooperation, ohne die diese Arbeit nicht möglich gewesen wäre, danke ich insbesondere Prof. Dr. Mark Helm, Dr. Patrick Keller und Dr. Isabell Hellmuth von der Johannes-Gutenberg-Universität Mainz sowie außerdem Prof. Dr. Yuri Motorin und Dr. Virginie Marchand von der Université de Lorraine.

Ich danke Daniel Buhl, Philipp Willnow, Manuela Aguirre Botero, Michelle Rosenthal und Maria Bozhinova, die durch ihre Bachelor- und Master-Arbeiten und Laborpraktika ebenfalls zum Gelingen dieser Arbeit beigetragen haben.

Besonders möchte ich mich bei allen Mitarbeitern der Abteilung Medizinische Mikrobiologie und Hygiene für die wunderbare Atmosphäre bedanken. Ein großes Dankeschön an Sébastien für die unermüdliche Hilfe bei allen Statistikfragen, Computerproblemen und ein offenes Ohr wenn mal wieder alles schief ging. Ein ganz lieber Dank geht insbesondere an Jana, Vedrana, Volker und Ulrike für die hilfreichen Ratschläge und die lustigen Stunden in unserem Büro. Des Weiteren möchte ich mich bei Suzan und Selina bedanken für die vielen guten Tipps und Tricks und die gute Stimmung im Labor.

Mein ganz persönlicher Dank geht an meine Familie und Freunde und besonders an meine Eltern, die mich immer bedingungslos unterstützt haben und mir dies alles ermöglicht haben. Zuletzt möchte ich Benjamin danken, der immer für mich da war und geholfen hat den Frust der Laborarbeit zu vergessen.